L-Università ta' Malta
Faculty of Engineering

MASTER OF SCIENCE IN ENGINEERING DISSERTATION

Evaluation of the Environmental and Financial Impacts of Faults in Bus Pneumatic Systems

MASSIMO BORG

Supervised by:
DR ING. PAUL REFALO

Co-supervised by:
DR ING. EMMANUEL FRANCALANZA

A dissertation submitted in partial fulfilment of the requirements for the degree of Master of Science in Engineering

by the

Faculty of Engineering

February 2022

Copyright Notice

Dedication

First and foremost, I would like to dedicate this dissertation to my parents Mary Anne and Charles, who not only supported me throughout the years, but also offered a loving and nourishing environment, helping me to develop my personality. I would also like to thank my significant other, Audrey, who offered endless love, affection and assistance throughout the years. Finally, I would like to dedicate this study to my grandparents Francis and Salvatore, who sadly passed away during the completion of this dissertation.

Abstract

In recent years, a push towards a cleaner transport sector has been given importance, with various regulations helping to achieve this goal. One of the major culprits of emissions in this sector are heavy vehicles, such as buses, which even though in minority, account for 27 per cent of all emissions. These types of vehicles make use of compressed air in the Bus Pneumatic System (BPS) to power auxiliaries, mainly the brakes, suspension and doors. From a review and problem analysis which was carried out in this study, these systems can be quite inefficient due to leakages and faults. Maintenance of BPSs is also often overlooked due to its effect on vehicle downtime. To address this problem, monitoring systems have recently started to be developed. Nevertheless, such systems are still limited and knowledge in this area is quite scarce.

Indeed, in order to better comprehend how a typical BPS operates, tests on an actual vehicle were performed during the study. It was concluded that to power the pneumatic auxiliaries, 4.4 per cent of the vehicle's total fuel is required. The next step was to understand how different factors, both operational and fault oriented, affect the system, whilst also finding factors which help in identifying and quantifying faults. This was possible by performing tests on a set-up designed to depict and monitor a typical BPS, containing the air suspension and pneumatic cylinder, both used frequently during bus use, where the pressure, flow rate and cycle time would be observed.

The results showed that a system leak and a faulty double acting actuator increased the volume of compressed air, whilst the cycle time was only affected when the faulty cylinder was induced. To find more parameters which help in identifying fault sources, the pressure standard deviation within each stop was analysed, where for both the leak and the faulty cylinder, a considerable decrease, i.e. 16 and 6 per cent, respectively, was recorded, as compared to the control. In addition it was concluded that the end effectors should not be actuated *separately*, since the test time was increased by 20 per cent. Furthermore, the real life repercussions of faults were also investigated, with the main outcomes being that in order to offset the annual emissions imposed by the leak per vehicle, 7 household solar panels would be required, thereby increasing the pneumatic fuel percentage to 5.6 per cent.

Key words: Sustainability, heavy vehicles, data monitoring, bus pneumatic system

Acknowledgments

First and foremost, I would like to acknowledge the valuable contribution and dedication offered by my tutors Dr. Ing. Paul Refalo and Dr. Ing Emmanuel Francalanza which paved way towards completing this thesis, whilst always offering enthusiastic support.

I would also like to express my gratitude to Mr. Angelo Mifsud from AIM Enterprises Ltd. together with Mr. Colin Borg and Mr. Joseph Grixti, since without their professional expertise, this project would not have been possible. Furthermore, I would also like to thank Mr. Josef Briffa and Mr. Joseph Curmi and all the technical staff at the Faculty of Engineering for their assistance throughout the entire study.

Finally, I would like to thank my parents, my brother Reuben, my girlfriend and her family who always offered encouragement and love not only during the completion of the dissertation, but throughout the years.

Table of Contents

List of Figures

List of Tables

List of Abbreviations

Phrase	Abbreviation
Artificial Intelligence	AI
Bus Pneumatic System	BPS
Bus Pneumatic Test Bed	BPTB
Carbon Dioxide	CO_2
Change in Pressure	Δ_P
Compressed Air	CA
Compressed Air Systems	CAS
Compressed Air Test Bed	CATB
Design of Experiment	DOE
Dynamic Pressure	$P_{Dynamic}$
Electronic Control Unit	ECU
Electronically Controlled Air Suspension	ECAS
European Union	EU
Human-Machine Interface	HMI
Internet of Things/Vehicles	IoT/IoV
Key Performance Indicator	KPI
Personal Computer	PC
Static Pressure	P_{Static}
Total Pressure	P_{Total}
Uncertainty Due to Accuracy	Δ_{Acc}
Uncertainty Due to Resolution	Δ_{Res}
Uncertainty Due to Standard Deviation	Δ_{Std}
United Nations	UN

Glossary of Symbols

Symbol	Definition
-	Minus
/	Division
+	Plus
±	Plus or Minus
×	Multiplication
≤	Equal To or Less Then
≥	Equal To or Greater Then
€/h	Euro per Hour
Euros	€
kg/h	Kg per Hour
Kilometre	Km
kW	Kilowatt
kW_P	Kilowatt Peak
L/h	Litre per Hour
milliAmp	mA
min	Minute
Nl/min	Normal Litres per Minute
Percentage	%
s	Second

Chapter 1- Introduction

1.1 Problem Outline

1.1.1 Inefficiencies Associated with Pneumatic Systems

Compressed Air (CA) has been used as an industrial utility for many years, with its uses ranging from industrial applications to the actuation of various auxiliaries in buses, with the latter being the focus of this study. There are plenty of reasons why companies opt to make use of this energy source, with the main ones being that CA is reliable, safe to operate and overall simple to set-up. Therefore, it comes as no surprise that CA is considered as the fourth utility [1–4].

Despite all these advantages, the generation of CA is highly inefficient with studies claiming that hybrid buses use 24 per cent [5] of their total electrical energy just to power the pneumatic compressor. Additionally, it is often the case that leaks are left unattended due to the downtime associated with their repair. In buses, it is estimated that this downtime costs companies around 21 per cent [6] of their total operational costs. This has not gone unnoticed and in recent years, pneumatic monitoring systems having the ability to alert users of faults have started to be developed for the BPS. However, only few are currently available, as the majority have still not reached commercialisation. Additionally, due to the lack of research relating to this sector, the further development of such systems is commonly hindered, meaning that additional studies regarding this area would provide beneficial information which helps in better comprehending the overall behaviour of these set-ups.

1.1.2 Sustainability Shift in the Automotive Industry

During the last few decades, devastating environmental impacts have been experienced, most noticeably global warming. Due to this phenomenon, it is estimated that if no drastic environmental improvements are made, the Earth's temperature will continue to rise by 2°C between 2030 and 2050, as compared to pre-industrial figures. The rise in temperature has currently resulted in climate change as in recent years an increase in the frequency of storms, followed by excessive high temperatures have been experienced [7, 8]. It could be said that the main reason for this phenomenon relates to the emissions of CO_2 gasses, with one of the main culprits being heavy

vehicles, making part of the transportations sector. This is especially true in the local scenario, since according to the National Energy and Climate Plan [9], Malta uses 15 per cent more energy for road transport as compared to its European Union (EU) counterparts.

These effects have not gone unnoticed and various efforts have been made to try to both mitigate and counteract them. Examples include the Sustainability Development Goals [10], by the United Nations (UN), which highlight various sustainable goals to be met by 2030 and the New Vehicles Directive [11] by the EU, emphasising the development of clean vehicles by 2030.

Although it is commonly thought that sustainability only relates to the environmental aspects, this is not the case since it also entails the holistic improvements for the economic and social pillars, as summarised in Figure 1.1 [12]. This means that not only do efforts help in making the environment greener, but also endorse the fulfilment of the individual well-being, thereby ensuring the distribution of wealth. Although it is difficult to do so, the Sustainability Development Goals, try to offer companies a realistic solution to fulfil all three areas. This is not a simple task however, since all companies in the industry are focused on increasing their profit margin, which commonly leads to a negative impact on all three pillars.

Figure 1.1: The Sustainable Development Goals created by the UN [12].

The depletion of natural resources is one of the main issues towards which the transport sector directly contributes. This is particularly due to the current dependence that the majority of vehicles have on fossil fuels, thereby affecting all three pillars. The legislations and goals set by both the EU and the UN however, forced innovation in

this sector to help in remedying these problems. Such advancements include the newly developed diesel engine by Bosch [13], which set an industry standard of 50 per cent efficiency, and the implementation of an electric drivetrain in Volvo [14] buses which is claimed to reduce the energy consumption by 80 per cent, when compared to conventional diesel buses. By being able to abide by all obligatory regulations, companies not only avoid fines being imposed but can also use their sustainability improvements to their marketing advantage, usually referred to as 'Green Advertising', i.e. pleasing stakeholders whilst also contributing to an increased number of sales [15].

For the purposes of this study, it is of paramount importance to mention that the current improvements regarding heavy vehicles mainly focus on the drivetrain. Although these abide by regulations and sustainable goals which emphasise the efficient use of resources, more specifically goals 7, 9 and 11 outlined in Figure 1.2, none focus on the BPS [10, 16]. While it cannot be guaranteed that improvements in this area will yield the same savings as those aforementioned, improvement in this sector cannot be overlooked. Indeed, it is evident that there is a lack of information in this area, whilst it is also known that all pneumatic systems are highly inefficient. Consequently, such information should incentivise further research within this sector since any achievable gains would still hold irrespective of the type of drivetrain being utilised by the vehicle.

1.2 Research Aim and Objectives

It can therefore be noted that the two major problems that plague BPSs refer to their inefficiency and restricted available knowledge within this area. Consequently, this study aims to further enhance comprehension of such set-ups via appropriate experiments with a view to understand the effects that leaks and faults induce on the system. Consequently, this would eventually lead to identifying factors which would help in better recognising and quantifying these fault sources, leading to more advanced monitoring systems for BPSs. Furthermore, through such actions, the study would contribute in improving the efficiency of such set-ups.

To be able to fulfil these aims, a set-up was designed and fabricated, building upon two systems by M.Borg [17] and K.Abela [18], which had previously been developed, and which contained the majority of the pneumatic and monitoring equipment, for a

BPS. This set-up was used to perform simulations in order to collect the required data to better comprehend the behaviour of a typical BPS, together with the effects implied by different types of faults. Additionally, through the literature review performed, a better understanding was achieved with regards to both literature findings relating to this area and also market research which helped in identifying current improvement efforts in this sector. In order to further extend the knowledge towards BPSs, whilst also identifying the real-life sustainable effects imposed by these systems, actual bus data was also collected. This was deemed crucial so as to confirm the legitimacy of the data being collected for the BPS via the test bed data, whilst also making it possible to establish real-life effects compounding these systems.

In order to maintain a structured approach to this research, the research method by C.R.Kothari [19] was adopted, as outlined in Figure 1.2. Although this entailed various steps, the structured manner by which it was presented made it possible to employ a holistic process by which each step would contribute towards the completion of the study.

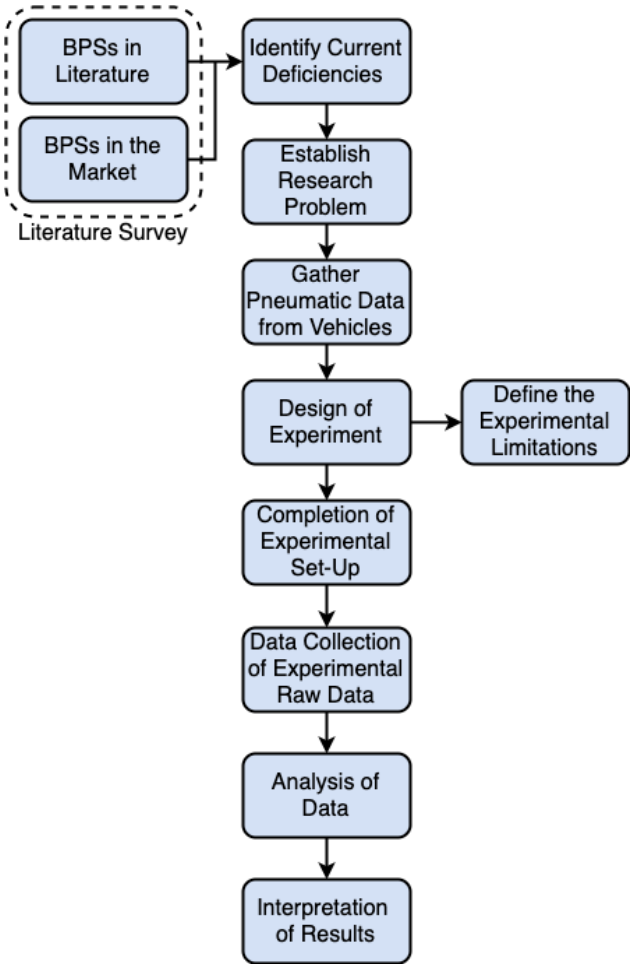

Figure 1.2: The steps adopted from C.R.Kothari [19]*, used to complete the study.*

Ultimately, the main aim of the study is to support the development of better monitoring systems catered for BPSs, hence contributing to a cleaner and more sustainable transport sector. The new knowledge generated from this study would also incentivise further research and knowledge generation in the field of BPSs.

1.3 Project Overview

This chapter introduced the BPSs and the aims rationale of the study. To this effect, Chapter 2 gives an overview of the key elements compounding pneumatic systems in buses. Based on this, Chapter 3, provides a thorough literature review with a view to provide the reader with a better understanding of the current knowledge in the field of BPS research and also report any advancements available in this industry. Chapter 4, presents the research gap and research problems which will be addressed throughout the remainder of the study. Moving on to Chapter 5, actual pneumatic bus data is collected in order to further comprehend the performance of a typical BPS. This data was used to establish the benchmark performance of such a set-up. In this light, Chapter 6 presents the experimental design so as to scientifically answer the research questions. Furthermore, Chapter 7 factually analyses the experimental data, whilst also establishing real life repercussions of BPSs. Finally, Chapter 8 concludes this study by summarising the main points which emerged from the collected data, together with realising future work potential and some concluding remarks.

Chapter 2- Compressed Air in Vehicles

This chapter provides an overview of Compressed Air Systems (CAS) utilised in the automotive industry, more specifically, in buses. Information includes knowledge regarding the working principles of such set-ups, together with the most frequently used end effectors in such vehicles. In turn, this will make it possible to comprehend these type of systems, therefore paving way to understand the literature review and state of the art presented in the following chapter.

2.1 Overview of Pneumatics in the Automotive Industry

CA is considered to be a vital form of energy storage, used in various applications depending on the industry [4]. In heavy vehicles, CA has always been utilised to power end effectors, such as the sliding doors and the air suspension, amongst others. In the last decade however, efforts in the automotive sector were also made to try and utilise this energy source to power the drivetrain of vehicles. The principle of how such a system works is that CA, which is stored in the vehicle's air tanks, is released at high pressures into the engine and subsequently converted into mechanical energy to the wheels, thereby moving the vehicle. On paper, this principle was quite a good concept and it was initially well received in 2012, since, these do not emit any toxic emissions, such as greenhouse gasses [20].

Despite this, although major companies, such as Tata [21], have developed various prototypes, currently none have been introduced into the market. This is due to the fact that although no emissions are emitted whilst the vehicle is in use, the production of CA is quite an energy intensive process thus, accounting for more CO_2 emissions than electric and fossil fuelled vehicles [22, 23]. Furthermore, it is also claimed that these type of vehicles emit up to 2.6 times [20] more greenhouse emissions per mile than the mentioned counterparts. Due to these shortcomings, the main application of CA in heavy vehicles, such as buses, has remained to power the auxiliaries and for this reason, this study will focus on CAS in heavy vehicles.

In principle, all CAS operate in the same manner, i.e. by making use of two main subsystems: the supply and demand subsystems, as shown in the illustration in Figure 2.1 [24]. These work conjointly to impart and convey CA throughout the entire system by making use of four different stages, as follows [24, 25]:

Supply Side Subsystem:

1. **Compression generation stage**: CA is generated by using compressors, which convert energy into CA, in conjunction with equipment, such as air inlet filters.
2. **Conditioning of CA stage**: By using adequate equipment, including pressure regulators, filters and dryers, the CA is filtered and adjusted to the required pressure to satisfy the requirements needed at specific points.

Demand Side Subsystem:

3. **Compressed air distribution stage**: The CA is conveyed to different points by using adequate pipes, fittings and valves, which are also strategically placed before the point of use.
4. **End usage stage**: Work is performed as a result of the pressure difference in the CA. The end use differs according to the application. In the case of heavy vehicles, CA is used to actuate various auxiliaries, such as the air suspension via the air bellows and the sliding doors via the double acting actuators, amongst others.

It is worth noting that in this study, focus will be made on the demand side subsystem of heavy vehicles, rather than the supply side.

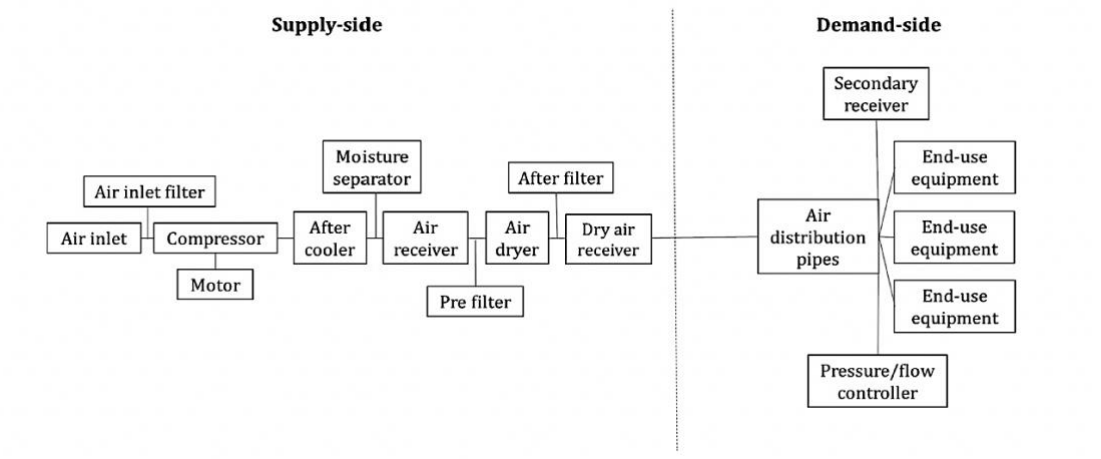

Figure 2.1: An overview of two main subsystems of a typical pneumatic system [24].

2.2 Main End Uses in the Automotive Industry

Upon analysing various systems, it became apparent that apart from pneumatic systems, there are other methods which may be adopted to actuate end uses. An example of this is by making use of electrical drives, such as the one shown in Figure 2.2 [26], which are utilised in Mercedes and Ford vans to operate their sliding doors [27].

Figure 2.2: The electrical drive used to operate the sliding doors [26].

Despite this, pneumatic systems are still preferred by automotive manufactures, including MAN [1], to power heavy vehicles' auxiliaries. The main reason for this is that overall, they are more resistant to outside elements and vibrations, making them a more durable option. This is especially the case because they have fewer moving parts, as compared to their electric counterparts, making them less prone to failure. In addition, the number of components required for pneumatic systems is less since each constituent utilises the same CA source. This is not the case for electric actuators, since each auxiliary works separately, hence requiring separate wiring looms. Finally, pneumatic actuators also allow the manufacturers to cap their actuation force, which is usually set to around 100 N [28]. This is particularly important for the sliding doors as it reduces the occurrence of injuries. Although it is possible to cap the force using the electric counterparts, the system is more complex since mechanical linkages would need to be utilised, making the system more bulky and less reliable. Furthermore, the pneumatic solution also offers an extra layer of safety since it is always possible to exhaust the system in the case of a malfunction whereas this cannot be done whilst using the electric counterpart [1–4].

In buses, the three most common end uses are the following:

- **Air suspension**: maintains and alters the vehicle's ride height by adjusting the bellows, whilst increasing the ride comfort by diminishing road vibrations and aiding to support the vehicle's weight.
- **Air brakes**: make the vehicle slow down by actuating the brake disks.
- **Sliding doors**: open and close by actuating the pneumatic actuators.

To operate, all of the auxiliaries, CA is required. In buses, this is achieved by using an engine driven compressor. Since the engine is directly coupled to the engine and so, is continuously running, a mechanical governor is used to control the compressor by monitoring the system pressure, thereby determining when it is in the loading or unloading phase. In the former scenario, CA is supplied into the system, whilst in the latter, the air is exhausted to the atmosphere. Generally the loading phase is triggered

when the pressure at around 6 bar and the unloading phase is triggered when the pressure of around 8 bar [29, 30]. To better understand BPSs, Figure 2.3 illustrates the layout of a typical BPS. The process commences with the compressor, which is directly coupled and driven by the engine using belts or gears, to produce CA at the desired 8 bar pressure. This CA is then conditioned via the air filter and dryer, to be stored in various supply tanks, which then provides the CA for all the end uses. As seen in the figure, the end-effectors comprise of 6 suspension bellows, three double acting actuators and 6 brake chambers [30–32].

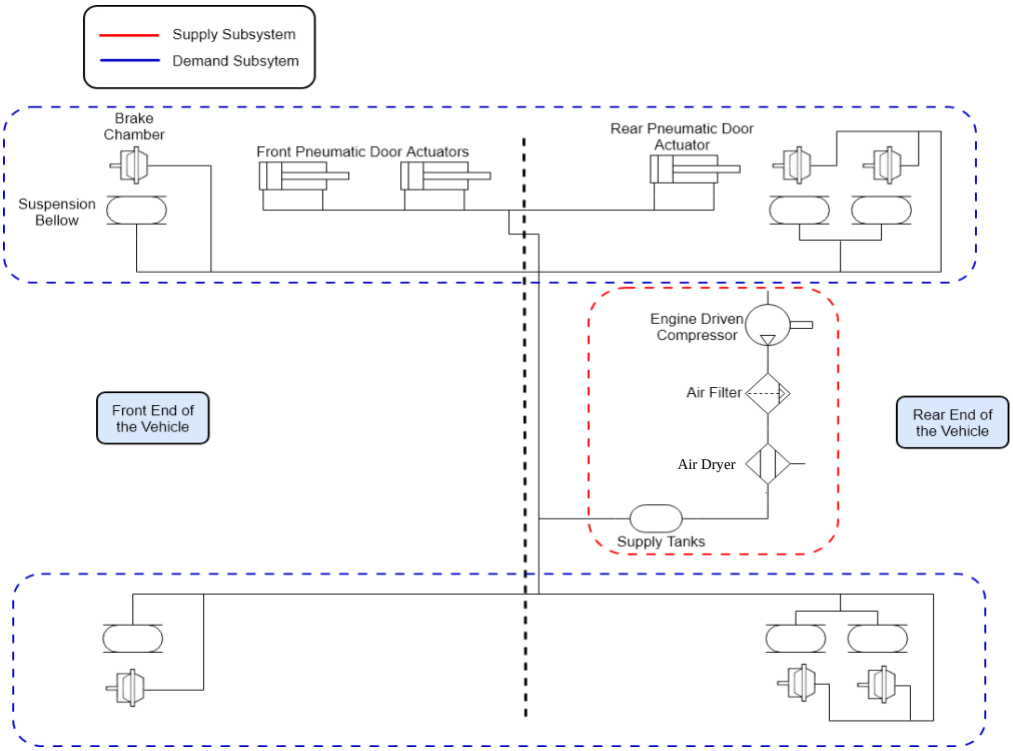

Figure 2.3: A basic illustration of a typical BPS.

2.2.1 Air Suspension

One of the main elements of BPSs is the air suspension and as aforementioned, it is tasked to support the weight of the vehicle whilst also mellowing down vibrations. Apart from making it possible to adjust the height of the vehicle, another advantage that these systems offer over the conventional spring counterparts is that they can produce considerably lower frequencies, resulting in a less stiff ride. To give perspective, typical spring set-ups have natural frequencies between 2 to 5 Hz, whilst air suspension set-ups have frequencies of around 1.5 Hz [33]. The working concept for how the ride height can be adjusted mainly comprises of the bellow and the levelling valve. The bellow inflates or deflates in order to adjust the height of the vehicle which is made possible due to the flexible rubber material construction,

allowing it to expand or retract on demand. Such constituents needs to withstand a considerable amount of force in order to support the vehicle, which can amount to an excess of 14 tonnes [34]. Therefore, these are usually 260 mm in diameter and are able to support loads of around 3.5 tonnes, at the 8 bar system pressure [35]. The levelling valve however, is responsible for controlling when the bellow inflates/deflates, to achieve the desired ride height. This is made possible by regulating the flow of CA into or out of the bellow. To better comprehend this set-up Figure 2.4 [5] depicts the air suspension set-up.

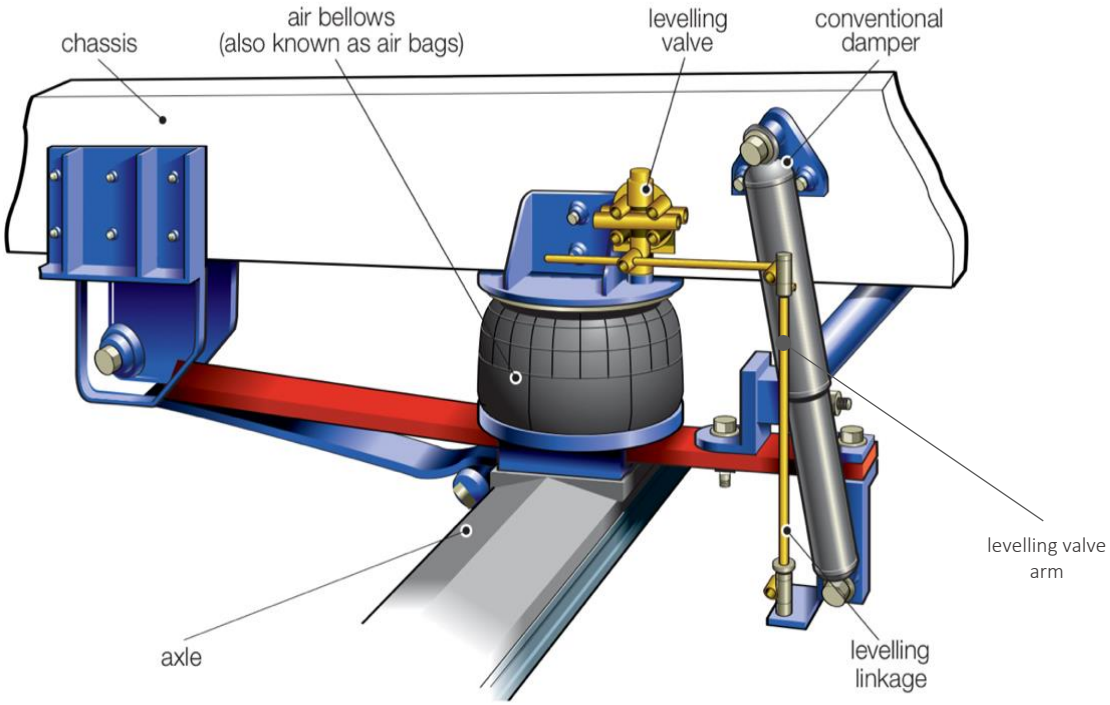

Figure 2.4: A typical suspension set-up of a heavy vehicle [5].

Although modern buses are virtually all classified as low-floor vehicles, where their step-down height from the bottom step to the ground is 300 mm, as compared to 350 mm found in high-floor vehicles, it might still be difficult for passengers to enter or exit the vehicle [36]. For this reason, the air suspension set-up is also responsible for the kneeling function. As the name implies, this function is performed when the

Figure 2.5: A bus kneeling [37].

bus kneels to one side, making it easier for people to enter the vehicle, as shown in Figure 2.5 [37]. To make this possible, the bellows deflate from the ride height setting (around 350 mm) to the kneeling setting (around 250 mm), as illustrated in Figure 2.6 [38]. This feature is standard in modern buses and works by using a separate kneeling valve to reduce the boarding height to around 200 mm [39–41].

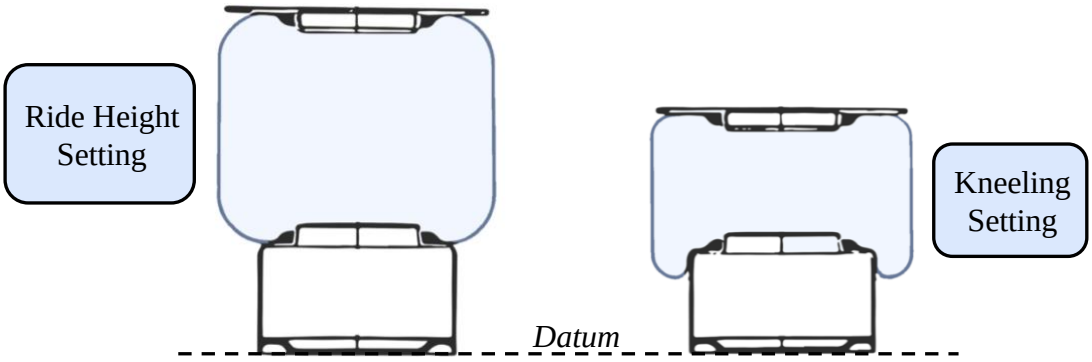

Figure 2.6: An illustration of a bellow during the ride height and keeling settings [38].

2.2.2 Air Brakes

Due to buses' heavy weight, a system had to be developed to be able to offer large braking forces, in excess of 6 kN [42], to adequately stop these types of vehicles. Consequently, air brakes were designed to address this issue, whereby these work using the same principles as their hydraulic counterparts, with the main difference being that they use CA instead of hydraulic fluid in order to actuate the brake chambers. The main advantage that these types of brakes have over the conventional set-ups is that they offer additional safety. This is because whilst a leak is induced, the air compressor can compensate for the loss of pressure until the problem is resolved, making it possible to brake the vehicle [43]. This is not the case for hydraulic systems however, which become less responsive when a leak occurs, due to the resulting pressure drop. Additionally, modern buses are also equipped with multi protection valves attached to the air dryer, which isolate faulty brake circuits, helping to prevent total braking failure [28, 42].

2.2.3 Pneumatic Sliding Doors

Typically, double acting cylinders, such as the one in Figure 2.7 [44], are used in vehicles to enable the doors' sliding movement and this is done by using CA to retract or extend the actuator. For this application, such constituents are capable of supplying around 2000 N [44] at the supply pressure. This makes it possible to smoothly open

the doors, which weigh around 130 kg [45]. In order to supply this force, the bore diameter is usually around 60 mm, whilst the stroke is typically chosen to around 150 mm [28].

Figure 2.7: Typical double acting actuators used to operate the sliding doors [44].

That said, MAN [1] has recently introduced pneumatic door motors which are used instead of conventional double acting actuators. The working concept is quite simple, where the CA is used to actuate the pneumatic drive, which rotates the turning column and opens the doors, as shown in Figure 2.8 [46]. Although not a lot of information is provided by the manufacturer, it could be said that such a set-up makes the overall system considerably less bulky since the actuator itself is around half the size of a typical double acting actuator. In addition, all the sensory equipment utilised to determine the position of the door is integrated inside the actuator assembly, helping to make the overall set-up less bulky.

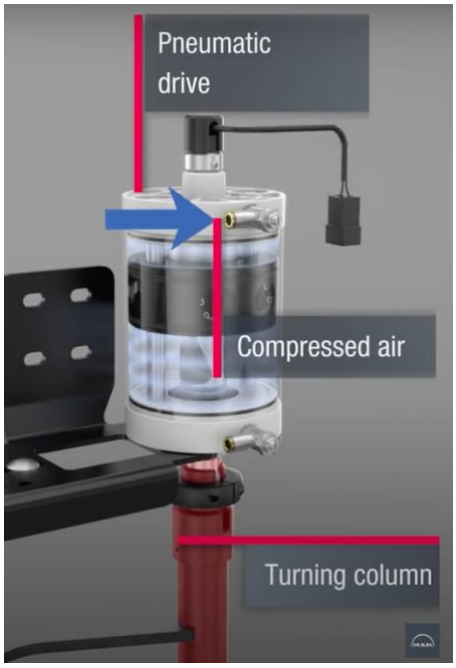

Figure 2.8: Newly developed pneumatic door motors by MAN [46].

2.3 Conclusion

The information in this chapter, is aimed at providing a better understanding of the working principles of pneumatic systems in heavy vehicles. This included a description of the most frequently used end effectors in this sector, mainly the air suspension, air brakes and the pneumatic sliding doors. Furthermore, by analysing other alternatives used to power such auxiliaries, the reason as to why pneumatic systems are still selected as the main actuation method is also highlighted.

Chapter 3-Literature Review Regarding BPSs

The purpose of this chapter is to better comprehend the state of the art of BPSs. In order to achieve this aim, this chapter reviews various literature sources, ranging from scientific papers to detailed market research. This review provides a deep understanding of this area, highlighting the type of systems used to diagnose BPSs and evaluate the environmental and sustainable impacts of faults in vehicle pneumatic systems, hence leading to identify a clear research gap.

3.1 Analysis of Current Literature Pertaining to BPSs

Before starting the literature survey, it was important to become familiarised with the information currently available regarding the study's area, mainly sustainability and monitoring of BPSs. Therefore, in order to search for these studies, the search tool 'HyDi', was used. To determine the holistic amount of research in this area, the first search was left quite open, with the search term being specified as *Pneumatic Systems* AND (*Heavy Vehicles* OR *Buses*) and the creation date set to 2010 and onwards. The number of retrieved documents was quite substantial with a total of 795 results. However, this included various subjects which were not relevant to this study, including material science and image processing. For this reason, the subject was then further specified to include relevant topics, such as engineering and technology, amongst others, which yielded a total of 471 relevant results. The source of these findings varied and included those highlighted in the pie chart in Figure 3.1.

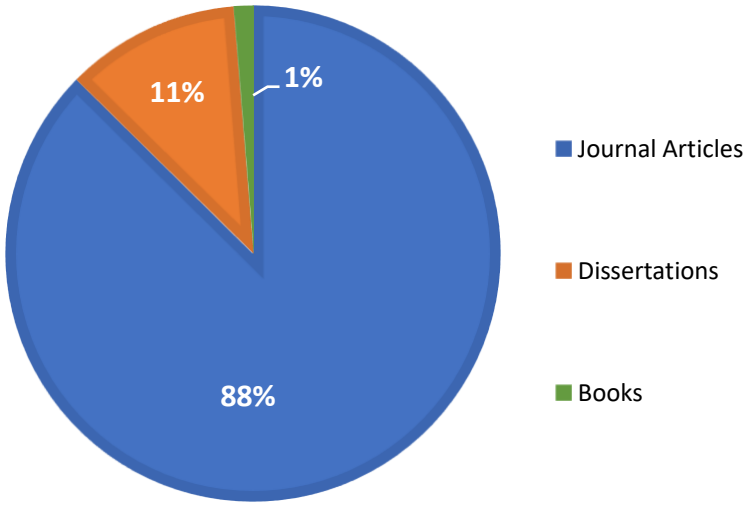

Figure 3.1: The different sources pertaining the findings for the first search.

By better understanding the information available, the next step was to start the actual search which provided literature which could be used throughout this chapter. This was done by further stipulating the resources area by also including the topics of sustainability and monitoring of BPSs. To do so, the research term was made more specific to narrow down the search results from the initial search. Therefore, the updated search term was updated to *Pneumatic Systems* AND (*Data Monitoring* OR *Sustainability*) AND (*Heavy Vehicles* OR *Buses*). As expected, the search yielded less results, where a total of 45 hits were obtained, which upon further inspection could be further narrowed down to 9. This showed that research regarding this area is limited and this will become more evident throughout this chapter. To give context, if the same search term was used but instead of specifying heavy vehicles or buses, the term industrial systems would be included, a total of 4,472 results would be obtained. By being able to perform the search process, which is summarised in Figure 3.2, the data available was better understood, making it possible to complete the literature survey found throughout this chapter.

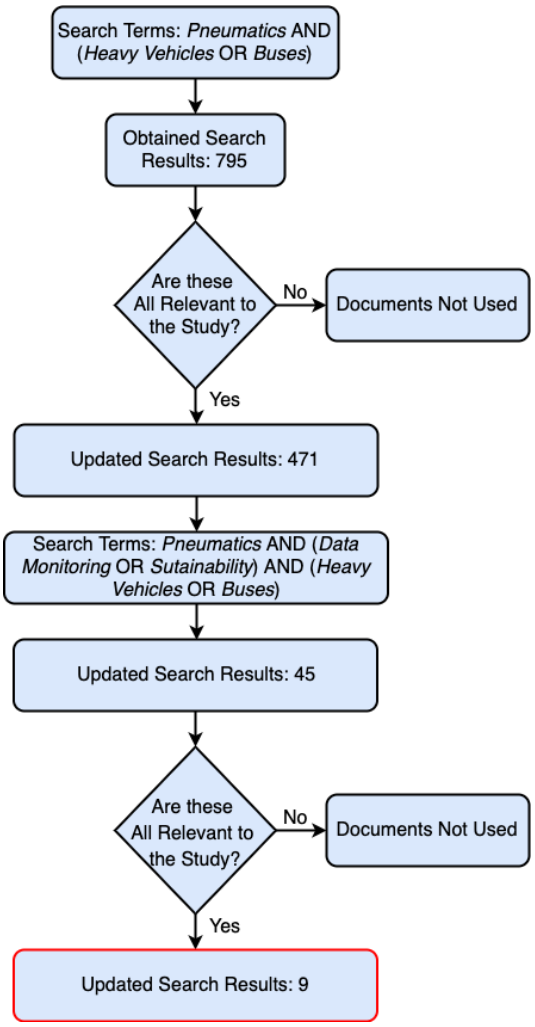

Figure 3.2: A summary of the literature search process.

3.2 CA Losses in BPSs

Despite having numerous advantages, all CAS have one detrimental aspect, which is that they are highly inefficient and thus being quite costly to operate. BPSs are of no exception as highlighted in the research carried out by D.Tretsiak *et al.* [5], where it was concluded that a typical electric compressor, used for hybrid buses, consumes around 24 per cent of the vehicle's electrical energy, as shown in Figure 3.3. Additionally, research in the industrial sector further confirms this aspect since according to multiple studies carried out on industrial CAS, it is claimed that such set-ups are only capable of converting around 5 to 30 per cent [47, 48] of their total input energy into an effective output. This could be attributed to the various losses that CAS frequently possess, which in the case of BPSs are mostly pertaining to the end usage stage in the form of leaks, making the system inefficient. It is also worth mentioning that the pneumatic auxiliaries found in buses, mainly the air suspension, cylinders and brakes are constantly utilised on a day by day basis. Therefore, their effects are imposed throughout a long time span whilst the vehicle is in operation.

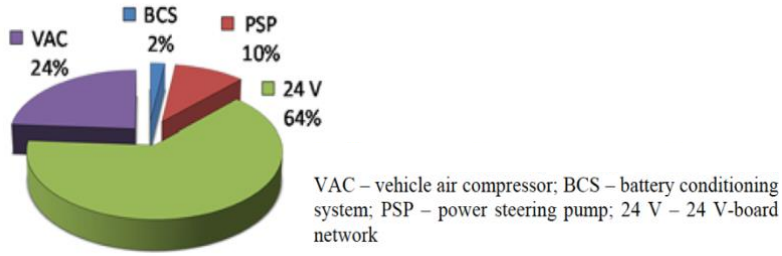

Figure 3.3: Breakdown of energy consumption of the vehicle [5].

In addition, it is also known that heavy vehicles, including buses, are major contributors to emissions. In a study completed by the EU, it was highlighted that 27 per cent [11] of emissions from the transportation sector, are a result of these type of vehicles, as show in Figure 3.4.

Figure 3.4: The breakdown of transportation emissions according to vehicle category [11].

These emit a variety of emissions, predominantly greenhouse gasses, such as CO_2, which directly contribute towards global warming and NO_x gases, which can cause serious illnesses, such as lung infections [49]. In Malta, these emissions have devastating impacts, where it is estimated that they account for around 500 premature deaths annually [50].

Currently, efforts are being made towards improving sustainability in the automotive sector and this is mainly evident by the new directives being issued by the EU, which focus on the reduction of CO_2 and NO_X emissions. One such directive is the New Vehicles Directive [51], which imposes that by the year 2030, 33 to 66 per cent of public buses need to encompass low emission drivetrains, meaning that they have to use other alternatives to fossil fuels, such as hydrogen or batteries. These efforts are proving useful since between 2017 and 2018, NO_x emissions have dropped by 4.1 per cent [52] in European member states. Locally, Malta Public Transport also proposed plans to integrate solar panel technology within its bus fleet [53]. It is claimed that this system will help in reducing fuel consumption by around 10 per cent annually, directly contributing to a reduction of around 2,700 kg of CO_2 emissions. Despite these improvements, research regarding BPSs is still quite restricted. However, it is known that in industrial systems, demand side improvements account for up to 70 per cent [54] of the total CA improvement potential, which is why this study mainly focused on the demand subsystem. As a result, this should give incentive for further research in pneumatics in the automotive sector, such as this study, helping to better understand these systems and improve their sustainable performance.

3.3 Investigation of Losses in BPSs

As discussed in the previous section, CAS are quite inefficient, and in BPSs this is mainly due to leakage losses. In order to further understand the repercussions that these losses have with regards to this sector, this section will further investigate these losses.

3.3.1 Leaks

One of the main reasons for CAS being so inefficient is the presence of leaks, which also lead to further losses, such as the drop in system pressure [55]. These can be a result of various aspects, including faulty components or piping leaks, which will be discussed in further detail throughout the study. Whilst it is difficult to identify leaks,

one of the common methods for detecting them is to pinpoint any audible hissing noises. Indeed, such noises are also claimed to cause health problems, including high blood pressure and hearing loss, amongst others [56]. However, this is considerably difficult and unreliable since this technique is highly dependent on how loud the external noises are [55]. In addition, if the leakage size is small the noise will not be audible, especially for heavy duty vehicles. For instance, a leak of 0.5 mm at a pressure of 6bar, results in a hissing noise of 36 dB [18]. In buses, this can be considered negligible due to the fact that modern diesel engines operate at higher noise levels of around 79 dB [57, 58]. In the industry, devices such as handheld ultrasonic air leak detectors shown in Figure 3.5 [59], are commonly used to pinpoint such leaks. These work by detecting high frequency noises generated by the fault. This not only makes the overall process easier but it is also makes it less phased by the ambient noise [60]. Although such devices help in locating the leaks, these are still not commonly used in the automotive industry. This is due to the fact that pneumatic systems found in heavy vehicles are very compact, hence making it difficult for the operator to manually manoeuvre through the whole set-up with the device [61].

Figure 3.5:A typical ultrasonic air leak detector [59].

In order to further understand the shortcomings that these leaks impose on BPSs, one has to quantify their effects. However, this information is not currently available due the lack of current information regarding this particular application. Nevertheless, to better grasp their consequences, industrial CAS were reviewed, with a view to help in further comprehending BPSs. One of the first indications that a system exhibits whilst it is exposed to leaks, is that the compressor's demand is drastically increased due to the additional work required to compensate for the pressure drops. This is supported by the research by Abdelaziz *et al.* [55], claiming that these loses can make the compressor waste its output by 20-50 per cent. R.Dindorf [62] also states that leaks are considered to be the preliminary source of losses, where these can make systems reduce their efficiency by 30 per cent. To further quantify these effects, an experiment was conducted on a shop floor by FESTO [63], where it was concluded that a system

operating at 8 bar and containing a 2 mm leak, resulted in an additional €3248 in annual electricity costs, translating to an additional 160 MNL of CA. Additionally, K.Abela [64] also investigated leakages in pneumatic end effectors, more specifically in double acting actuators. The investigated leak was caused by one of the seals due to wear and tear. As the name implies, seals are used to create a closure between the cylinder bore and the piston, with Figure 3.6 highlighting some of these seals. By performing multiple simulations it was concluded that this seal leak, which was estimated to be between 0.5-1 mm in diameter, would contribute to an additional 34 per cent of CA consumption. Furthermore, the research performed by K.D.Prajapati *et al.* [65] also states that this type of wear consumes 67 per cent of the total energy required to power an actuator.

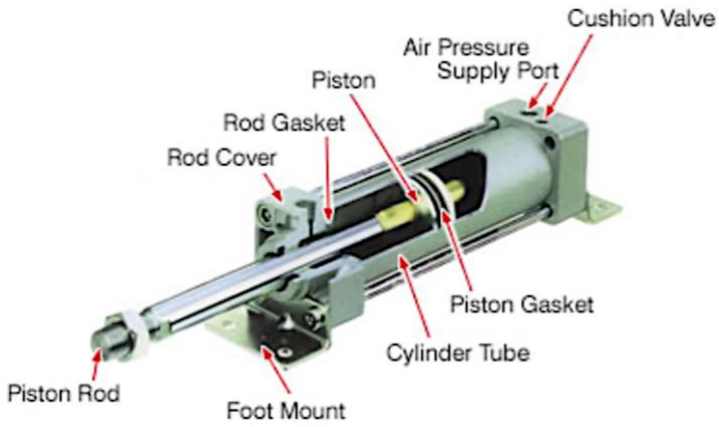

Figure 3.6: A cross-section of a typical double acting actuator [117].

In buses, leaks not only contribute to an increase in the compressor's output but will also increase the engine's demand since these are directly coupled together, as discussed in *Section 2.2*. Although the effects have not yet been documented, the increase in the engine's demand directly contributes to more fuel being consumed and emissions emitted. In the industry, the emission by-product was investigated in the same study by K.Abela [64], where leaks were induced to be able to determine how an industrial based system would react to them. Ultimately, it was established that whilst the system was running at 6 bar with a 1.5 mm leak, an additional 1.77 tonnes of CO_2 would be emitted annually which equates to an increase of 64 per cent. It is also good to mention that this figure is highly dependent on both the method and efficiency of the power station in question, since these affect the overall carbon footprint of the power station.

Furthermore, CA leaks in the automotive industry have also resulted in safety hazards, directly affecting braking performance. This is because, although modern vehicles come equipped with multi protection valves, as stated in *Section 2.2.2*, these still do

not entirely prevent the occurrence of brake delays. Consequently, this can result in devastating impacts with one such example being an accident which occurred in Pennsylvania, where an air leak led to delays in braking, resulting in one casualty [66]. To further investigate this issue, S.Ramarathnam *et al.* [67] performed a study dedicated to finding the effects of leaks on the braking performance. It was concluded that the issue caused by leaks was that although the vehicle still brakes, the pressure inside their brake chambers takes more time to build up, inhibiting the system from reaching its intended pressure therefore, contributing to an increase in the vehicle's stopping distance. This was clearly exhibted in the performed simulations, where a bus containing a leak of an unkown size was made to travel at 60 mph and to brake abruptly. The results showed that the stopping distance was increased by 2.7 m due to a 0.1 s lag of pressure build up, with the results shown in Figure 3.7. Currently, no additional studies could be found which further investigated the impacts of leaks in the braking system. However, these findings highlighted the detrimental effects that leaks can impose on the vehicle's safety.

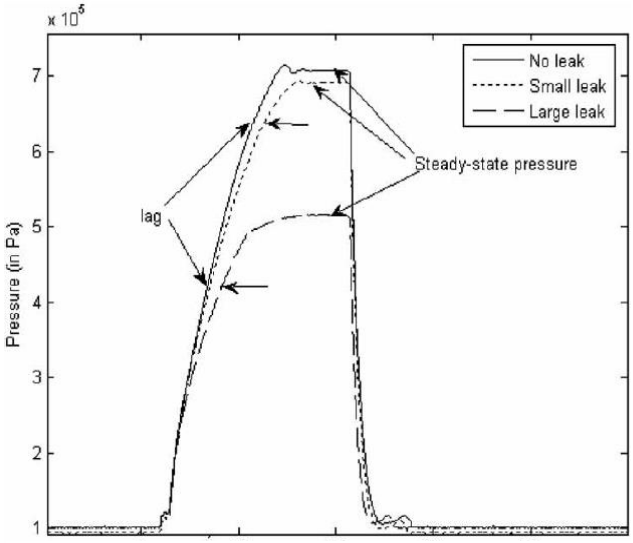

Figure 3.7: The results for the experiment showing a drop in pressure whilst leak is induced [67].

3.3.2 Lack of Maintenance

The upkeeping of equipment is key to extend its lifetime, whilst also preventing the occurrence of faults, such as leaks. In BPSs, this is no exception although it is common for companies to turn a blind eye to maintenance. The main reason for this is that maintenance causes a considerable amount of downtime. It is estimated that for transit buses, maintenance costs are the second highest expense category, which accounts for 21 per cent [6] of the overall operational costs. Just to give perspective the overall consumables used in a vehicle, including fuel and oil, account for around the same cost percentage. However, this is still not a valid excuse to deter from performing adequate maintenance procedures, since as aforementioned, this not only reduces the overall efficiency of the system but may lead to safety hazards.

As described in *Section 2.2*, air filtration is an essential aspect in the generation of CA since it prevents any unwanted debris from entering the system. This is especially important in the case of buses since these vehicles are continuously exposed to different types of debris, such as sand, with the latter causing a considerable amount of damage since it can easily ingress inside different equipment whilst also being insoluble. Failure to upkeep this system and to follow the service interval specified by the manufacturer, results in leakages in the supply side subsystem which is mainly due to the corrosion caused to the filter housing assembly. This is due to the fact that the metal housing making up this component is exposed to the elements and starts to erode over time, accelerating the corrosion process. Another common mishap is that the air filters are not correctly seated into their housing which also allows CA to leak. In turn, this not only increases the compressor's demand, directly contributing to an increase in the vehicle's fuel consumption and emissions, but it will also increase the overall downtime during its daily service. This is due to the pressure drop caused by the leaks, which prevent the system pressure to build up to the desired 8 bar setting [28]. According to the Ministry of Transportation in Ontario, it is estimated that leakages can result in pressure drops of up to 2.8 bar every 10 minutes [30]. Such drops in pressure inhibit vehicles from resuming their journey since modern vehicles are inoperable until the required pre-set pressure is reached [28].

Moreover, the demand side subsystem is also affected by leaks if proper maintenance intervals are not kept since, as discussed in the previous section, auxiliaries, such as the double acting actuators for the doors, are prone to seal wear. This type of wear is principally caused due to friction where it is estimated that seals receding in these components are exposed to copious amounts of friction, generally amounting to 90 per cent of all friction in such components [68, 69]. Seal wear also prevails by vibrations, which are frequently encountered in buses due to road irregularities. This wear may not only cause the development of air leaks but may also cause components to stick-slip, where the constituent is not able to actuate smoothly due to sudden jerks [70, 71].

In order to try and prevent injuries whilst maintaining bus pneumatic components, various standards have been introduced, specifying instructions on how to safely repair them. This includes ISO 3583:1984 [72] which specifies the user on the correct pressure levels that air brake connections should possess. Such instructions however, only prevent injuries if the maintenance intervals stipulated by the manufacturers are

observed, averting catastrophic component failure [73]. Unfortunately, this is not always the case and one common area where maintenance is often lacked is the air suspension bellows. Due to copious amounts of wear and tear that bellows experience, they tend to rupture over time, reducing the vehicle's suspension ride height. When this occurs during service, maintenance personnel often try to quickly remedy the problem by replacing the bellows roadside, instead of towing the vehicle back to the workshop. This means that in some instances, not all the necessary precautions are taken, such as fully de-pressurising the system. As a result, these disregarded actions can result in the bellows to blow, causing bodily harm [74].

3.3.3 Synopsis of Losses in BPSs

Despite not being able to find a vast amount of information relating to this sector, it could still be noted that the main culprit for pneumatic losses in these vehicles are leaks, affecting both the supply and demand subsystems. Their effects mainly contribute to an increase in the fuel consumption and excess emissions. The lack of safety was also a by-product of the mentioned leaks where the vehicle's braking performance was considerably hindered, whilst also making repairs more dangerous. One of the main reasons as to why these leaks prevail is due to lack of maintenance since companies opt to overlook them due to their incurred costs and downtime, resulting in bigger and more substantial leaks.

3.4 Energy Saving Techniques in Automotive Pneumatic Systems

In order to rectify the losses confounding pneumatic systems to improve the system's performance, it is important to be able quantify the losses. To make this process easier, various techniques and equipment have been designed for use with CAS [18, 60]

The first step towards rectifying prevailing losses is to be able to identify them. To do so, specific parameters have to be monitored in order to identify the performance of the particular system. Some commonly monitored parameters in CAS are system pressure, electrical consumption and CA flow rate. These make it possible to have a good overview of the performance of several subsystems compounding the entire set-up [18, 60]. In order to observe these parameters, adequate sensory equipment is

required to log them. Table 3-1 [60] compiles the relevant measuring device required to monitor the mentioned parameters.

Table 3-1: Typical parameters used to measure the performance of CAS together with their respective measuring device [60].

Parameter	Measuring Device
Pressure	Pressure transmitter/ gauge
Electrical consumption	Power Meter
Air flow rate	Air flow sensor

Typically, measuring devices, such as multimeters, have been quite basic and had limited functions. In recent years however, more advanced data logging systems have been introduced on the market which are capable of remotely monitoring and logging parameters at specific time increments. An example of such device is the KEW 6305 Power Meter by Kyoristu, shown in Figure 3.8 [75]. As the name implies, it is capable of logging the system's power in real time whilst also having additional features, including an automatic wire checking function, amongst others.

Figure 3.8: The Kyoristu KEW 6305 Power Meter [75].

The use of this equipment makes it possible to use other methods to be able to further monitor and improve the performance of these systems. Throughout the remainder of this section, these methods will be reviewed and examined in further detail.

3.4.1 Audits and Assessments Relating to BPSs

Although it is possible to monitor the system's performance by solely using monitoring equipment, it is not always fully effective in achieving the required improvements. For this reason, audits can be used in conjunction with recorded sensor data, to methodically monitor and analyse the system's or its subsystem's performance in further detail. By doing so, one would be able to determine any encountered trends which may not always be as evident [60, 76].

In order to ensure that a proper audit is performed, various standards have been formulated which guide the user on how such a procedure should be performed. With regards to pneumatic systems, the standard ISO 11011:2013 was specifically formulated for CA audits. This standard gives a guide on how to:

- Set requirements for conducting and reporting the results for the entire system;
- Divide and analyse the CA system in terms of both the supply and demand subsystems;
- Identify energy saving opportunities, together with the documentation of any relevant savings;
- Establish the responsibility and roles required to implement the saving opportunities.

Furthermore, another standard relevant to monitoring CAS is ISO 50002 [77], which gives guidance on how to perform an energy audit, where various principal requirements are stipulated on how to adequately perform such a task. In a typical energy audit, the aim of performing such a procedure is to:

- Determine the current energy performance of the system;
- Identify adequate energy efficient approaches;
- Designate and delineate the findings.

Keeping in theme with energy audits, the main ones found relating to buses were audits for bus organisations which investigated the financial and environmental aspects emerging from changing the drivetrain. Two such assessments were conducted, one by A.Thiruvengadam *et al.* [78] and the other by Volvo [79]. The audit performed by the former focused on comparing the performance of EURO 5 Cummins diesel engines equipped in buses, similar to those found in Maltese buses, to newer EURO 6 diesel engines. Eventually, it was concluded that by converting to the newer diesel engines, an average of 7.9 per cent [78] could be saved on both fuel consumption and CO_2 emissions. The audit performed by Volvo focused on converting the entire bus fleet in the city of Gothenburg from a fossil fuel based drivetrain to an electric one. After various tests, the results showed that the changes could contribute to €10.6 million in annual fuel savings, whilst also eliminating 33,000 tonnes of CO_2 emissions, offsetting the emissions of 3,000 Swedish households [79].

In order to realise the potential that energy audits can have on improving CAS, audits for industrial applications were also reviewed where Shanghai [60] claims that in industrial applications, these type of audits are capable of saving up to 50 per cent of the energy used. A good example of this is the audit performed by L.Caruana *et al.* [80] for Toly Products Malta, where improvements, such as leakage repairs, were done in conjunction with adequate calculations and tests. Ultimately, the energy savings reflected on the annual energy costs, claiming savings of around €4,000 throughout the entire factory. These enhancements also helped in improving the sustainability of the system, where it was also calculated that the mentioned arrangements resulted in 14.17 tonnes of CO_2 emissions being saved, translating to a reduction of 32 per cent.

Whilst reviewing audits which related to heavy vehicles, another type of audit was also found and therefore, to further enhance knowledge towards such vehicles, these were also reviewed [81, 82]. This audit could be classified as a performance audit, where public transport companies analyse and asses the performance of the overall service so as to perform any necessary improvements. In doing so, energy saving improvements were generally not considered. An example of these audits was the one performed by the National Audit Office [81] in 2020 where a thorough assessment was completed with regards to Malta's public transport service. Several factors were analysed, although the main ones relate to inspection parameters, such as tyre condition and infrastructure conditions, including bus cleanliness. However, none of the mentioned parameters included aspects regarding BPSs, such as specific maintenance intervals or ideal performance values, which suggests that this subsystem was not given attention. Ultimately, it was highlighted that the focus of this audit was to improve the overall service and reduce downtime, by streamlining physical inspections using an IT based shift for routine checks, via databases. This makes the overall process less prone to human error. Another performance audit was also performed by the Auditor-General [82] in Victoria Australia. Although focus was also made on improving the punctuality of the service, the approach taken to improve the service was different, where the main suggestion was to change the time tables for the bus routes, in order to make it possible to divide the demand of the passengers with nearby trams.

Recently, efforts have also been made to try and make the auditing process for heavy vehicles easier with an example being the service being offered by JRS Innovation

[83], which makes it possible to carry out audits specifically designed for these type of vehicles. This service entails making use of a smartphone application entitled 'Bus and Inspection & Maintenance', so as to construct custom checklists for the required audits, using intuitive flow charts. An example of such a flow chart is shown in Figure 3.9. Although this checklist can also be applied for BPSs however, it is currently difficult to do so. The reason being that the lack of information regarding the behaviour of such a system, considered essential to completing the audit, makes it hard to do so. All in all, it can be said that although not numerous, efforts are being made towards improving and facilitating the auditing process for the public transport sector. Furthermore, the potential improvements recorded in industrial applications should further incentivise the development of audits in vehicle CAS.

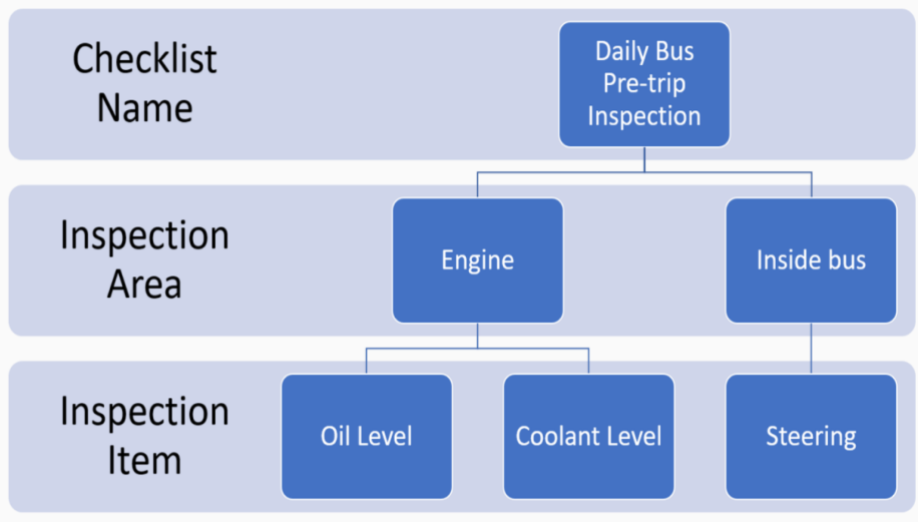

Figure 3.9: An example of the flow chart layout used to create a custom bus audit [83].

3.4.2 Key Performance Indicators for BPSs

To ensure that a system is operating at the required level or to further improve the system's, a benchmarking process can be performed. This process entails comparing the performance of the set-up in question to another one, which is known to operate at a correct standard [60]. This is done using Key Performance Indicators (KPIs) which are considered as performance measures. To give context, common bus related KPIs include the Maintenance Cost per Bus Mile, the Mean Distance Between Failures and the Fuel Consumed per 100 km [84]. In the automotive sector, it is difficult to develop KPIs, since information is often not made publicly available. This was documented in the report published by the Energy Sector Management Assistance Program [85], where it was also claimed that information, such as the buses' fuel consumption, is often kept secret, both to the general public and in some instances, even to the

company's employees and executives. Consequently, pneumatic KPIs related to the automotive industry could also not be found.

This aspect was also observed by M.Trompet [86], and his report further highlighted the lack of KPIs currently established for buses in the public transport sector. For this reason, work was carried out with bus organisations to perform a benchmark process, developing relevant KPIs to be used for audits in this sector. During the development of the new KPIs, various areas entitled 'Success Dimensions' were analysed and these highlighted the areas that the KPIs would be focusing on. These ranged from financial to environmental ones. The environmental dimension however, was overlooked by the bus organisations with focus given to other dimensions, such as the Customer Success Dimensions, which revolved around improving the overall service's reliability and punctuality. The reason for this was that focus was made on increasing the number of customers, rather than looking for ways of improving the sustainability of the BPS.

To better comprehend how typical KPIs are adopted within CAS, examples highlighting the optimal performance of industrial applications, were also reviewed. These included the specific energy consumption of a system, which should be in the range of 85-130 Wh/Nm^3 and the mechanical efficiency of power tools, which should be in the range of 10-15 per cent [64]. By having this information available, the user is able to adequately monitor the performance of the system. Benedetti *et al.* [87] also states that by using KPIs, improvements in industrial pneumatic systems can account for 20-30 per cent in energy savings. By considering the potential that these performance measures have, it becomes evident how beneficial it would be to develop tailor made KPIs for buses, more specifically for BPSs, making it possible to properly monitor their performance whilst performing any relevant improvements.

3.5 Current Efforts to Improve the Efficiency of BPSs

In order to improve the efficiency performance of BPSs whilst also remedying losses, such as leaks, studies and systems have been developed to try and improve upon these aspects. The improvements range from advancements in the auxiliary systems, to the development of sophisticated monitoring systems. In this section, these improvements will be discussed in further detail.

3.5.1 Energy Efficient Air Compressors

Although this study focuses on the demand side of BPSs, it was still deemed important to include some improvements residing in the supply side of these vehicles, mainly the compressor, in order to provide a comprehensive literature review of BPSs. Unlike in industrial applications, where it is possible for the user to size or change parameters relating to the air compressor to improve the system's efficiency, this is not the case for BPSs [60]. As a result, both WABCO [88] and Voith [89], have recently introduced newly developed engine driven air compressors which focus on further improving the efficiency of these systems.

The compressor by WABCO utilises an integrated clutch, which allows it to have on-off capabilities, meaning that whilst the compressor is in the off-loading phase, it can be completely switched off. This improvement promises fuel savings of 1000 L per 150,000 km [88], which translates to around 2 per cent of the annual consumption. Similarly, the compressor by Voith also utilises an integrated clutch however, it also makes use of the dual stage concept, meaning that that two cylinders are used for two separate compression stages. This means that in the first stage, the air is compressed to an intermediate pressure, whilst in the second stage, the air is compressed to the desired pressure. Figure 3.10 [89], highlights the difference in workloads between a single and dual stage compressor whilst the air is compressed. It is claimed that this set-up helps in reducing the overall annual fuel consumption to around 3 per cent which amounts to 1 L per 100 km [89].

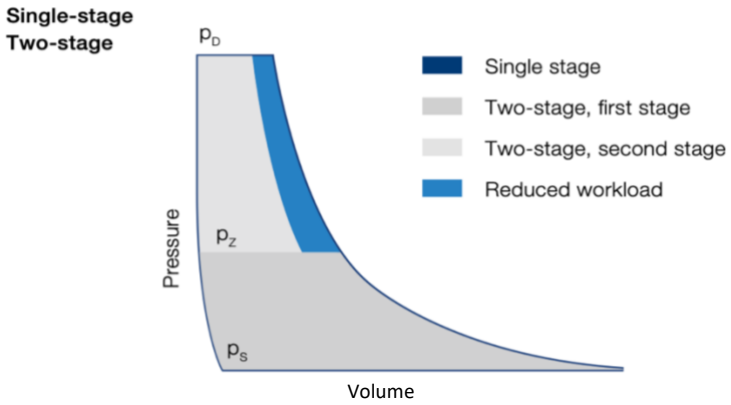

Figure 3.10: The difference in workloads between single and dual stage engine driven compressors [89].

3.5.2 Electrification of Sub-Systems

With technology advancing at a rapid pace, the concept of electrification has been quite popular in recent years. In vehicles, such as buses, this concept has been mainly

applied to their drivetrain, as highlighted in the audits in *Section 3.4.1*. However, further studies have been made towards electrifying specific subsystems, including in BPSs, with Steinert *et al.* [90] and Anderson [91] claiming that this is a promising solution to improve the vehicle's energy efficiency.

One such example is the set-up designed by M.Khodabakhshian *et al.* [92], where the air brake system in a hybrid bus was converted into an electromechanical one. The principle of how this works is by having a controller which is used to determine the required demand that the brake system has to provide, whilst also determining when to apply the mechanical and electrical brakes. By having an electric braking system, the vehicle would be able to slow down without using any additional energy. This is achieved by making use of magnets and slip rings situated in the vehicle's electric motors, which together offer enough resistance to automatically slow the vehicle down, whilst recuperating and storing energy. This phenomenon is called regenerative braking [93]. The results obtained during one test cycle are shown in Figure 3.11. From this data, it could be noted that the energy used by the electromechanical brake was negligible since most of the braking was done using regenerative braking, allowing the vehicle to slow down automatically. It was claimed that the system was able to save around 1.5 per cent [92] of vehicle's fuel. That said, it was also concluded that this was dependent on the driving style, since it was highly affected by the amount of braking being done. Apart from fuel savings, this also helped in making the vehicle safer since this braking set-up could be better integrated with the traction control system, offering better vehicle stability whilst driving.

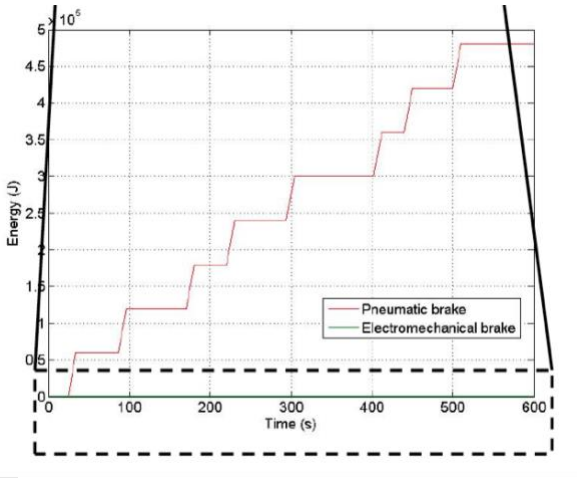

Figure 3.11: The results obtained whilst comparing the electromechanical set-up to the a pneumatic set-up [92].

Another pneumatic auxiliary which has been electrified is the air suspension system, more specifically the valves utilised. As described in *Section 2.2.1*, the adjustment in the vehicle's height is made by the mechanical levelling and kneeling valves. Although these are still utilised, modern buses make use of an Electronically Controlled Air

Suspension (ECAS) solenoid valve which encompasses the two valves in a compact package. Such a set-up also requires electric height sensors to determine the actual height of the vehicle, rather than using mechanical linkages. An example of this system is the one developed by WABCO [94], where it is claimed that equipped vehicles average a fuel reduction of 3 to 5 per cent [94].

In contrast to the previously mentioned electric conversions, the one designed by Vapor Bus International [95], is by comparison quite simple whereby they designed a retro fitting kit to replace all the pneumatic door actuators with the electromechanical motors found in Figure 3.12 [95]. No savings were mentioned however, these components do not use CA, thereby reducing the demand of the compressor. Consequently, less fuel would be consumed which also translates to less emissions.

Figure 3.12: The electromechanical motor used for the conversion of the pneumatic cylinders [95].

Although it can be noticed that various companies are pushing towards the electrification of these subsystems, one main disadvantage arises when adopting such set-ups. This is that a considerable amount of additional equipment and sensors would be required in order to perform these conversions. Therefore, it is good to point out that although such improvements help in improving the sustainability performance of these vehicles, it could also be argued that they make the maintenance process more complex due to the fact that additional equipment and sensors may become faulty overt time, hence contributing to an increase in the downtime of the vehicles [2–4].

3.5.3 Monitoring of BPSs

Leaks can be considered to be one of the leading causes of losses in pneumatic systems, whose effects range from additional fuel consumption to excess emissions. This gives incentive to address such faults, with R.Saidur *et al.* [76] also claiming that by remedying such problems in industrial applications, a 42 per cent increase in the system's sustainable performance can be achieved. In BPSs, this has not gone unnoticed, with one of the main efforts to try and mitigate these effects being to quickly identify them to reduce the maintenance downtime. Therefore, in this subsection,

detail will be given about the development of different systems which help in addressing this issue.

3.5.3.1 Manual Monitoring of BPSs

The process of finding and repairing leaks in CAS has always been difficult, due to fact that it is difficult to pinpoint the source of the fault. This is especially true in BPSs where the system is made as compact as possible in order to fit in the vehicle's footprint. As highlighted in *Section 3.3.2*, maintenance has often been deterred by companies in order to avoid the downtime associated with such repairs. To try and address this problem and make the overall repair process faster, the American Transport Association [96], recently released a checklist specifically catered for BPSs which contains common problems frequently encountered within these systems. Additionally, suggestions were also given on how to solve different types of issues. Some of these examples are shown in Table 3-2.

Table 3-2: A checklist specifically designed for CAS in vehicles [96].

Symptom: Air system is slow to build pressure	
Possible Cause(s)	**Suggested Action(s)**
Air system leaks	Perform leak-down test on air subsystems. Listen for audible source or use soapy water to isolate the leaks (chamber, valve, hose, etc.). Repair as necessary.
Compressor unloader malfunction	Follow compressor manufacturer recommendations for determining proper operation of compressor unloader.
Damaged compressor head gasket (reciprocating compressor)	An excessive leak around the head gasket may be caused by flow restriction downstream, a dead-headed compressor, malfunctioning governor or a defective/missing safety valve. Check for restrictions or faulty safety valve, and repair as necessary. Replace compressor.

In the case that the user is still not able to identify the source of the problem, monitoring devices and detectors can be used in order to locate the issue. The most common type of monitoring device is the hand held ultrasonic leakage detector described in *Section 3.3.1*, whose current design makes it difficult to use in buses, due to its size. WABCO [61] however, have designed a leakage detector specifically to counter this problem, which includes a flexible sensor, as shown in Figure 3.13, making it easier to reach tight spaces. To ensure

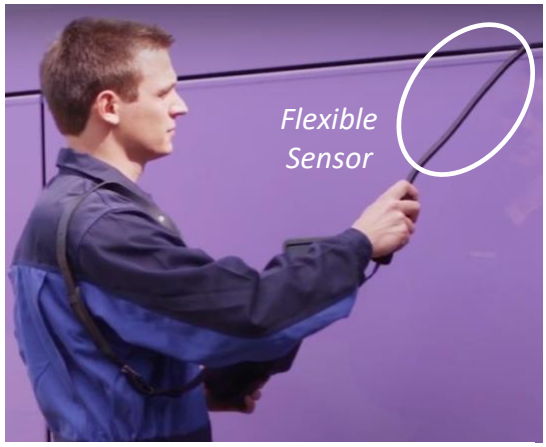

Figure 3.13: The ultrasonic leakage detector by WABCO [61].

that these devices are used correctly, the standard ASTM E1002 was also developed to guide the user on how to adequately use such equipment. In this standard, one finds detail on how these detectors should be calibrated, together with the correct approach on how to identify and estimate the size of a leak [80].

3.5.3.2 Remote Monitoring of BPSs

Although the methods mentioned in the previous section help in identifying leaks, they are still quite rudimentary and dependent on the personnel doing the repairs. Apart from this, with the increased number of sensors used in various pneumatic auxiliaries, systems are becoming more complex, increasing the potential of faulty components. This therefore, also contributes to an increase in the maintenance down time. In the automotive industry, this issue was addressed by automating the monitoring process however, the primary focus was given to monitoring the drivetrain of the vehicles. An example is the system designed by P.Killeen *et al.* [97], which catered for a bus fleet and was capable of monitoring drivetrain parameters, such as the coolant temperature and oil pressure. Furthermore, during the last decade such set-ups have also started to be optimised for use with the BPS.

One of the ways to develop such set-ups is to use existing sensors situated in the vehicle. For example, Volvo [98] utilised pressure sensors present in both the air suspension and air brake systems to be able to monitor them. By doing so, lights could be installed in the vehicle's dashboard, which triggered when the pressure significantly dropped, such as in the case of major leak [98–100]. An example of these lights can be seen in Figure 3.14, which include the warnings for the air brake and air suspension systems [98].

Figure 3.14: Anterior (left) dashboard warning for air brake leak and posterior (right) dashboard warning for air suspension leak [98].

That said, as highlighted in the study by A.Eriksson [99], these systems have one major shortcoming. This relates to the fact that although the system is capable of detecting the pressure loss resulting from leaks, it is mostly effective when these faults are significant, which is not always the case. For this reason, such systems will not be

triggered when the leak is small. Another shortcoming is that although the system informs the user when a significant leak is present, the location is still not known and it will be up to the maintenance personnel to determine its exact location.

To address the aforementioned problems, A.Eriksson [99] designed a system capable of monitoring the pneumatic system of a truck, which is very similar to a BPS, by again using pressure sensors built into the vehicle and a custom algorithm. The overall leak detection process was quite complicated, which can be summarised by the three steps in Figure 3.15.

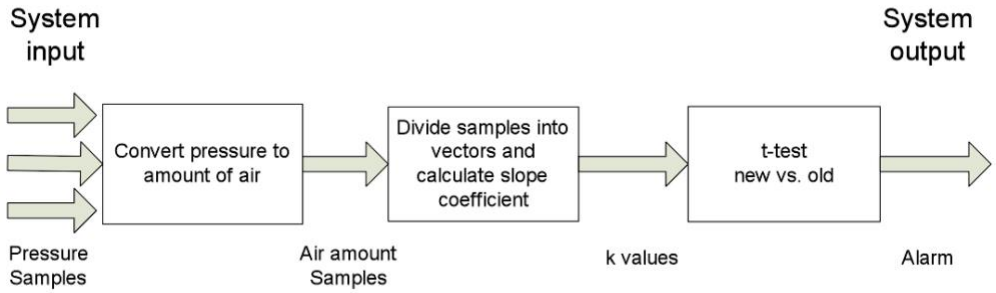

Figure 3.15: A summary of the leak detection algorithm [99].

The first step entails using pressure readings for the particular pneumatic circuit being monitored and multiplying this value to the tank volume. This provides the amount of CA (in litres) being used by the circuit and is denoted by *A*. By obtaining this value, the second step is to differentiate *A* with the time elapsed, resulting in the slope coefficient *K* (i.e. the usage rate in L/s). In the final step, the value obtained for *K* is used in a t-test where the result is compared to previous ones in order to establish if there is a significant change. Figure 3.16, shows an instance when the system was being tested whilst induced with a leak of unknown size. From this figure, it could be seen that the algorithm was capable of detecting the presence of leakages, where it determined that when the t value dropped below -3.4, a leak was present. The system was also designed to locate the source of the fault and this was done by comparing the pressure drop values across different points in the pneumatic circuit. Ultimately, the system encountered two major problems, firstly it was not capable of correctly locating the leak, which could be attributed to the fact that a 10 Hz setting was used to fetch the pressure values, which may have been too slow to accurately identify the changes caused by the fault. Secondly, the system often gave false alarms with the reason being that the amount of air used was also affected by the driving style. This is because if

auxiliaries, such as the air brakes, are used more frequently, more CA is consumed and the algorithm associates this consumption to a leak.

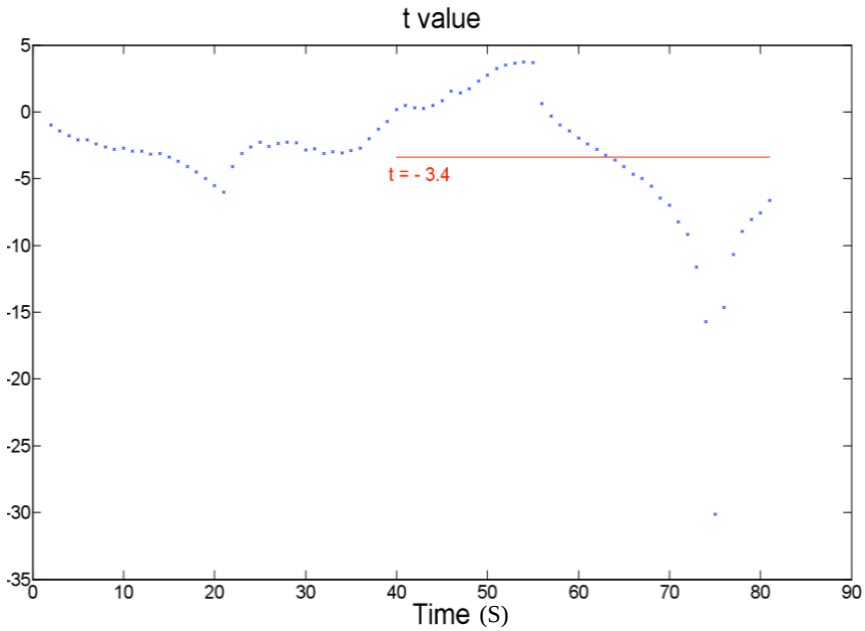

Figure 3.16: An instance where the system detected a leak [99].

Another set-up by M.Borg [17] was also designed to monitor the pneumatic system of buses. Unlike the system by A.Eriksson [99], this concept was not made to work with built-in pressure sensors but rather relied on data logged from external air flow sensors, placed throughout the whole pneumatic circuit. The performance of the set-up however, could not be fully assessed since it was not possible to fully implement the set-up in a vehicle.

To further enhance knowledge regarding pneumatic monitoring systems, industrial oriented set-ups were also reviewed. Consequently, it was noted that these are still not widely available and the ones currently offered in the market focus on the supply side of the system, such as the 'Sigma Air Utility' by KAESER [101]. Furthermore, the equipment typically utilised in these set-ups is not well suited for use in buses. This is mainly due to the operating conditions that the vehicles come exposed to, together with the space restrictions imposed by the overall set-up. Therefore, it could be concluded that current industrial pneumatic systems are not well suited for use in BPSs.

3.5.3.2.1 Dynamic Control of BPSs

In the previous subsection, various methods were discussed on the development of systems capable of monitoring the BPS. Upon further research, another category of monitoring systems was also found, which not only monitored the vehicle pneumatic

systems but was also capable of dynamically controlling the supply side of the set-up. Though this study is focused on the demand side, it was still deemed important to include these systems since currently, these set-ups have only been applied to the supply subsystem and are important for a comprehensive literature survey.

An example of such set-ups is the one designed by D.Tretsiak *et al.* [5] implemented on a hybrid bus which makes use of an electrical compressor. The principle of the set-up was a custom-made algorithm, designed to control both the compressor operation time and the compressor pressure, in order to consume the least possible amount of electrical energy. This was done using sensors, valves and two additional air tanks. By obtaining values for the CA flow, system pressure and compressor power, it was possible to control the valves, which allowed the compressor to be switched on or off accordingly. An example of how the algorithm works is by determining the driving style, which allows it to sense factors, such as the frequency of the regenerative braking, which produces a significant amount of surplus electrical energy, making it possible to charge the vehicle's battery. When the system identifies this surge in energy, the compressor is switched on so as to use this surplus energy instead of the stored energy from the vehicle's battery. A summary of the operation of the algorithm is shown in Figure 3.17 [5].

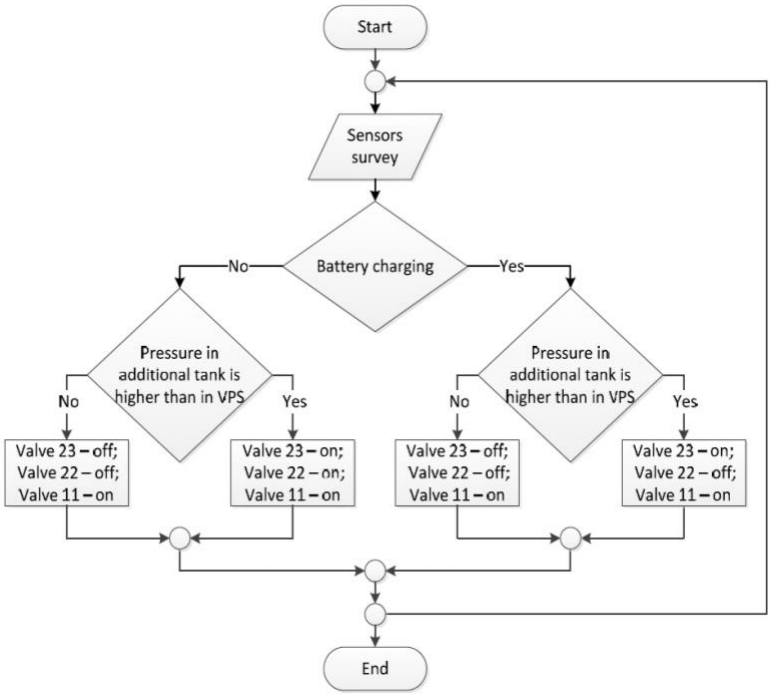

Figure 3.17: The flow chart used for dynamic compressor control [5].

By being able to perform these improvements, the compressor was optimised to work less frequently. This could be confirmed by the logged data results in Figure 3.18,

which shows the compressor switch on frequency. Ultimately, it was concluded that by performing this upgrade, the frequency of compressor utilisation was reduced by 27.8 per cent which contributed to an energy reduction of 24.3 per cent.

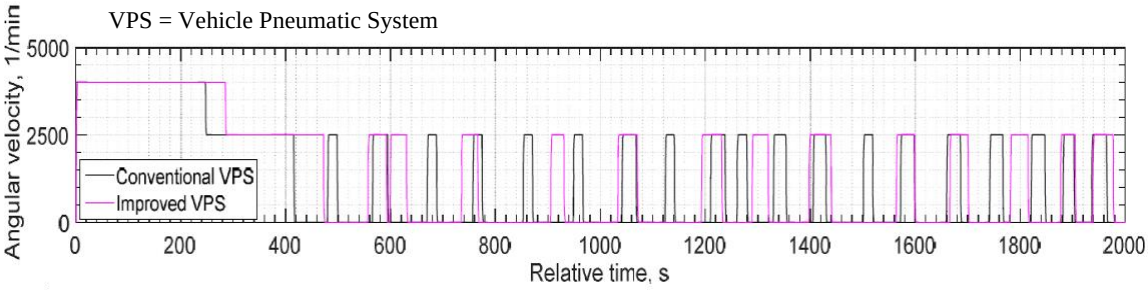

Figure 3.18: The switch on frequency of the compressor for one of the tests [5].

Another dynamic set-up was also designed by J.Laurikko [102] and again, focus was made upon improving the frequency operation of an electric compressor for an electric bus. Although the set-up was not described in a lot of detail, the system made use of data, such as timing parameters, from sensors already fitted into the vehicle and the vehicle's Electronic Control Unit (ECU), considered as the 'brains' of the vehicle, together with pressure readings from pressure sensors. This data was then used in conjunction with a custom-made algorithm in order to monitor the pressure throughout the system, so as to control the compressor. By being able to adjust the compressor's loading, it is claimed that 35 per cent of electrical energy was saved.

3.5.3.2.2 Internet of Vehicles (IoV)

In an effort to make systems smarter, the concept of Internet of Things (IoT) has embedded itself into various applications. Such smart systems are deemed to be 'smart' since they are able to be connected online, making it possible for the user to interact and communicate with the system [5, 102]. This concept has also been applied to the automotive industry and has been labelled as Internet of Vehicles (IoV).

Although not common, there have been efforts pushing towards the development of smart monitoring BPSs. Three such examples are the set-ups by D.Tretsiak *et al.* [5], J.Laurikko [102] and M.Borg [17], described in the previous sections. All three systems used a similar method to convey data to the user, with the process summarised in Figure 3.19 [5]. What happens is that the data from the vehicle's sensors, which is utilised to monitor the system, is transferred to a micro-computer and conveyed to a server, making it accessible to the user. Such a system offers the advantage in that it

allows users to remotely monitor the vehicle's performance even if they are not physically present in it.

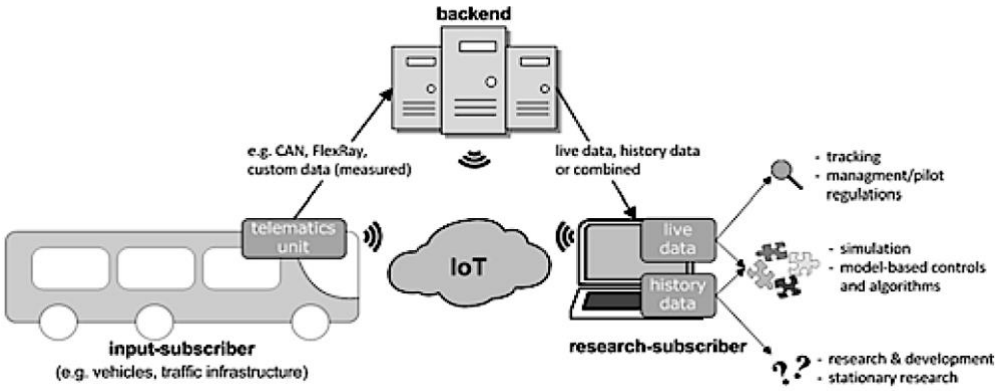

Figure 3.19: An overview of the system's data transfer process [5].

In order to further enhance the intelligence of the system, the cyber-physical system by M.Borg [17], also included an alarm system which automatically informs the user when the system detects a leak. This was done by using the application IBM Alert Notification Service, which automatically pushes alert notifications through a server when the system experiences any abnormal activities. Furthermore, this system also placed emphasis on security by using various protocols, which can be considered to be standard rules which dictate specific functions whilst the data is being transferred. The following four protocols were mainly used: LoRaWAN, MQTT, SSL and HTTPS, which all ensured that the data, both inside each node and whilst being transferred, were secure. Figure 3.20 [17] gives an overview on how these protocols were applied throughout the system.

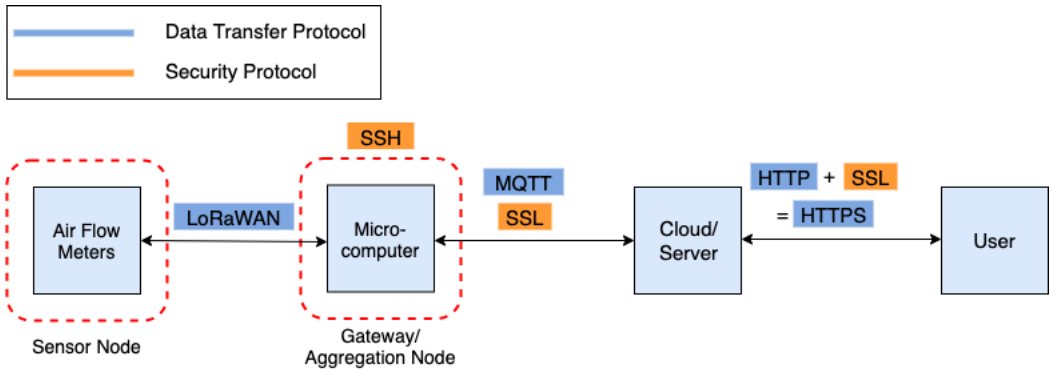

Figure 3.20: An overview of the system's data transfer process [17].

3.5.4 Overview of the Improvements in BPSs

By analysing this section, it could be noted that energy audits can help in highlighting the performance deficiency of CAS, helping to reduce the amount of energy used whilst also reducing emissions. However, it is evident that these are not applied to

BPSs, as the majority of the audits found in this sector focused more on improving the overall bus service. Another highlighted aspect was that information regarding this sector is often not made publicly available. As for efforts to improve the sustainability of BPSs, various enhancements have been made, especially with regards to the auxiliaries found in such vehicles, ranging from the supply to the demand side subsystems. Monitoring systems, specifically designed for BPSs, were also developed to be able to make the overall process less human dependent and simpler. Furthermore, systems capable of dynamically controlling the supply side subsystem have also been designed and the concept of IoV has also been introduced to BPSs. Despite this, it could be noted that there is still room for improvement for these systems, especially when it comes to monitoring systems in the demand side.

3.6 Experiments Pertaining to CAS

In order to understand and study the behaviour of a particular system or to be able to confirm, or deny a particular hypothesis, one needs to perform relevant experiments. This is done to gather the required results, produce an adequate analysis and if possible, improve the system's performance. For instance, M.Borg [17] wanted to investigate how a BPS reacts whilst being exposed to various fault sources, such as leakages or faulty components. To do so, a test-bed replicating two frequently used end uses (i.e. the air suspension system and the pneumatic cylinders) was designed. This set-up is depicted in Figure 3.21 [17].

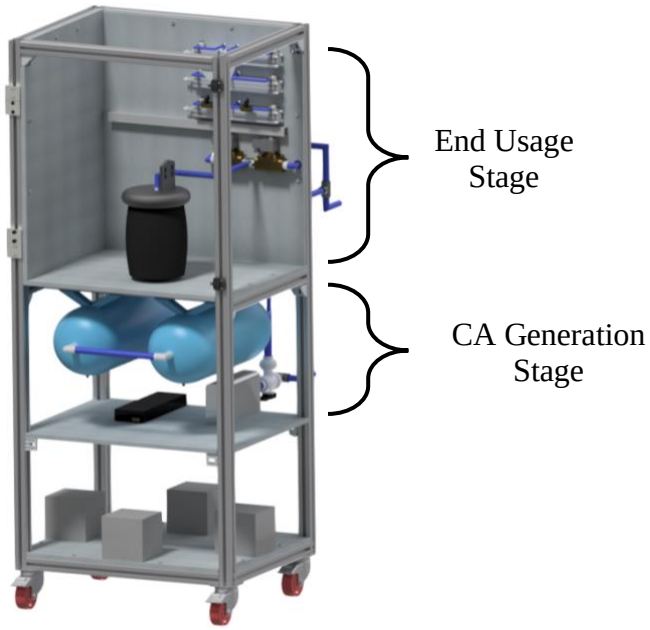

Figure 3.21: The set-up designed by M.Borg [17].

To perform such experiments, a systematic approach has to be conducted in order to properly perform experiments. In the case of CA studies, this is frequently done using the concept of Design of Experiment (DOE), where one plans, designs and analyses the required experiment [103]. Whilst performing such an analysis, variables have to be altered in order to record and establish the relationship that these have with the measured output responses. Such variables are referred to as input variables and can be categorised either as controllable or uncontrollable input variables, where the former refers to parameters which can be easily altered by the user. For example, in the pneumatic study performed by K.Abela [64], where he wanted to better comprehend the behaviour of industrial pneumatic set-ups, the input parameters, system leakage diameter and input pressure, were altered in order to record the output parameters system pressure, CA flow rate and actuation timing. Similarly, the set-up by M.Borg [17] also allowed the user to adjust various input parameters relating to pneumatics, such as the leakage diameter and the inclusion of faulty actuators, to be able to record the system pressure, CA flow rate and actuation timing. Conversely, as the name implies, uncontrollable input factors are parameters which cannot be easily controlled by the user. For instance in pneumatic systems, such parameters include the ambient temperature and humidity, which have an influence on the behaviour of the CA fluid flow [18].

There are various ways how one can perform pneumatic experiments however, it is commonly the case that single and full factorial experiments are performed.

Single-factorial experiments are considered as the most straightforward type of experiment since only one controllable input factor is altered per experimental run. An instance of this is the experiment performed by K.Abela [64], where, the leakage diameter was the factor being altered throughout the experimental runs, with the output response being the CA volume per test. A similar experiment was also performed by FESTO [63] however, instead of varying the leakage diameter, the input pressure was varied to record the volume consumption per test.

On the other hand, full-factorial designs investigate all the possible outcomes from the parameters being investigated. In the case that the factors are run at two levels, then the total number of experiments needed are 2^k, where k is the number of factors. An example of such an experiment is shown in Table 3-3 where K.Abela [64] performed

additional experiments using this method to further comprehend the behaviour of the pneumatic set-up. This meant that for each input factor (i.e. the input pressure and leakage diameter), their high and low levels were investigated, in order to better understand the interaction between them and the outputs recorded.

Table 3-3: An instance of a two-levelled factorial experiment [64].

Run	Input Pressure (bar)	Leak Diameter (mm)	Air Volume (NL/min)	Total Energy (Wh)
1	6 (high level)	1.5 (high level)	969	168.1
2	6 (high level)	0.0 (low level)	326	63.5
3	3 (low level)	1.5 (high level)	517	95.6
4	3 (low level)	0.0 (low level)	171	33.3

3.7 Conclusion

Based on the understanding of BPSs in Chapter 2, this chapter served to evaluate literature concerning the assessment of losses, including leaks and faults, within BPSs, whilst also helping to further understand their repercussions which range from additional emissions and downtime to safety concerns. This was followed by a review of various solutions which address these issues. This was complemented with extensive market research which was performed to not only review the improvement opportunities, but to also better understand how the faults can be monitored and how the monitoring process can be improved. Finally, experiments pertaining to CAS were reviewed, whilst also highlighting how they are typically performed, in order to perform a comprehensive pneumatic study.

Chapter 4-Research Gap and Research Problem

4.1 Analysis of the State of the Art

Through the in-depth analysis of the literature provided in Chapter 3, it can be concluded that BPSs are generally quite inefficient, with the main cause of inefficiencies being leaks or faulty components. In addition, the identification of leaks is not a straight forward process, especially when the system is compact such as the one found in buses. Consequently, it is often the case that repairs are overlooked due to the downtime associated with their maintenance.

Despite the current lack of information regarding BPSs, which becomes apparent when analysing aspects such as audits, it cannot be said that no developments are being made towards further improving the sustainable performance of these set-ups or the development of monitoring systems. Table 4-1 includes an overview of several of these solutions.

Table 4-1: The attributes of some of the studies/systems discussed in Chapter 3.

Attribute	**M.Borg** [17]	**A.Eriksson** [99]	**D.Tretsiak *et al.*** [5]	**J.Laurikko** [102]	**M.Trompet** [86]	**WABCO** [88, 94]	**Volvo** [98]	**M.Khodabakhshian *et al.*** [92]
Supply Side Improvement			x	x		x		
Demand Side Improvement	x	x				x	x	x
Manual Inspection					x			
Automatic Inspection	x	x	x	x			x	
System Benchmarking					x			
IoV Capabilities	x		x	x				
Detection of Faults	x	x					x	
Dynamic Control of Supply Subsystem			x	x				
Use of Built-In Sensors		x	x	x			x	
Use of Additional Equipment	x		x					x

In order to assess the performance of a set-up and identify any potential improvements, audits need to be performed. To help in completing this task, the benchmarking process is usually implemented, whereby the system is compared to a known well-functioning set-up. This is done using KPIs since these serve as metrics by which to compare the performance values. However, as underscored in the study by M.Trompet [86], these are currently quite limited for buses especially for their pneumatic system. This was further subsidised by his bus benchmarking process, where it was noted that companies were not concerned about evaluating metrics relating to BPSs, further highlighting the lack of information in this sector.

One of the main reasons for faults prevailing is that maintenance is often overlooked due to the downtime associated with the repair. To reduce this downtime, monitoring systems have been developed which aim at making the maintenance process faster. Such a system is the one developed by Volvo [98], where by using sensors already present in the vehicle's pneumatic system, it is able to trigger lights on the dashboard when faults are detected. However, it was noticed that this set-up is only capable of detecting large leaks. More advanced monitoring systems were also designed by both A.Erikkson [99] and M.Borg [17], each taking different approaches. The main difference between both set-ups was that the former, again made use of built-in sensors, whilst the latter made use of additional air flow sensors. Despite this, it is good to mention that the system by A.Erikkson was not deemed reliable since it triggered frequent false alarms and was not able to locate the fault source whilst the system by M.Borg could not be reviewed since it was not fully implemented.

Furthermore, supply oriented monitoring systems have also been developed which allow for dynamic compressor control capabilities. Two set-ups could be found, designed by D.Tretsiak *et al.*[5] and J.Laurikko [102]. These systems were able to automatically adjust the demand of the compressor, according to the current need. Both systems recorded significant savings whereby the system by D.Tretsiak *et al.* recorded an energy saving of 24.3 per cent and the system by J.Laurikko, recorded an energy percentage saving of 35 per cent.

Another advancement to monitoring set-ups is the integration of IoV into the set-up, allowing for remote monitoring of BPSs. The systems by D.Tretsiak *et al.* [5], J.Laurikko [102] and M.Borg [17] were three of such set-ups and all worked using the

same principle. This entailed transferring the recorded sensory data onto a server which makes it accessible to the user. The set-up by M.Borg also included an alert notification system, which remotely informs the user when a problem is encountered.

Whilst performing the market research, it was also noted that a lot of focus has been given by manufacturers to improve several auxiliaries, both supply and demand oriented, with A. Kochsiek [104] also claiming that these improvements have reached their pinnacle. With regards to the supply side auxiliaries, WABCO [88] developed a compressor with full on-off capabilities and it was claimed that this improvement contributed to a reduction of 2 per cent to the annual fuel consumption. Moving onto demand side improvements, it noticed that various auxiliaries have been electrified. Such an example is the set-up developed by WABCO [94] where an electronic air suspension system was designed to make use of various height sensors. It was claimed that this set-up helped in reducing the vehicle's fuel consumption by 3 to 5 per cent. M.Khodabakhshian *et al.* [92] also made use of the electrification concept, where the air brakes were converted into an electro-mechanical system, helping to reduce the annual fuel consumption by 1.5 per cent. It was also highlighted however, that the results achieved for this set-up were highly dependent on the driving style. Whilst adopting such a system however, one needs to keep in mind that the converted auxiliaries will contain more sensors and therefore will become more complex, which can make repairs more complicated and time consuming.

4.2 Research Gap

Ultimately, based on this comprehensive literature survey, an evident research gap could be identified. Although improvements have been performed to several vehicle pneumatic subsystems, together with advancements in monitoring systems, research regarding this area is still currently in its early stages. This could be noticed through the overall lack of information available, as compared to industrial pneumatic systems. As a result, it is still not known how faults, such as leaks and defective components, affect the system itself and its overall sustainability or which parameters have the greatest impacts on BPSs. Furthermore, parameters which may help to reliably identify the presence of faults in BPS have still not been clearly recognised. By being able to better understand such systems, whilst gathering the required information, it would further help in comprehending the system's behaviour. This would not only promote the implementation of processes, such as audits for CAS (or BPSs), but it will also

make it possible to perform further advancements in monitoring systems, making them operate more efficiently, autonomously and reliably. Therefore, by addressing these shortcomings, the sustainable performance of these systems could be improved, whilst reducing the maintenance downtime.

4.3 Research Questions

Based on extensive literature reviewed in Chapter 3, it could be established that the main priority for this study is to comprehend the effects that inefficiency sources, such as leaks, have on BPSs, whilst also identifying variables which make it possible to easily identify and quantify these faults. Consequently, data has to be collected from an actual bus in order to better comprehend the BPS. In addition, a system would also have to be designed to be able to perform adequate simulations, depicting a typical BPS, whilst also being able to easily alter and log demand parameters. As a result, the following research questions where established;

1. How much fuel/energy do elements in a typical BPS consume during operation (e.g. the bellows, doors and brakes)?
2. What are the effects that different parameters have on the performance of the BPS?
3. Which parameters can be used to identify and quantify fault sources in BPSs?

4.4 Research Objectives

In order to perform the required experiments, so as to answer the questions in *Section 4.3*, a set-up capable of depicting a BPS whilst also monitoring the required variables has to be developed. To do so, two set-ups by M.Borg [17] and K.Abela [18] would be utilised conjointly with, the one by the former containing the most frequently used elements found in a typical BPS, whilst the one by the latter containing the majority of the data logging equipment. In addition, a data collection session has to also be performed on an actual vehicle to better understand the behaviour of BPSs.

By using the mentioned set-ups, the following research objectives were devised to be able to commence and complete the study:

1. Collect actual vehicle data, to better comprehend the performance of BPSs;

2. Implement a set-up capable of depicting the required simulations;
3. Establish an adequate design of experiment in order to depict real life scenarios during simulations;
4. Record the required data in order to be able to factually answer the research questions.

Therefore, the rest of the study will focus on answering and completing both the devised research questions and objectives. To do so, preliminary pneumatic tests were performed using actual buses, the results of which presented in Chapter 5, in order to better comprehend the behaviour of such systems. Consequently Chapters 6 and 7 will describe the simulations to be performed in the lab, highlighting various aspects including the DOE and the set-up used, whilst also explaining and factually assessing the obtained results.

Chapter 5 –Preliminary Data Collection in a BPS

5.1 Monitored End Uses

In order to better comprehend the behaviour of BPSs, a preliminary data collection session was performed on an actual bus in order to acquire benchmark values, which could be utilised throughout the rest of the study.

The first step towards performing the tests was to identify the scenario and constituents to be monitored during this process. The main criteria whilst choosing the scenarios was that the actions to be logged had to be frequently performed during normal bus operation. After analysing various scenarios, it was determined that two of the most frequent actions performed by a bus are the actuations whilst the vehicle is at a bus stop and the application of the front and rear air brakes, which make it possible for the vehicle to slow down on the stop.

During a typical bus stop, the bus performs the following actuations:

1. The pneumatic door actuators open and the bus kneels, simultaneously, in order to allow the passengers to enter or exit the vehicle.
2. Once all passengers board and exit the vehicle, the doors are closed and the bus's ride height is restored to its original setting.

Furthermore, whilst the vehicle is braking, the brake chambers are actuated. By being able to comprehend what actuators are used during a bus stop and braking, it was deemed appropriate to choose both scenarios to be monitored during the preliminary tests. This is because these would encapsulate the use of the three most frequently utilised end uses in a typical bus, as was also highlighted in *Section 2.2*. In addition, to further comprehend the BPS, another test was also undertaken whilst the CAS was initially being filled up. As a result, the following five tests were performed:

- Monitoring of the initial system fill-up;
- Monitoring of the pneumatic cylinders;
- Monitoring of the suspension bellows;
- Monitoring of the front and rear brakes.

5.2 Data Logging Equipment

In order to perform all five tests, adequate data logging equipment had to be used. To determine this apparatus, the parameters to be monitored had to be identified. For the purpose of the preliminary tests, the aim was to determine the amount of CA that each constituent consumes whilst it is in use. Therefore, to be able to monitor the CA volume, an air flow meter was required. Additionally, in order to log all this data, a dedicated data logger was also required to record all of the sensory data, whilst also making possible for the user to interact with the system. Ultimately, the equipment listed in Table 5-1 was chosen to be used for all the tests. It is good to note that pressure was not measured during the data collection session, due to the fact that this parameter does not contribute towards quantifying the CA volume consumption for the components.

Table 5-1: Equipment utilised during experiments

Component	Supplier Code	Function
Human-Machine Interface (HMI)	Omron NB7W-TW01B	Utilised as a gateway between the user and the system, whilst also logging the sensor data from the sensor.
Air flow sensor	SMC PFMB7501	Responsible for monitoring the air flow of the constituent.

It is worth mentioning that the main reason for choosing this sensor was that it had an adequate flow range value of up to 500 NL/min whilst also being compatible with the HMI unit. In addition, the resolution for the logging was set to 0.5 s, making it possible to obtain a good amount of data, thereby helping to adequality analyse the actuations. In order, to make this set-up portable, all the equipment was enclosed into the housing shown in Figure 5.1.

Figure 5.1: The data logging equipment used in its enclosure.

Due to being limited to a single sensor, it was not possible to collect all the data simultaneously. Consequently, the set-up had to be connected according to the constituent to be monitored. To give an overview of how the logging equipment was integrated with the pneumatic system, Figure 5.2 shows a simplified schematic of the pneumatic system, highlighting where the equipment was situated for each test. Further detail about the logging set-up and the sensor placement, will be discussed throughout this chapter.

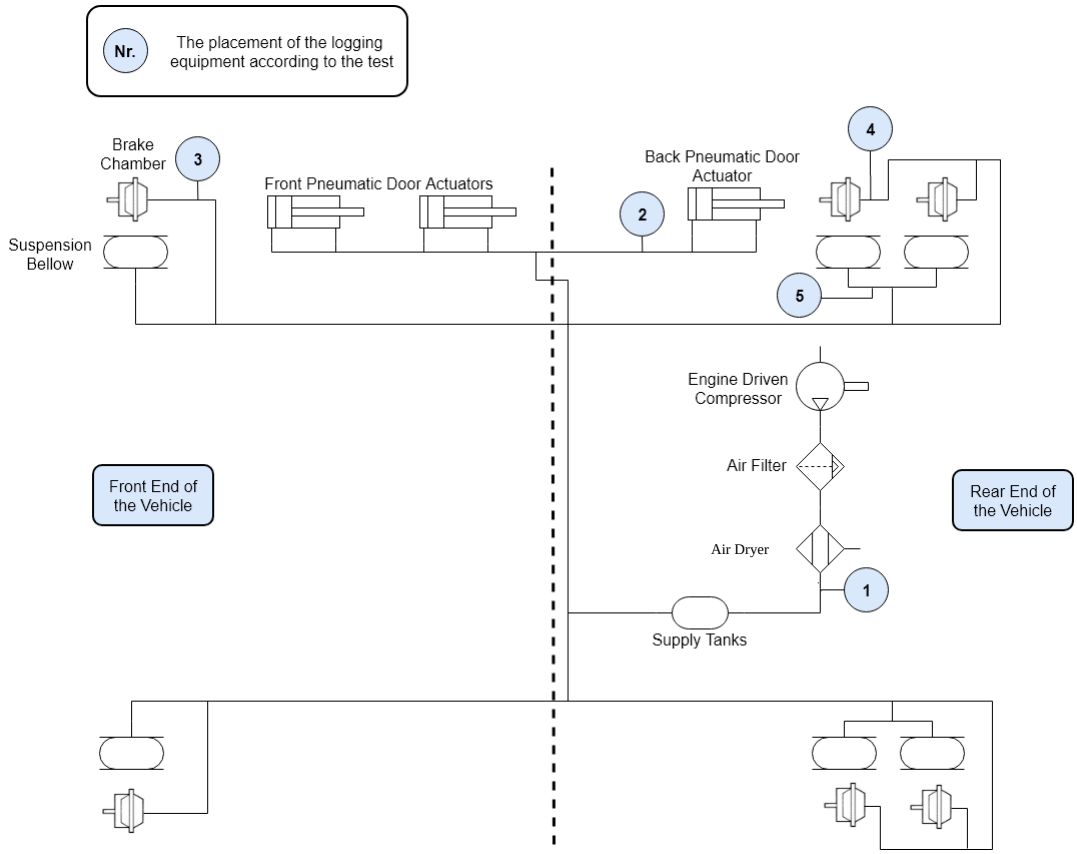

Figure 5.2: A simplified schematic of the pneumatic set-up.

5.3 Data Collection

By determining what scenarios were to be monitored and the equipment required to log the respective end effectors, it was possible to perform all the tests, with the obtained results tabulated in Table 5-2. Indeed, the remainder of this section will give further detail about the results of each test.

Table 5-2: The data obtained for all five tests.

Test Nr.	System Investigated	Average Volume Consumed (NL)	Average Time to Complete Action (s)
1	System Fill-Up	1,103	219
2	Pneumatic Cylinder	3.66	5.3
3	Front Brake Chamber	4.85	/
4	Rear Brake Chamber	5.22	/
5	Suspension Bellow (*Inflation*)	38.52	7.2

5.3.1 System Fill Up Simulations

Before starting its first journey, a bus has to wait for its pneumatic system to be fully pressurised. In this regard, the first test was performed with the aim of better grasping what occurs during this scenario.

To complete this test, the logging equipment was set-up as shown in the illustration in Figure 5.3, where the air flow sensor was connected downstream of the pre-conditioning equipment and in series with the system. Subsequently, the CA then flowed to various tanks, in order to supply all of the required constituents. By doing so, the sensor measured the CA flow which was being supplied to the entire pneumatic system.

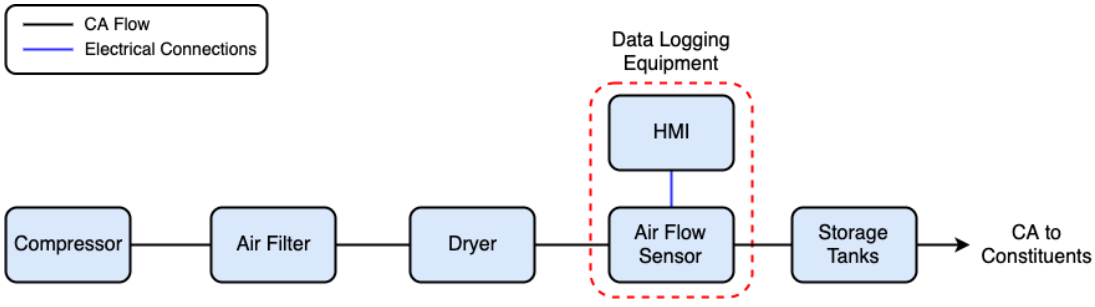

Figure 5.3: The set-up to monitor the system fill up.

Once all the equipment was set-up, the experiment could commence and the results are depicted in Figure 5.4. By calculating the area under the graph, the total volume required to fill up the entire system from empty could be determined. This resulted in a total of **1,103 NL** of CA, which took the compressor a total of 219 s to fill the system. Indeed, it was observed that the air flow values varied throughout the entire simulation. The reason for this is that since the compressor is directly coupled to the engine, the

driver revs the engine to speed up the fill up process, resulting in fluctuations. Since this is highly dependent on the particular driver, the time required to fill up the entire system is variable. However, it can be said that the volume remains constant since the system pressure is always left the same.

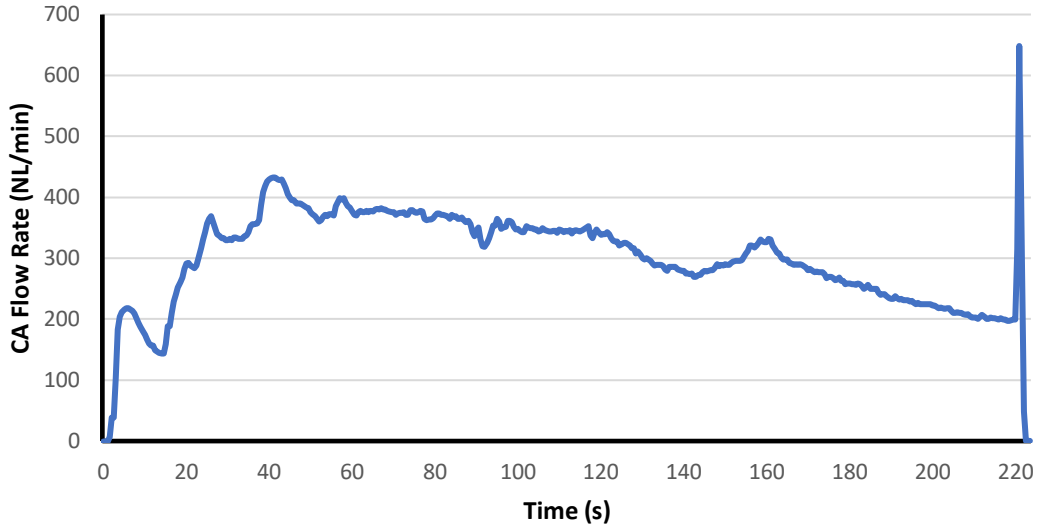

Figure 5.4: The CA flow rate whilst the system was initially being filled.

5.3.2 Bus Stop Scenario

This scenario depicts all the actions performed during a typical bus stop, more specifically the actuation of the pneumatic cylinders and the bellows. Therefore, during this test, both constituents were monitored so as to have a good insight on what occurs during this situation.

5.3.2.1 Pneumatic Cylinder Simulations

In order to monitor the extension and retractions of the cylinders, the data logging equipment in Figure 5.5 was used.

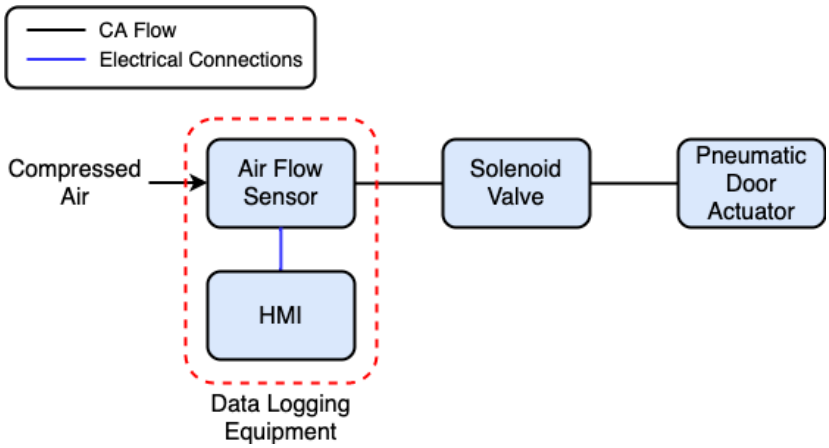

Figure 5.5: The set-up utilised to monitor the door.

e of the door cylinder actuators. As a result, the meter was placed in series with the CA

flow, upstream to the solenoid valve responsible to open and close the door. By placing the sensor prior to the respective valve, it made it possible to monitor the CA flow during both the extension and retraction phases.

Once the equipment was set-up, the simulations for this scenario could commence. This entailed opening and closing one of the doors for six successive times, resulting in 12 separate actuations. In Figure 5.6, the CA flow data for the first cycle is show in further detail.

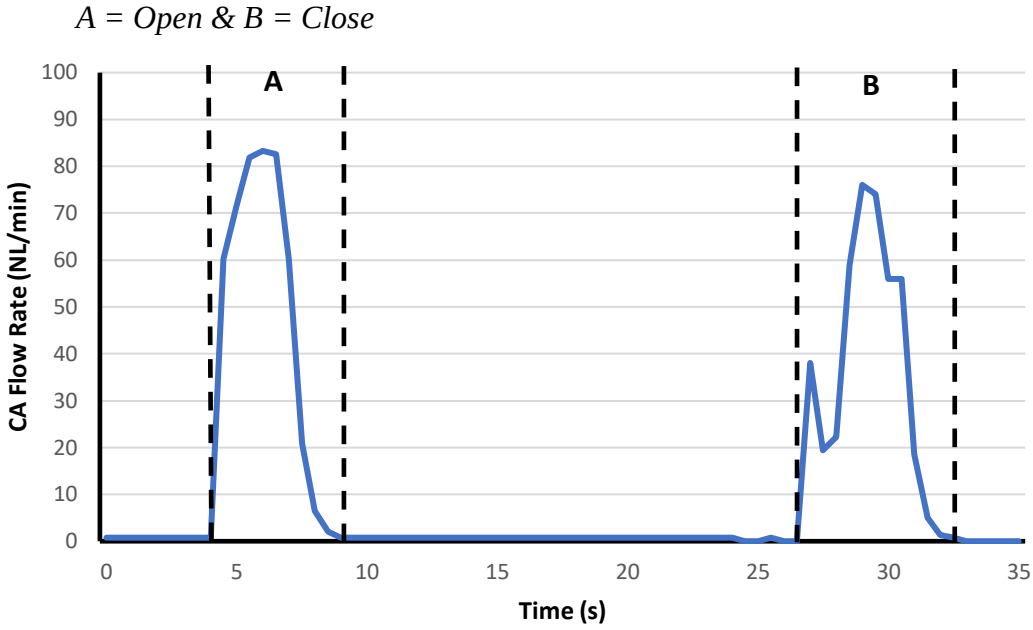

Figure 5.6: The CA flow rate for the first cycle whilst monitoring one of the cylinders.

By obtaining this data, the time to actuate the double acting cylinder could be determined, where the average time to fully extend the component was 5.1s, whilst to fully retract it was 5.5 s. It is good to mention however, that these durations were approximations, since it was not possible to log the actual switching of the relevant solenoid valves. Additionally, it could also be determined that the average CA volume to actuate the constituent was **3.66 NL**.

5.3.2.2 Suspension Bellow Simulations

The aim for this simulation was to monitor the behaviour of the suspension bellow whilst undergoing the kneeling procedure. Consequently, this could be done by monitoring one of the suspension bellows, as can be seen in Figure 5.7.

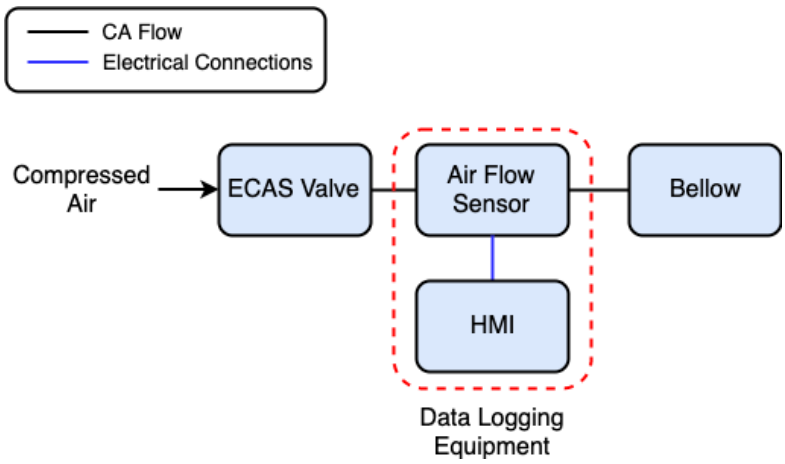

Figure 5.7: The set-up utilised to monitor the bellow.

As depicted in Figure 5.7, the air flow sensor was again placed in series with the CA flow, in between the ECAS valve and the bellow, with the former encompassing both the kneeling and levelling valves, as documented in *Section 3.5.2* This made it possible to monitor the flow of CA being supplied to the constituent.

During the test, the suspension bellow was inflated and deflated for 6 times in order to depict typical kneeling behaviour. Figure 5.8, shows the CA flow results for the second cycle can be seen.

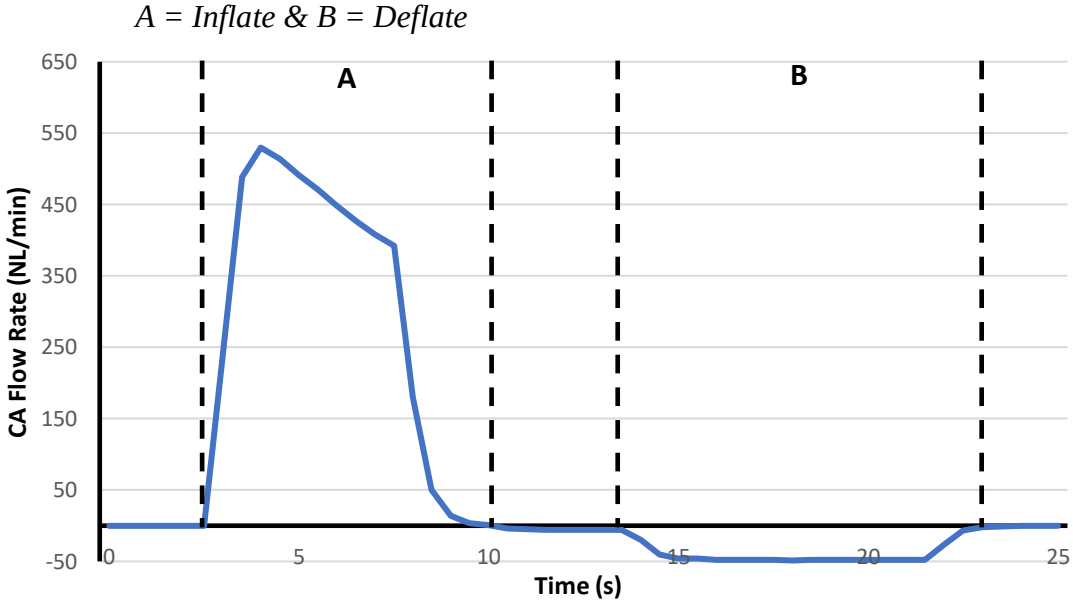

Figure 5.8: The CA flow rate for the second cycle of the bellow simulations.

The graph showed that the amount of CA used to inflate the bellow was considerably more than to actuate the cylinder, with the average to fill the end effector being **38.52 NL**. Similarly, the time taken to inflate the bellow to its ride height was more,

with the average being 7.2 s. It was observed that after each fill up cycle, i.e. Zone B, troughs were present. This represented the kneeling function, whereby the bellow was being deflated hence exhausting CA. Moreover, the reason that the maximum negative flow rate value during the deflation was only 50 NL/min, as compared to 520 NL/min whilst being inflated, was a result of the negative capping induced by the air flow sensor.

5.3.3 Brake Simulation

The final set of tests revolved around the vehicle's brakes. Due to the fact that when the brakes are applied, both the front and rear disk brakes are used to slow the vehicle down, both sets were monitored to gather knowledge on the whole braking set-up.

5.3.3.1 Front Brake Simulations

To analyse the behaviour of the front brakes, it was deemed appropriate to survey one of the front brake chambers. To do so, the logging equipment was placed as shown in Figure 5.9.

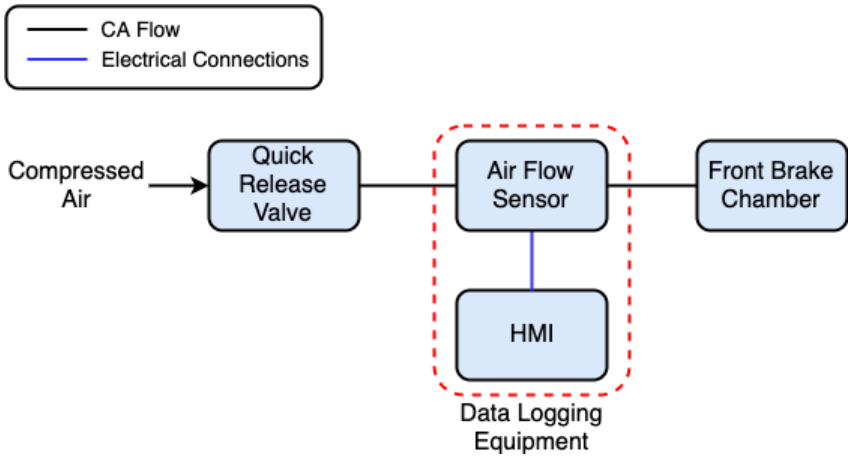

Figure 5.9: The set-up to monitor the front brakes.

The set-up consisted of two main constituents, being the quick release valve and the brake chamber, with the air flow sensor being connected in between both components. The braking effect was achieved via the brake chamber, which actuated the disk brakes when the pedal was pressed. In order to release the brakes, the quick release valve was tasked with exhausting all the air from the chamber.

The performance of the front brakes was analysed by fully applying and releasing the brakes for four successive times, with Figure 5.10, showing the CA flow for the third cycle.

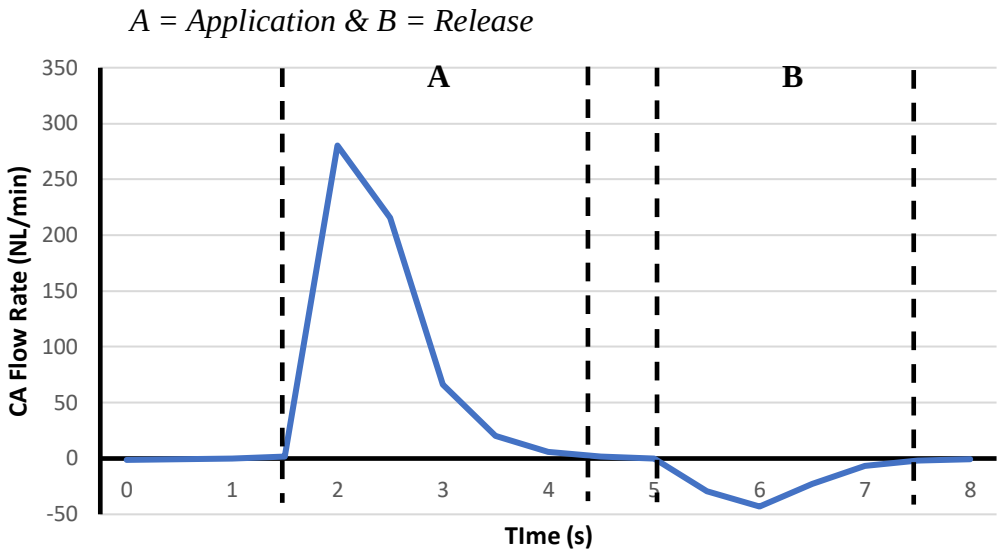

Figure 5.10: The CA flow rate for the third cycle for the front brake simulations.

During this test, the average CA volume required for each front brake application was measured at **4.85 NL**. Troughs, such as the one denoted by B, represented the brake being released and the CA being exhausted to atmosphere.

5.3.3.2 Rear Brake Simulations

Similar to the previous test, it was deemed appropriate to monitor one of the rear brake chambers, in order to better comprehend the behaviour of the system. This was done by using the set-up in Figure 5.11.

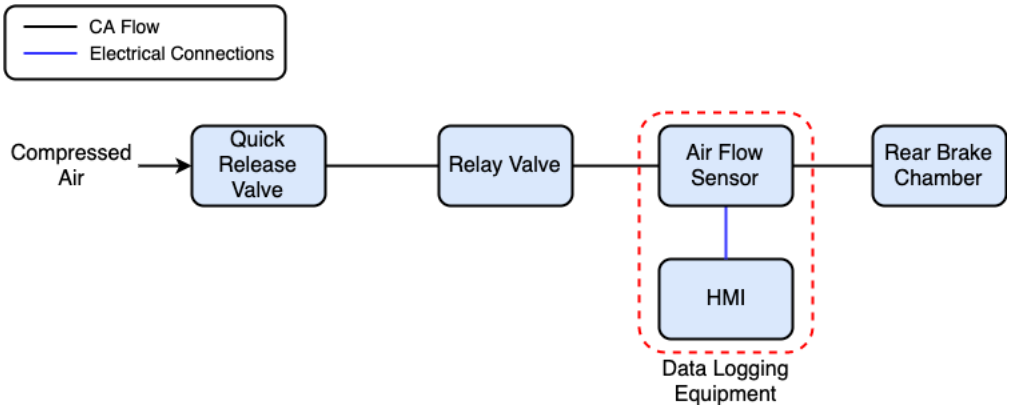

Figure 5.11: The set-up to monitor the rear brakes.

From this illustration, it could be noted that this brake set-up was quite similar to the previous one, with the only difference being the relay valve, ensuring that this circuit was always pre-charged with CA. This guaranteed that no delays in the brake application would occur, which may arise as a result of the rear brakes being situated further away from the CA reservoir.

For this test, the same procedure adopted for the other braking system was utilised, whereby the brakes were fully applied and released for four successive times. The CA flow data for the third cycle can be seen in Figure 5.12.

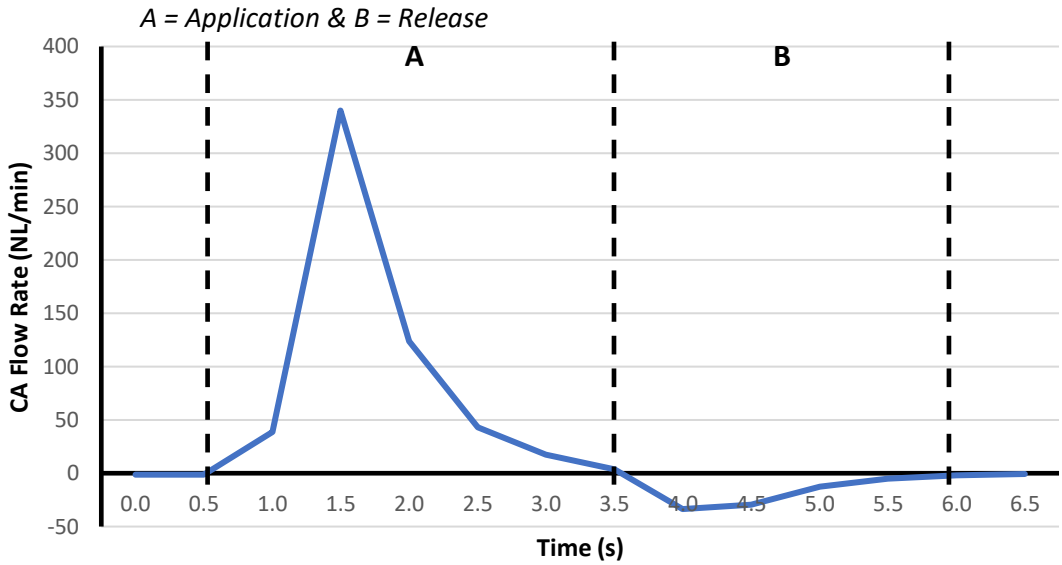

Figure 5.12: The CA flow rate for the third cycle of rear brake simulations.

From the results, it could be determined that this brake set-up behaved very similarly to its counterpart. In addition, the volume to actuate the chamber was also comparable, resulting in an average of **5.22 NL** of CA.

5.4 Performance Dissection for BPS

The next step towards further comprehending BPSs was to go into detail about the actual performance of these systems, making it possible to answer the first research question. In order to do so, it was deemed appropriate to determine the scale by which the pneumatic system affects a typical bus. By using the compiled data in previous section, it was possible to determine the volume of CA required to complete a single bus stop. During each stop, the following components were utilised;

- Three cylinders;
- Three suspension bellows (to kneel the vehicle to one side);
- Two front disk brakes and four rear brakes.

Therefore, it could be determined that by using the data in Table 5-2, each stop consumes **168 NL** of CA. Furthermore, it was also required to establish the number of bus stops per hour. This was done by taking Route 21 as an example, which departs from Valletta and stops at Sliema, whilst encountering 49 bus stops in an hour. By using this data and Equation 5.1, the volume of CA consumed per hour could be calculated.

$$Consumed\ CA\ volume/hr = Nr.of\ stops/hr \times CA\ volume/stop \quad Eq.\ 5.1$$

$$Consumed\ CA\ volume/hr = 49 \times 0.17Nm^3 \ = 8.33\ Nm^3/h$$

The next step was to establish a relationship between the drive train of the vehicle and the pneumatic compressor and this could be done by using the data gathered in *Section 2.2*, which is summarised by the illustration in Figure 5.13.

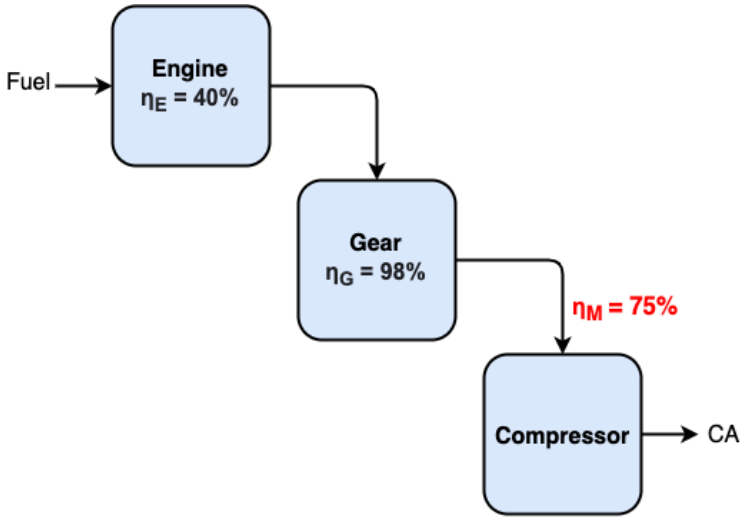

Figure 5.13: The relationship between the engine and the compressor.

It is known that the compressor is directly driven by the engine via gears and that modern EURO V diesel engines and gears are around 40 per cent [105] and 98 per cent [106] efficient, respectively. With regards to the compressor however, the efficiency value is not currently available. Therefore, for the purpose of this study, the 24V DC EXTREME 3 electric compressor by Nardi [107] was chosen to be utilised throughout this analysis. The reason for this selection was that this component was similar to those used to operate pneumatic systems in smaller vehicles, hence ensuring that the obtained results were as realistic as possible. This compressor made use of an

electric motor, which generally can be considered to operate at 75 per cent efficiency [108].

By using the chosen compressor, it was also possible to determine the specific energy consumption of a typical vehicle pneumatic compressor. This was possible through the use of the recorded data which was gathered and used in Equation 5.2.

$$Specific\ Energy\ Consumption = \frac{Power \times Time}{Compressor\ Discharge} \qquad Eq.\ 5.2$$

$$Specific\ Energy\ Consumption = \frac{(24V \times 33A) \times 0.017h}{0.069Nm^3} = 195.1\ Wh/Nm^3$$

By determining the volume required per bus stop, the energy consumption of a typical vehicle compressor and the relationship between the drivetrain and the compressor, the energy being supplied to the engine by the fuel could be determined using Equations 5.3 and 5.4.

$$Consumed\ energy/h = CA\ volume/h \times Energy\ Consumption \qquad Eq.\ 5.3$$

$$Consumed\ energy/h = 8.17 \times 195.1\ = 1.59\ kWh/h$$

$$Energy\ supplied\ by\ fuel = \frac{75\%\ of\ Consumed\ energy/h}{Engine\ Efficiency \times Gear\ Efficiency} \qquad Eq.\ 5.4$$

$$Energy\ supplied\ by\ fuel = \frac{0.75 \times 1.59}{0.4 \times 0.98} = 3.05\ kWh/h$$

Since 1 L of diesel has a calorific value of 10 kWh/L [109] and the amount of energy being supplied to the engine to power the pneumatic system is 3.05 kWh/h, the pneumatic system requires **0.31 L of diesel per hour**, which translates to **4.96 L daily**. It is also known that on average, modern buses use a total of 35 L of fuel per 100 km [110, 111] and that the bus travelling via Route 21 drives an average of 20 km per hour. By extrapolating this data, one can deduce that this particular bus requires a total of **7 L per hour** of diesel to operate, with most of this consumption being attributed to the drivetrain. Consequently, it could be concluded that the pneumatic system uses **4.4 per cent** of the total fuel as compared to the total demand, with the drivetrain contributing to the most fuel consumption. Moving onto financial repercussions for a fault-free set-up, it could be concluded that the BPS costs the

operator **€0.37 per hour** in fuel costs, keeping in mind that the current price of diesel per litre is €1.21 [112]. Moreover, since 1 litre of diesel emits 2.62 kg [113] of CO_2, **0.80 kg** of CO_2 would be emitted each hour to power the pneumatic system.

5.5 Sensitivity Analysis

Once a benchmark for the overall performance of a typical BPS was established, it was deemed appropriate to also perform a sensitivity analysis. This investigation helped in determining how varying factors that compounded the system's performance, affect its behaviour. These factors were:

1. Engine efficiency and average fuel consumption per 100 km;
2. Specific energy consumption;
3. Number of stops per hour;
4. Distance of route per hour.

During this process, all factors were varied by ±25 per cent, with the monitored output response being the resulting pneumatic fuel percentage, as a ratio of the total, which can be represented by Equation 5.5.

$$Ratio = \frac{Fuel\ Consumed\ by\ Pneumatics}{Total\ Fuel\ Consumed} \qquad Eq.\ 5.5$$

The obtained results are displayed in Figure 5.14.

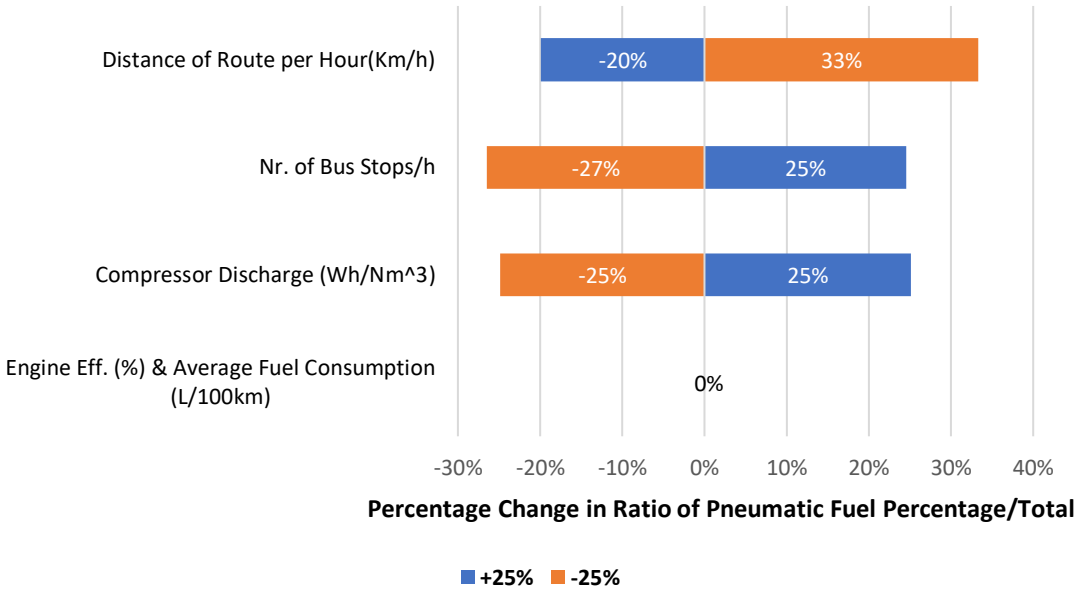

Figure 5.14: The sensitivity analysis for the BPS.

The results showed that whilst altering the number of stops per hour and the compressor discharge, the output response was also altered by around ±25 per cent, which shows that that these parameters affect the pneumatic percentage linearly. On the contrary, it could be argued that for the route distance per hour, the system behaved differently. In fact, it reacted opposite to the previous scenarios since its output response decreased whilst the parameter was increased, and vice versa. The reason for this is that as the route distance decreased, the engine fuel consumption decreased, hence contributing to the fuel percentage increase in the pneumatic system. Conversely, when the distance increased, the engine fuel consumption increased, which decreased the percentage of the pneumatic fuel consumption. Furthermore, due to the fact that when calculating the pneumatic percentage, Equation 5 was used and the distance change correlated with the drive which pertained in the denominator, the inverse relationship meant that the percentage did not increase linearly by ±25 per cent.

With regards to the engine efficiency and the average fuel consumption, these are linked together since if the engine is more efficient, the fuel consumption decreases, whilst if the engine efficiency is reduced, the fuel consumption increases. Through the obtained results, it became evident that whilst inversely varying each of these parameters by ±25 per cent, the system reported the same percentage as the control test. This was attributed to the fact that the relationship correlating to the pneumatic percentage was relative, therefore the changes made for both linked parameters compensated for each other. From this analysis it could also be concluded that whilst varying each parameter by ±25 per cent, the maximum variation obtained for the pneumatic percentage was 33 per cent, meaning that maximum obtainable fuel percentage for the pneumatic system, as a consequence of variations, is 5.3 per cent.

In order to further comprehend the behaviour of BPSs, it was also deemed appropriate to analyse the relationship of compounding factors. To do so, the effects that a route has on the overall fuel consumption were analysed. This therefore, entailed varying the values for the number of bus stop per hour and the route distance per hour, using two actual routes. These were;

- Route X1 which is from Luqa to Ċirkewwa, encounters 24 bus stops per hour, and the travelled distance being 31.9 km in one hour [114].

- Route 49 which is from Valletta to Għadira, encounters 57 bus stop per hour and the travelled distance being 25.2 km in one hour [115].

The reason for choosing these two routes was that as compared to the benchmark scenario, one bus travels a longer distance and encounters less bus stops, whilst the other travels less distance and encounters more stops. The obtained results showed that the scenario for Route X1 consumed a total of 11.17 L of diesel (0.15 L for pneumatics), whilst the scenario for Route 49 consumed 8.82 L of diesel (0.35 L for pneumatics). For both scenarios, the amount of diesel consumed was more than the control, which was as expected due to the longer distance travelled. It could also be noticed that the distance travelled had a greater impact than the number of stops due to the fact that the drivetrain consumes more fuel than the pneumatic system.

5.6 Conclusions

By performing these tests, vital information was gathered with regards to the behaviour and consumption of three of the main end effectors typically used in typical bus operation, i.e. the pneumatic cylinders, the air suspension and the air brakes. Therefore, by using the obtained data, it was computed that each stop consumes 168 NL of CA and 4.96 L of diesel daily, which translates to 4.4 per cent of the total fuel consumed. A sensitivity analysis was also performed in order to determine how the system reacts whilst varying multiple parameters. From this assessment it could be concluded that the maximum possible value for the pneumatic fuel consumption due to possible variations is 5.3 per cent. Ultimately, this chapter made it possible to answer research question one, enabling the quantification of energy and fuel required to operate a typical BPS.

Chapter 6 – Experimental Procedure for a BPS Test Bed

Based on the literature and state of the art review, and actual data collected from a BPS as presented in Chapters 3, 4 and 5, a better understanding of BPSs was acquired. This information paved the way to develop the experimental design which would be used to answer the remaining research questions, i.e. to determine the effects that different parameters pose on the performance of the BPS and the factors that can be used to identify and quantify the presence of faults. In this chapter, details will be provided about the development of the experiment, comprising of the experimental procedure and the set-up, utilised to perform the simulations.

6.1 Experimental Approach

The first step towards performing the simulations was to comprehend what had to be represented during the experiments hence acknowledging the hardware and cyber elements required to complete the devised experiments. This section delves into the different stages required to complete the experimental procedure.

6.1.1 Design of Experiment

In order to adequately comprehend the interactions between the input factors and the recorded output responses, multiple experiments had to be performed whilst systematically altering the input factors. This design process entails different stages and so, in this subsection, one finds all the elements required to complete the experimental design process, so as to observe in detail the interactions taking place.

6.1.1.1 Experimental Aim

As aforementioned, the information compiled in the previous chapters would help in developing the required experiments. Consequently, the aim of this study was to be able to factually answer the research questions by devising a realistic scenario to be performed during the tests using an adequate set-up. This would make it possible to better understand the behaviour of BPSs, whilst establishing and quantifying the factors which significantly affect it.

6.1.1.2 Experimental Limitations

Before commencing the experimental design process, it was important to determine the limitations inherent to the experiments performed. These include;

1. The system pressure was limited to 6 bar since the compressor used in the Industrial Automation Lab at the University of Malta supplies CA at a maximum of 7.2 bar. Another compressor, similar to those found in buses, was supposed to be used however, it was not delivered due to the supply issues.
2. Due to the space limitations imposed by the lab, an actual bus set-up could not be used.
3. The air brake sub-system was not included due to its complexity and the limited space available.
4. The curb weight of a bus is typically around 12 tonnes which was not possible to replicate with the given space restrictions.

6.1.1.3 Experimental Methodology

The first step towards developing the tests was to choose the scenario to be performed during the simulations. From the tests performed in Chapter 5, it could be determined that during a bus stop, various actuations take place, with the main constituents being the pneumatic cylinders and the suspension bellows. This meant that whilst the vehicle is at a bus stop, multiple actuations take place repeatedly on a regular basis, ensuing the consumption of a considerable amount of CA. For this reason, it was deemed appropriate that this scenario would be depicted during the simulations, so as to help in better investigating BPSs, whilst also answering research questions two and three.

Bus Stop Scenario

As mentioned earlier, the tests to be performed during the simulations will all depict the bus stop scenario. Consequently, this represents four main stages;

1. The doors are opened and the suspension bellows are deflated, making it easier for the passengers to leave and board the vehicle.
2. A time delay to allow sufficient time for the passengers to enter and exit the vehicle.
3. Once all the passengers board the vehicle, the doors are closed whilst the suspension bellows are inflated to their original ride height.
4. A time delay until the vehicle reaches its next bus stop.

In order to replicate the mentioned stages, whilst also abiding by the dimensional restrictions imposed by the lab, it was not possible to use an actual bus set-up. For this reason, it was deemed appropriate that to perform the simulations, the following end effectors would be required;

1. Two double acting actuators, representing two sliding doors.
2. One bellow representing an air suspension system for a single front wheel.

By identifying the required end effectors, the actuations relating to each component could also be determined. The reason being that although the actuations for the double acting actuators were quite simple, as they could only be fully extended or fully retracted, this was not the case for the bellow since it could be stopped at intermediate positions. This is made possible by using the ECAS valve, whereby it regulates the CA flow inside the bellow. To better comprehend the bellow's actuations, Figure 6.1 provides an illustration of the three most common pre-set height positions that it can adjust to.

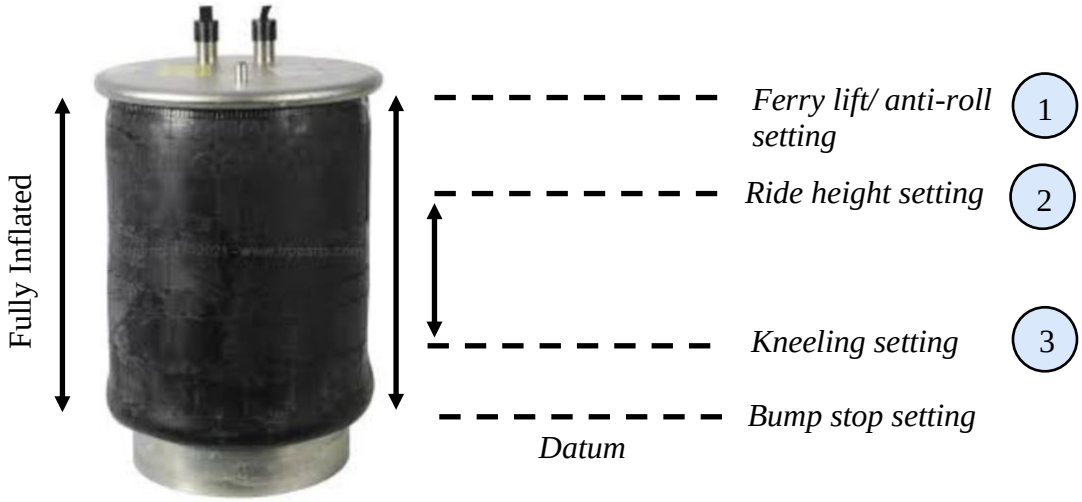

Figure 6.1: The common pre-set height positions used for the bellow.

The first setting offers two functionalities and occurs when the bellow is fully inflated. It is either used when the vehicle is boarding a ferry, so as not to scrape its undercarriage or to activate the anti-roll function. The latter is mainly used when the vehicle is turning alongside a bend and in order to keep the vehicle steady, where the height of the bellows are modulated to prevent the vehicle from rolling.

The second setting is the most used setting and is usually around 80 mm lower than the previous one. This is the height that the bus utilises whilst it's being driven and offers a balance between ride comfort and handling.

The final height setting, whilst the vehicle is in use, is the kneeling setting and is around 100 mm shorter than the second position. This is the lowest setting, apart from the bump stop setting, making it easier for people to enter and alight from the vehicle.

To replicate the bus stop scenario, the bellow has to transition from the ride height setting (*Position 2)* to the kneeling setting (*Position 3*) and vice versa, whereby, as stated earlier, an actual bus makes use of the ECAS valve to handle these settings. This solution however, was not possible to replicate during the simulations since an actual bus set-up could not be used. As a result, the chosen solution was to modulate the pressure inside the bellow, which will be discussed in detail further on in this section.

By obtaining a better understanding of the actuators to be utilised and how they would be actuated, the experiment could be developed to emulate the bus stop scenario. Table 6-1 summarises all the actuations during the experiments.

Table 6-1: A summary of the actuations taking place during the bus stop scenario.

Stage	Performed Actuations	Depicted Situation
A	• Double acting actuators; From fully retracted to fully extended. • Bellow; From *Position 2* to *Position 3*.	• Opening the doors and bellow kneels so as passengers can enter/leave the vehicle.
B	• Five second time delay	• Arbitrary time for passengers to enter vehicle.
C	• Double acting actuator; From fully extended to fully retracted. • Bellow; From *Position 3* to *Position 2*.	• The doors are closed and the bellow is inflated to its original ride height.
D	• Five second time delay	• Arbitrary time for vehicle to reach its next stop.

6.1.1.4 Process Factors

As attested by J.Antony [103], the main purpose for performing an experiment is to be able to alter various parameters in a controlled manner, so as to comprehend the system's behaviour. By identifying the experiments to be simulated, the next step was

to establish the experimental process factors to be altered. These could be categorised into two:

- Operational Input Factors
    - Bellow pressure and actuation sequence

- Fault Oriented Input Factors
    - Leakage diameter and faulty components

These two types of factors were chosen due to the fact that these made it possible to understand the system's behaviour whilst altering functional aspects associated with the operation of the BPS and also the effects imposed by different fault sources. Additionally, the output factors: system pressure, CA flow rate and cycle time will also be used to monitor the system's performance whilst altering the input parameters.

Rationale of Process Factors

During the tests, it was deemed appropriate to alter four input parameters, two operational and two fault oriented, in order to measure their response via the output factors. Below, one can find the rationale for the selection of all these factors.

Operational Factors

Bellow Pressure

During its service, a bus utilises its ECAS valve to regulate the vehicle's height in order to retain its ride height and perform the kneeling function. This works by constantly monitoring the bus's height and adjusting it accordingly. As stated in *Section 6.1.1.2* it was not possible to use an actual bus for the experiments therefore, another method had to be devised in order to replicate the function of such a set-up.

It is known that in order to increase the ride height, the ECAS valve provides CA to the bellow to inflate it, whilst deflating it to decrease its height. Whilst the bellow is expanded and retracted, the pressure inside the component is constantly being varied, due to the fact that the volume of CA inside it is also changing. To further understand this aspect, it is good to recall Figure 2.6, which illustrates the bellow during both settings, highlighting the difference in volume. From this figure, it could be seen that during the ride height setting, the volume of CA inside the component was increased, making it expand, whilst during the kneeling setting, the volume of CA inside it

decreased, contributing to the decrease in its height. This change in volume also affects the force exerted by the bellow, since during inflation, the force is increased, whilst during deflation, the force is decreased. This force modulation makes it possible to counter act external forces, such as the weight of people boarding the vehicle. For this reason, it was deemed appropriate that in order to depict the kneeling and ride height settings, the bellow's pressure would be adjusted accordingly. This would make it possible to investigate the constituent's behaviour whilst varying its pressure. In order to understand the forces being exerted whilst the component is being inflated/deflated, the bellow found in the set-up by M.Borg [17] was utilised. Figure 6.2 [35] provides the graph supplied by the manufacturer, showing the typical behaviour of the constituent.

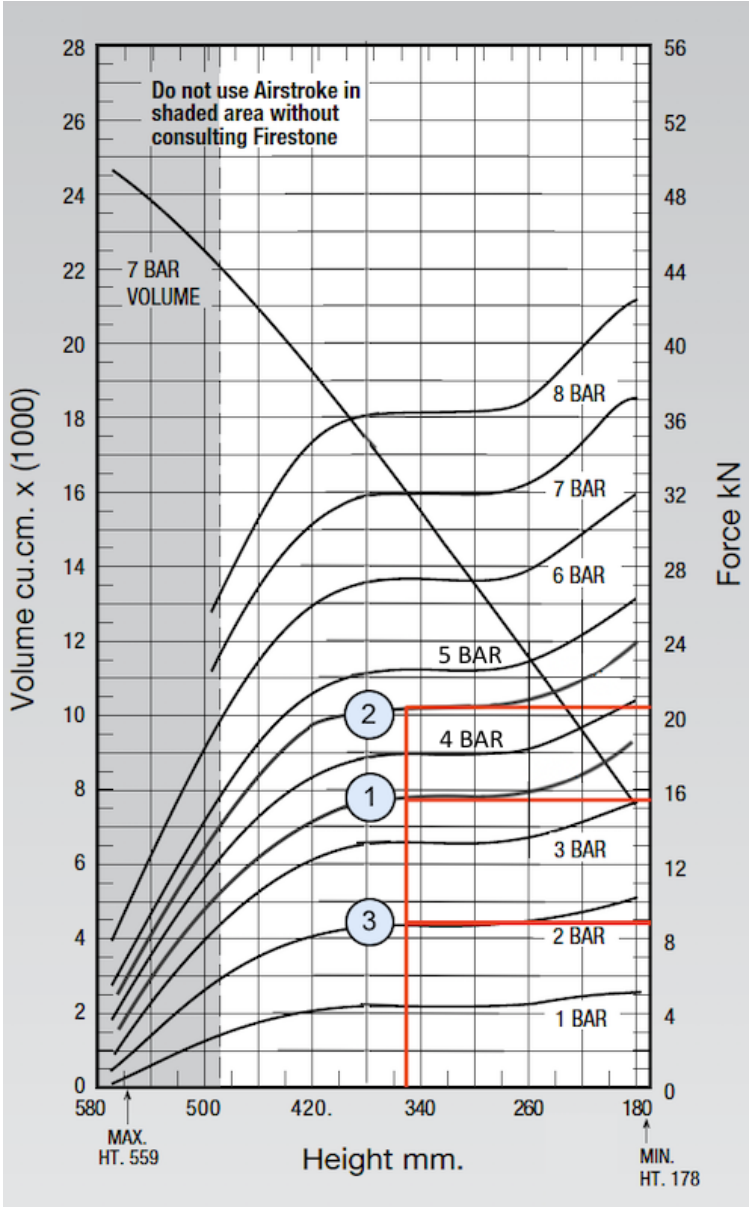

Figure 6.2: The force characteristics for the chosen bellow [35].

With regards to ride height, although not every bus has the same setting, it generally varies between 320 mm and 380 mm. Therefore, during the simulations, a ride height of 350 mm was utilised [28]. Consequently, the chosen bellow pressures were set at 3.5 and 4.5 bar whilst inflated at its ride height setting, in order to simulate different bus loading. These specific pressures were chosen due to the fact that the compressor available at the lab operated at a maximum pressure of 7.2 bar. Therefore, these pre-set pressures ensured that the system operated reliably. By referring to Figure 6.2, the force exerted for each of these pressures could be determined, with point 1 indicating the force at 3.5 bar (i.e.15.5 kN), whilst point 2 indicating the force at 4.5 bar (i.e. 20.5 kN). Through literature, it could also be determined that whilst the bellow is in its kneeling setting, the pressure can vary from 1.5 bar to 2.5 bar, depending on the vehicle [28]. For this reason, the kneeling pressure during the simulations was set to 2 bar. At this pressure, the force exerted by the bellow amounts to 9 kN and is indicated by point 3 in the graph. This is made possible due to the fact that during kneeling, the weight of the bus is not fully supported by the bellow but rather shared by the axle, chassis and shock absorbers. This, allows the bellow not to further compress itself hence maintaining the 2 bar pressure [116].

Sequence of Actuations

As aforementioned, once all the passengers have boarded or left the vehicle and the bus is ready to continue with its journey, the doors are closed and the bellow's height is restored to its original ride setting. In order to do so, the driver has to press two sets of buttons, one to retract the cylinders and the other to inflate the bellow, as shown in Figure 6.3. For this reason, the sequence of the actuations depends on how the driver chooses to press these buttons, i.e. either *simultaneous*, which operates both constituents together, or *separately*, which operates the cylinders and the bellows consecutively. Therefore, this aspect was also investigated during the simulations, making it possible to investigate the effects, if any, that the actuation sequence posed on the BPS.

Figure 6.3: The buttons used to operate the auxiliaries.

Fault Oriented Factors

Leakage Diameter

The impacts of leaks on CAS were well discussed in *Section 3.3.1*. Therefore, during this test, it was beneficial to further investigate the impacts imposed by leaks with regards to BPSs. During the simulations, the leakage diameter could be altered between two values, either 0 mm or 0.82 mm. This was done using metal piping with drilled holes, with further detail about this set-up explained throughout the study. The former represented a scenario where the system was fault-free therefore, no leaks were present, whilst the latter conveyed a scenario where a fault was present in the form of a system leak.

Faulty Actuator

In order to understand the impacts that faults have on BPSs, it was deemed appropriate to also introduce another fault aspect, mainly in the form of a defective component. From the literature in *Section 3.3.1*, it was determined that one prevalent form of wear in double acting actuators is seal wear. For this reason, the fault to be simulated was wear in the piston seal, for one of the double acting actuators. Recalling Figure 3.6 [117] from the previously mentioned section, this seal is the one seated into the piston, which consequently moves with the piston during extension and retraction. Furthermore, during the simulations, two double acting actuators were used, i.e. either two fault-free actuators, or one fully functional and one faulty, so as to compare the performance between them. As a result, the total number of double acting actuators required for the set-up were three.

In Table 6-2, one can find the chosen input factors summarised.

Table 6-2: The input parameters to be altered during the simulations

	Input Parameters	**Different Parametric Alternatives**	
Operational Factors	Bellow Pressure	4.5 bar	3.5 bar
	Actuation Sequence	*Simultaneous*	*Separate*
Fault Oriented Factors	Leakage Diameter	0	0.82 mm
	Faulty Actuator	No	Yes

Output Factors

In order to identify any occurring interactions, so as to comprehend the system's behaviour, output parameters would need to be recorded. By, looking at the studies by K.Abela [18] and M.Borg [17], discussed in *Section 3.6*, it was established that three parameters were important in order to adequately monitor a pneumatic system since they encapsulate the surveillance of various elements of the set-up. These are:

- System pressure;
- CA flow rate;
- Cycle time.

In addition, during the simulations, the bellow pressure had to be modulated and to do so, the pressure inside the component had to be monitored. Consequently, a total of four parameters were altered during the experiments, with Table 6-3 providing detail on which sensors were required to adequately monitor these factors.

Table 6-3: The output factors to be monitored during the simulations.

Output Factor	**Required Sensor**	**Measured Units**
System Pressure	Pressure Transducer	bar
CA Flow	Air Flow Sensor	NL/min
Cylinder Actuation Time	Reed Switches	s
Bellow Pressure	Pressure Transducer	bar

6.1.1.5 Sources of Error

During all the simulations, an uncontrollable element of error was always present, with the main one being the variations in the ambient pressure. This directly contributes to changes in the CA temperature which may result in variations in the recorded values. In order to try and mitigate the occurrence of such variations, the following two procedures were performed;

1. The lab was well ventilated, to ensure adequate ventilation for the set-up.
2. Throughout all tests, the temperature of the lab was kept constant by using an air-conditioning system.

Additionally, all experiments were performed within the same five-hour time interval. This was done to not only minimise the variations in ambient temperature but also to keep constant the atmospheric pressure and humidity, which can also have an effect on the recorded results. The final precautionary measure was to perform an additional cycle per experiment to compensate for any pressure fluctuations which may have resulted whilst the set-up was not in use, whilst also doing three repeats per experiment to account for any variations between repeats.

By establishing the input factors to be altered, the output parameters to be logged and the factors which may inadvertently affect the results, the DOE was completed. Figure 6.4 summarises all of the factors in question whilst performing the experiments.

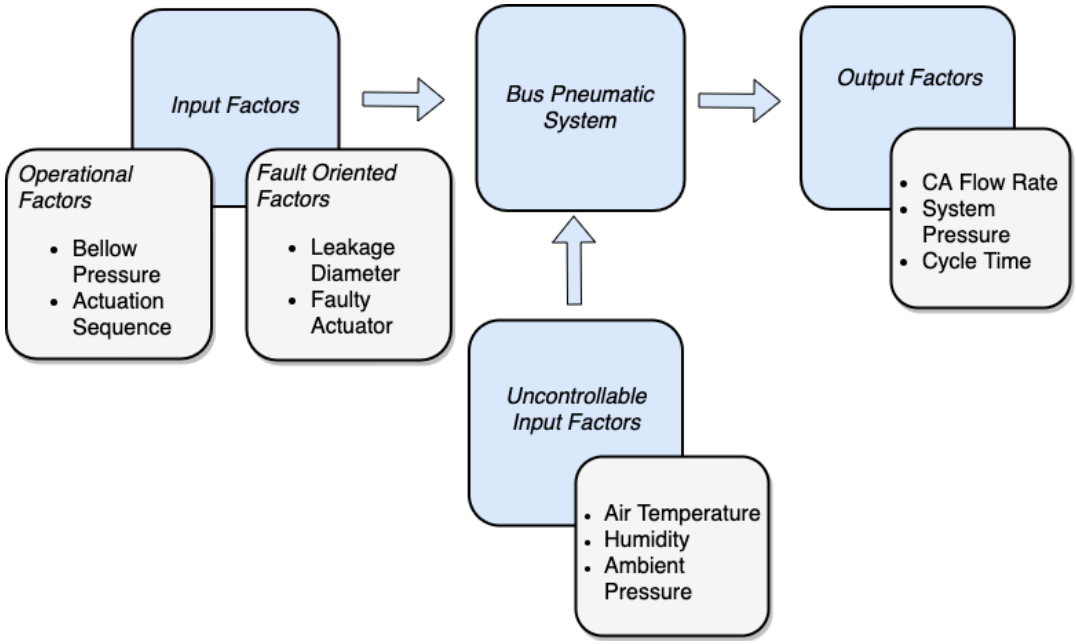

Figure 6.4: All the of the factors involved during the experiment.

6.1.1.6 Experiment Runs

Whilst performing the simulations, a control experiment would first be performed, before altering the previously mentioned parameters. This would represent a BPS in perfect working order, allowing one to establish benchmark values which would be used throughout the remainder of the study. As a result, the leakage diameter would be set to 0 mm, the sequence of actuations would be set as *simultaneous*, the bellow pressure set to 4.5 bar and the state of all actuators would be fault-free. Once this experiment is performed, the parameters could then be altered and in Table 6-4, one can find all the experiments that would be performed.

Table 6-4: The experiments to be performed during the study, together with their input factors.

Leakage Diameter (mm)	Sequence of Actuations	Faulty Components	Bellow Pressure (bar)
0	*Simultaneous*	No	4.5
0.82	*Simultaneous*	No	4.5
0	*Separate*	No	4.5
0.82	*Separate*	No	4.5
0	*Simultaneous*	Yes	4.5
0.82	*Simultaneous*	Yes	4.5
0	*Separate*	Yes	4.5
0.82	*Separate*	Yes	4.5
0	*Simultaneous*	No	4.5
0.82	*Simultaneous*	No	3.5
0	*Separate*	No	3.5
0.82	*Separate*	No	3.5
0	*Simultaneous*	Yes	3.5
0.82	*Simultaneous*	Yes	3.5
0	*Separate*	Yes	3.5
0.82	*Separate*	Yes	3.5

6.2 Experimental Set-Up

Once the design of experiment process was completed, together with identifying the process factors to be altered and monitored, it was possible to better comprehend what

was required to perform the simulations. Therefore, the next step involved the development of the set-up to be used.

To develop the required set-up, two pre-designed systems were used: the bus pneumatic test bed (BPTB) by M.Borg [17], which is the same researcher as this study, and the compressed air test bed (CATB) by K.Abela [18]. This offered the foundation for set-up providing the following two elements:

1. Pneumatic Subsystem;
2. Control Subsystem.

For this reason, this sub-section will be further divided to explain each subsystem in adequate detail, whilst also explaining any additions made to the systems.

6.2.1 Pneumatic Subsystem

As the name entails, this subsystem encompasses all the equipment relating to the pneumatic side of the system. The schematic in Figure 6.5 illustrates all the pneumatic components used for the simulations.

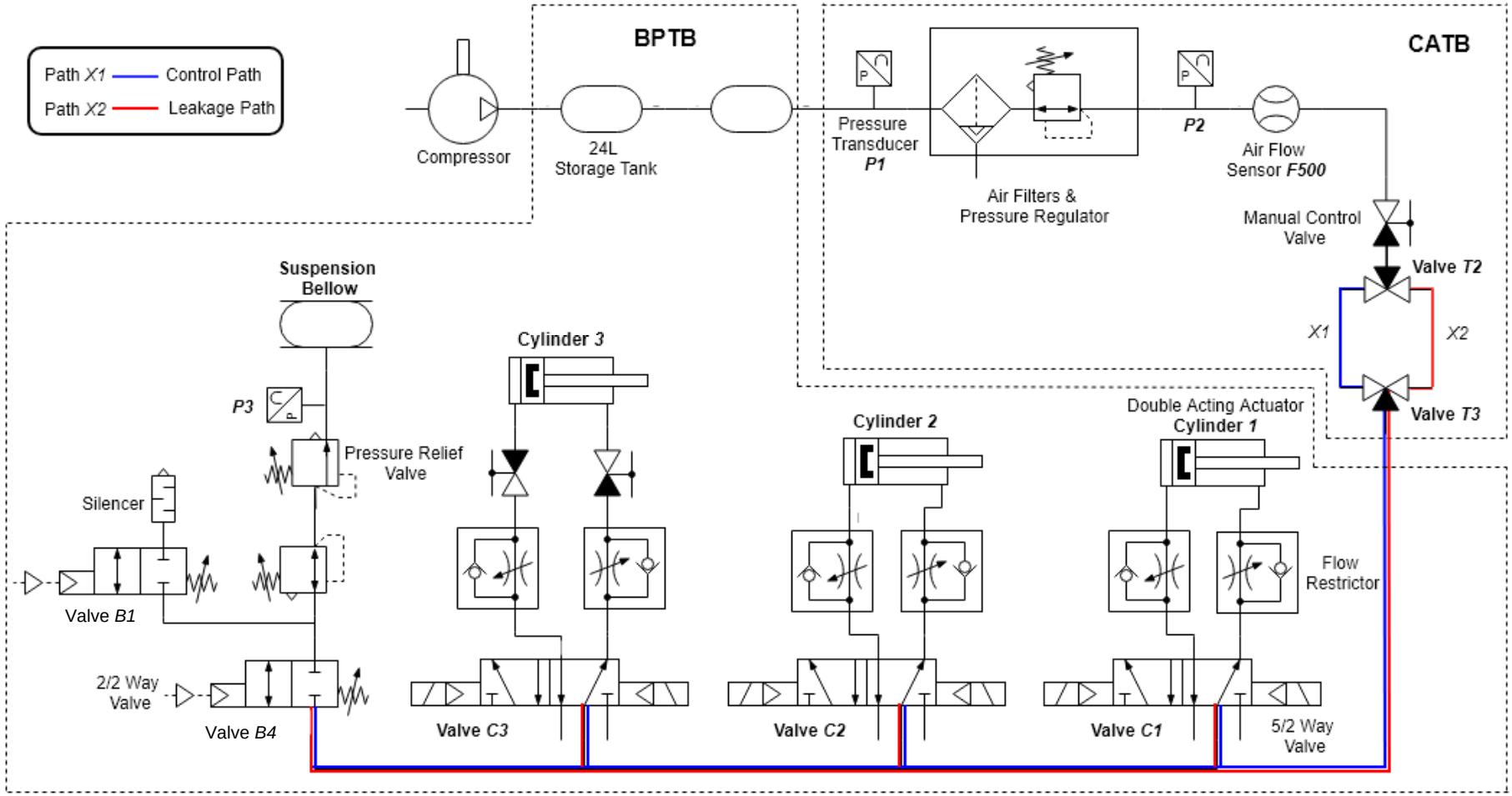

Figure 6.5: The pneumatic schematic of the set-up.

From Figure 6.5, it could be noted that CA flows through different stages along the whole set-up, starting from the generation of CA, up to the end uses. Therefore, the process started with the air generation stage, producing CA via the compressor and stored into two 24 L air tanks. The CA was then transferred throughout the whole set-up via pipes and fittings situated in the air distribution stage and through the air preparation stage, where three sets of filters and a pressure regulator were tasked to condition and filter the CA, making it useable for the other components.

In order to introduce leaks into the system, the leakage simulation stage was introduced. This entailed making use of valves, *T2* and *T3*, which were responsible for guiding the CA towards paths *X1* or *X2*. To better understand this concept, Figure 6.6 [18] shows an illustration of the set-up. To induce leakages, a metal pipe, with a drilled hole of diameter 0.82mm, was introduced in path *X2* and this was fitted via push fittings. Additionally, *T3* was the point where the CATB was connected to the BPTB.

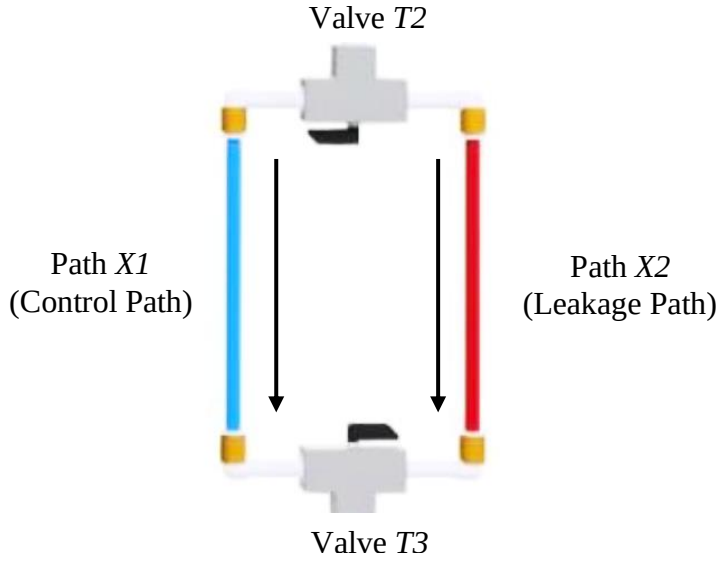

Figure 6.6: The set-up used to introduce the 0.82mm system

The final stage was the end usage stage and this contained all the end effectors. To actuate these constituents, 5/2 way solenoid valves (i.e. Valves *C1, C2 and C3*) were used to control the three double acting actuators, whilst the bellow was actuated via two 2/2 way solenoid valves (i.e. Valves *B1* and *B4*). The reason for using two valves for the bellow was so that Valve *B1* would inflate the component whilst Valve *B4* would exhaust air, hence deflating it. In order to control the speed of the actuations, each double acting actuator was also equipped with two flow restrictors, whereby one was tasked to control the speed of the extension whilst the other, to control the retraction. For the faulty cylinder (i.e. Cylinder *3*), two two-way ball valves were also included so that each port could be closed, hence ensuring that no leaks were present

when it was not in use. With regards to the bellow, care was taken to ensure outmost safety whilst it was used. Therefore, it was also deemed appropriate to add a pressure regulator, pressure relief valve and flow restrictor, upstream to the component. The reason being that the former allowed for direct pressure control whilst the latter, exhausted CA in the case of excessive pressure build up. For the required application, the pressure setting for the relief valve was set at 6 bar.

Throughout the set-up it could also be noted that various sensors were used. Firstly, pressure sensor *P1*, was utilised to monitor the pressure of the CA being supplied by the compressor, whilst pressure sensor *P2* was utilised to monitor the pressure post conditioning, i.e. the system pressure. Another transducer was also added (i.e. *P3*) which was responsible for monitoring the pressure inside the bellow. The CA flow rate was monitored and to do so, flow meter *F500* was used to measure the CA flow rate for the system. To summarise the whole pneumatic set-up, Table 6-5 includes all the equipment that was used for the simulations.

Table 6-5: All the pneumatic equipment used from both pre-designed set-ups.

Constituent	Quantity	Set-up Component Position
24L Storage Tank	2	BPTB
Pressure Regulator	2	BPTB & CATB
10μm Air Filter	1	CATB
3μm Air Filter	1	CATB
0.01μm Air Filter	1	CATB
1/8” Three-way valve	2	CATB
Aluminium Pipe with hole ø0.82mm	1	CATB
5/2 Way Solenoid Valve	3	BPTB
2/2 Way Solenoid Valve	2	BPTB
New Double Acting Actuator	2	BPTB
Faulty Double Acting Actuator	1	BPTB
Suspension Bellow	1	BPTB
Flow Restrictor	7	BPTB
Pressure Relief Valve	1	BPTB
Two-Way Valve	2	BPTB
5-500 NL/min Air Flow Meter	1	CATB
0-10 bar Pressure Transducer	3	BPTB & CATB

6.2.2 Control Subsystem

In order to systematically actuate the pneumatic actuators, and to use the recording equipment mentioned previously, a control system was required. Therefore, the purpose of this system was to interface all of the equipment and comprised of the following three main components:

1. Interfacing devices
2. Input devices
3. Output devices

These were all integrated together as shown in the schematic in Figure 6.7.

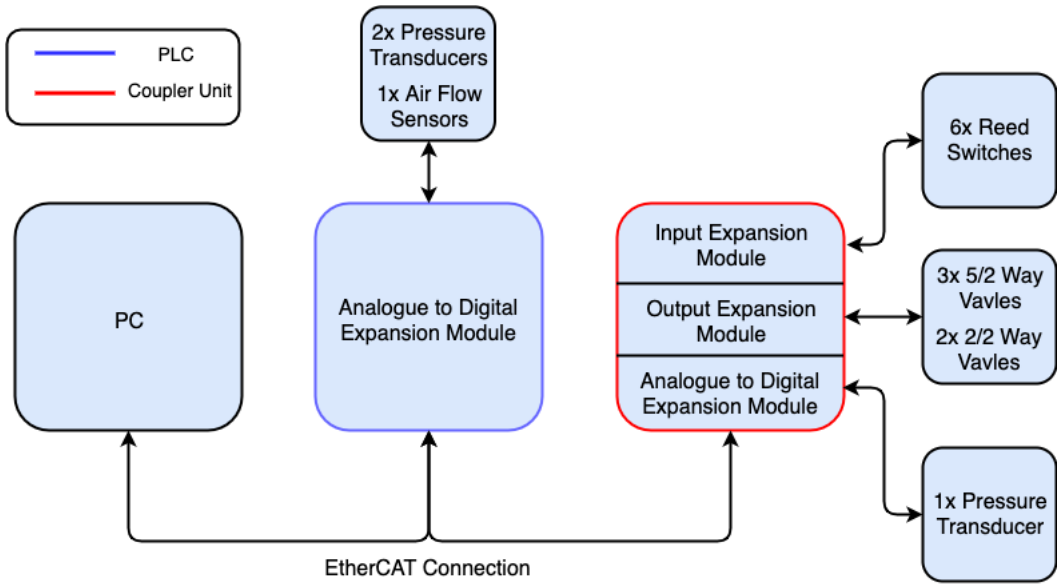

Figure 6.7: The schematic for the control equipment.

With regards to the input devices, two types were used in the set-up: reed switches and measuring sensors. The reed switches were responsible for detecting the position of the double acting actuators whereby, two of these were required for each actuator, one to provide a signal when the component was fully extended and the other to provide a signal when it was fully retracted. The second type of input devices were the sensors mentioned in the previous section, which included the air flow sensors and pressure transducers. With regards to transducers *P1* and *P2*, two different sensors were utilised. The reason being that since the system pressure was one of the main output parameters to be monitored (i.e. *P2*), the accuracy required for this measurement was more than that for the unregulated pressure (i.e. *P1*), with further detail about this aspect being discussed throughout the study. Similarly, the transducer added to monitor the bellow's pressure (i.e. *P3*) did not require the same amount of accuracy as that of *P2* since it would only be used to achieve the desired pre-set cut of pressures.

Therefore, the same sensor was chosen, as that of *P1*. In contrast with the previously mentioned devices, output devices convert a signal into a particular action and two types were included: 5/2 way and 2/2 way solenoid valves, used to actuate their respective actuator, as highlighted in the previous section.

The final type of control devices required to make the system functional were the interfacing constituents. These devices were responsible for integrating the input and output devices, whilst also allowing for data transfer between all parties. The main interfacing device was the programmable logic controller (PLC), and this could be considered as one of the main components of the system. The reason being that it was responsible for handling the data processing and the communication between the devices and the user, via a personal computer (PC). In order to better organise the wiring between both set-ups, a coupler unit was also used to connect the majority of the input and output devices to it. It is worth mentioning however, that to connect the input and output devices to this unit, expansion modules are required. Three of these modules were used, one for the measuring sensors, so as to convert the analogue readings into digital ones, one for the input devices and one for the output devices.

To summarise, Table 6-6 provides all the equipment encompassed in this section, together with the set-up by which they were located in.

Table 6-6: All the control equipment used from both pre-designed set-ups.

Device Type	Product Model	Quantity	Set-up Device Position
Input Devices			
Reed Switch	SMC D-M9PL	6	BPTB
Air Flow Sensor	Omron PFMB 7501	1	CATB
Pressure Transducer (*P1)*	WIKA Model S-10	1	CATB
Pressure Transducer (*P3*)	WIKA Model S-10	1	BPTB
Pressure Transducer (*P2*)	WIKA Model A-10	1	CATB
Output Devices			
5/2 Way Valve	SMC SY7220-5YO-02F-Q	3	BPTB
2/2 Way Valve	JORC FLUIDRAIN 1603	2	BPTB

Interfacing Devices			
Coupler Unit	Omron NX-EC2203	1	BPTB
PLC	Omron NX102-1020	1	CATB
Input Expansion Sleeve	Omron NX-ID5442	1	BPTB
Output Expansion Sleeve	Omron NX-OD5256	1	BPTB
Analogue to Digital Expansion Module	Omron NX-AD3208	1	CATB

6.3 Physical Set-Up

By being able to understand the overall system and the equipment used, the next step was to see how all the equipment, would be physically integrated into the set-up. To do so, Figure 6.8 depict renders for the CATB and BPTB. It is good to note that the equipment that was not labelled in the CATB was not used for this study.

To fit inside the lab, both set-ups were designed to be as compact as possible. To give perspective, the overall dimensions for the CATB were 1000 by 600 by 2000 mm whilst the BPTB was 800 by 700 by 2000 mm. Furthermore, it could also be noted that the CATB contained the main sensors for logging the parametric data, whilst the BPTB contained all of the end effectors used during the simulations. In order to connect both set-ups together, point A was the point where the CATB was connected to the tanks of the BPTB. Furthermore, the compressor and inverter were not installed since they were not delivered due to supply issues.

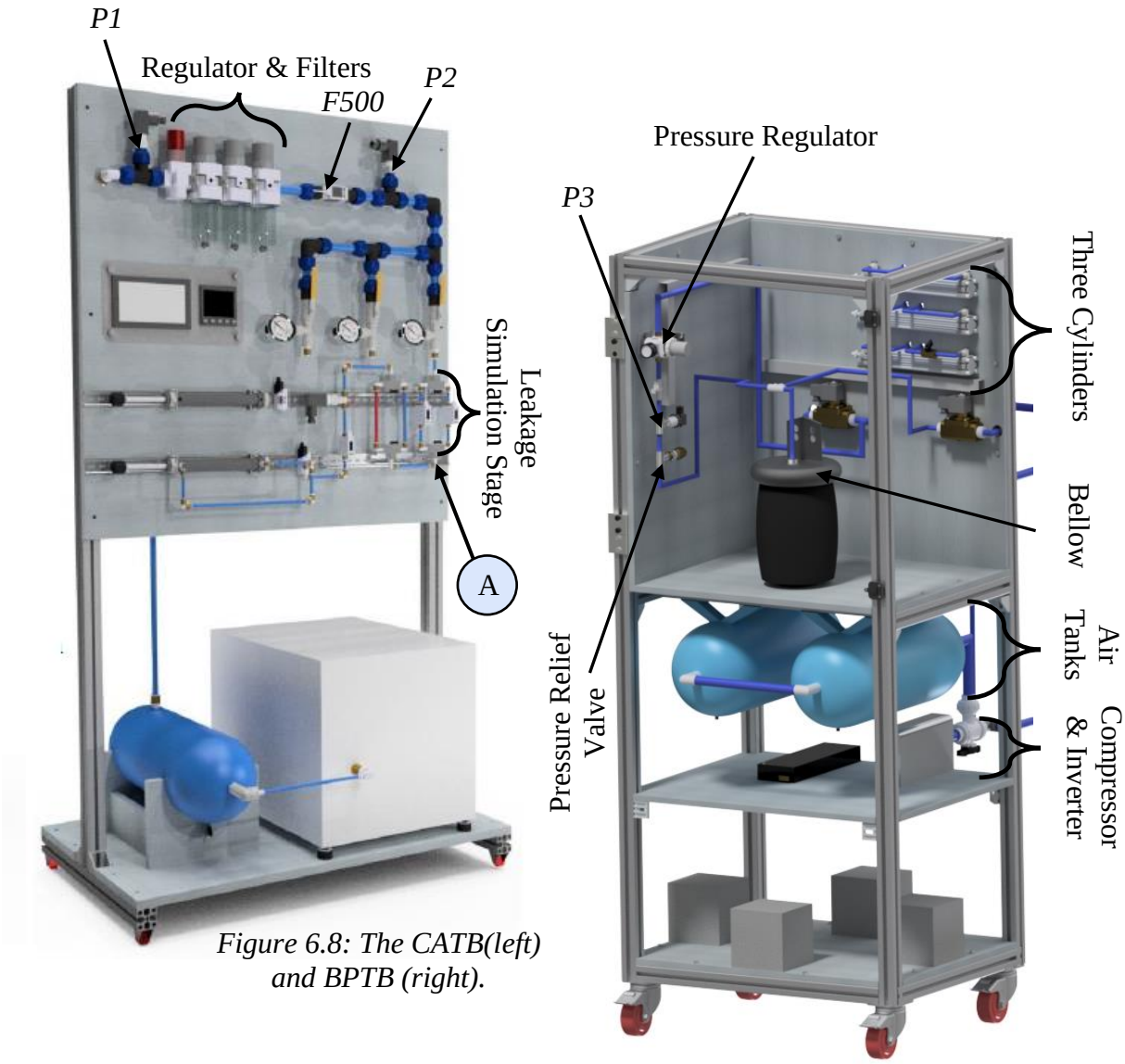

Figure 6.8: The CATB(left) and BPTB (right).

6.3.1 Bellow Frame Design

From the previous section, it could be established that the overall physical structure for both set-ups was deemed adequate for the intended application since they could store all of the required equipment. However, it was noticed that whilst analysing the bellow, there was no structure which was capable of offering an opposing force to it whilst at *Position 2*, as is done in an actual bus owing to its weight. For this reason, it was deemed appropriate to design and implement a frame structure which would be used during the simulations to fulfil these requirements. The following sub-sections will go through the design process of this frame.

Frame Specifications

As discussed in *Section 6.1.1.3*, the bellow inflates and deflates to alter the ride height of the vehicle. However, in a bus, the bellow also supports the vehicle's weight which provides a means to restrict the bellow from over extending. For this reason, a solution,

in the form of a frame, had to be devised so as to provide an opposing force. This frame had to serve the following functions:

1. Define and restrict the bellow's extension height;
2. A means of enclosure so as to offer an opposing force.

The designed frame was installed inside the BPTB therefore, it also had to comply with the imposed space restrictions. Table 6-7 outlines the dimensional specifications of this set-up.

Table 6-7: The space restrictions that the frame had to comply with.

Attribute	Specification
Length	≤ 640 mm
Width	≤ 540 mm
Height	≤ 840 mm

Conceptual Design

By determining the functional aspects and the dimensional specifications of the frame, the design process could commence. Whilst numerous designs were considered, three were drawn as the final contenders. The design for each of these concepts is shown in Figure 6.9.

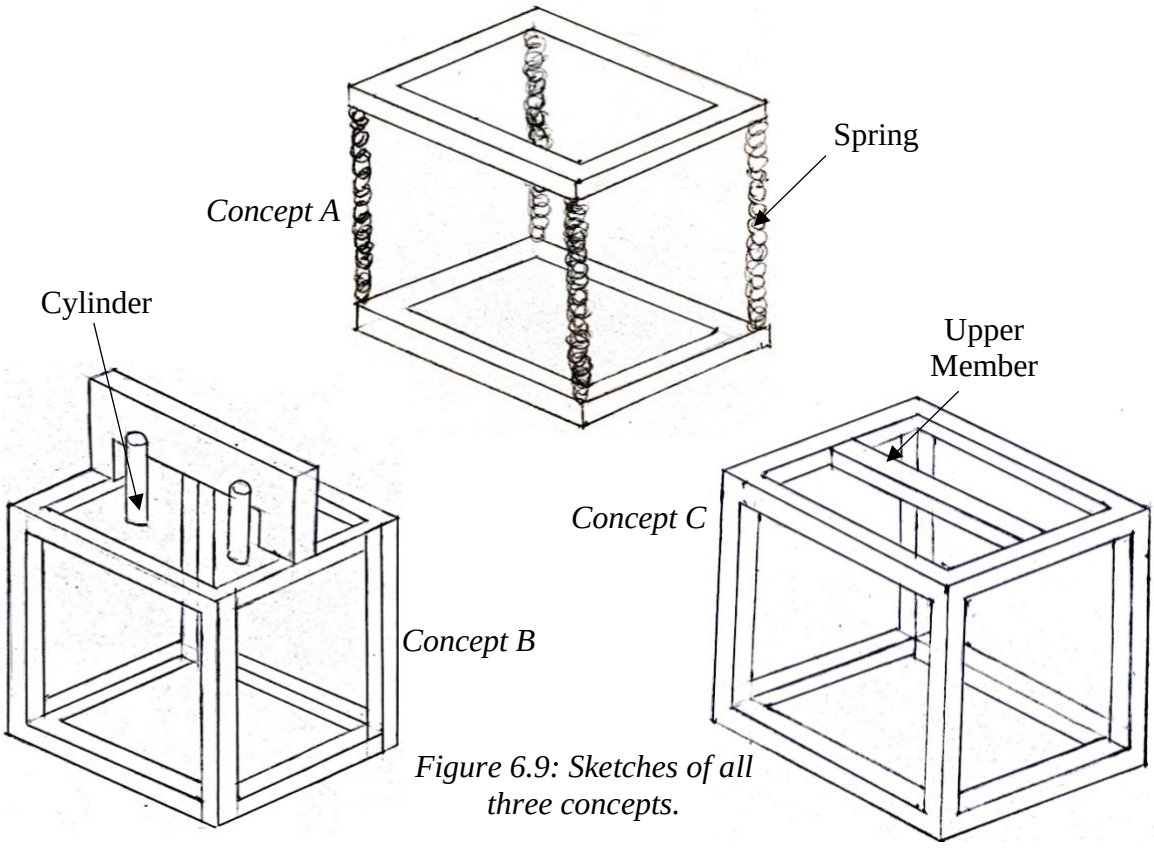

Figure 6.9: Sketches of all three concepts.

The premise of all three designs was a rectangular prism frame, making it possible to enclose the bellow. The difference between the three approaches was the way how the bus's weight would be replicated on to the bellow. In Concept A, the weight of the bus would be replicated using multiple springs placed across the frame offering a resistive opposing force during inflation, whilst Concept B would simulate this force using double acting actuators which act on top of the bellow. Concept C however, took a different approach since the weight would be simulated by the bellow itself. This is done by having a fixed member on top of the frame, offering an equal resistive force from the bellow, whilst being pressurised. In order to decide which concept would be most appropriate for the required application, the decision matrix found in Table 6-8, was used.

Table 6-8: The decision matrix to choose between concepts.

Property	Concept A	Concept B	Concept C
Safety	--	++	++
Compactness	-	-	+
Ease of assembly	-	-	+
Number of components	++	++	-

Where + is high and – is low

Ultimately, Concept C was chosen since it achieved the highest score in the decision matrix. The main advantages were that it was considerably safer than Concept A, since no springs would be required, and that it was significantly less bulky than both Concepts A and B, which needed large springs or double acting actuators to replicate the bus's weight.

Detailed Frame Design

The next step was to further evolve Concept C. However, in order to do so, the material used for its construction had to be chosen. From Figure 6.2, it was determined that the force exerted by the bellow whilst it is actuated at a maximum of 6 bar system pressure, at the chosen ride height (i.e. 350 mm), would be 2.75 tonnes. As a result, the material used had to cope with these forces. To compute such forces, the free body diagrams in Figure 6.10, Figure 6.11 and Figure 6.12 were used to better understand the forces on the upper portion of the frame. It is good to note that the dimensions for the vertical

members were set to 0.35 m in order to allow the bellow to elevate till that point, whilst the length of the horizontal member was set to 0.37 m, to allow it space to expand.

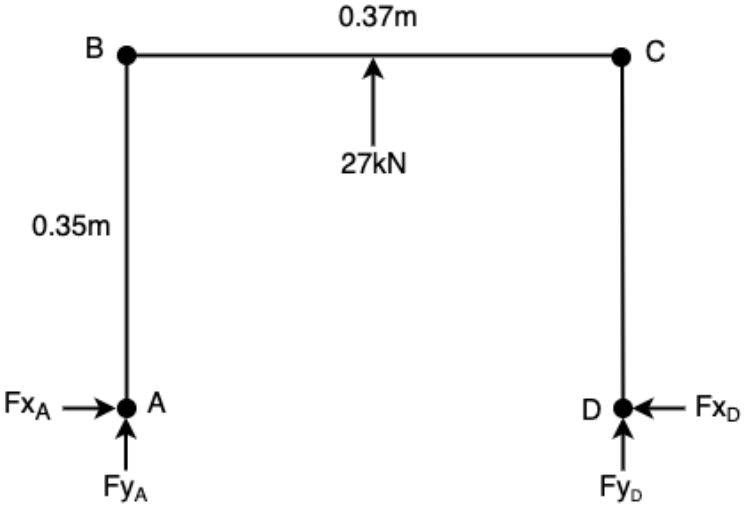

Figure 6.10: The free body diagram ABCD.

$$\Sigma F_y: Fy_A + Fy_D + 27 \times 10^3 = 0 \qquad \textit{Eq. 6.1}$$

$$\Sigma F_x: Fx_A = Fx_D \qquad \textit{Eq. 6.2}$$

Considering *ABC*

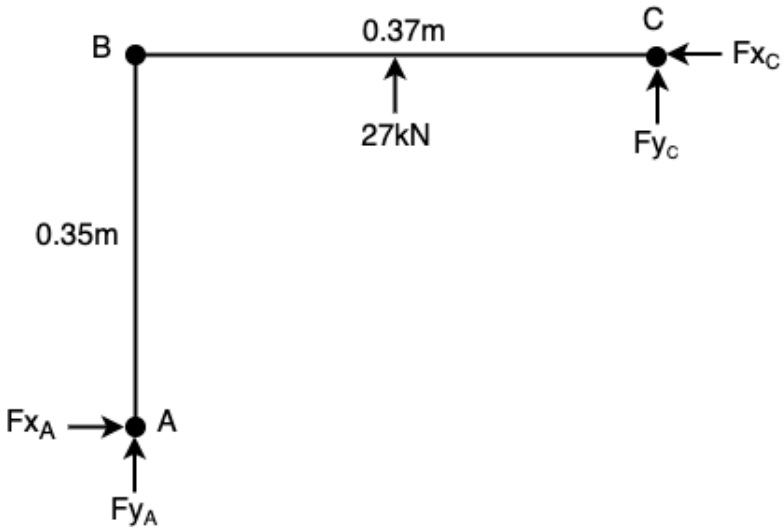

Figure 6.11: The free body diagram ABC.

$$\circlearrowright \Sigma M_A: -0.35Fx_C - 0.37Fy_C = 0.185 \times 27 \times 10^3 \qquad \textit{Eq. 6.3}$$

$$\circlearrowright \Sigma M_C: -0.35Fx_A + 0.37Fy_A = -0.185 \times 27 \times 10^3 \qquad \textit{Eq. 6.4}$$

$$\Sigma F_y: Fy_A = -27 \times 10^3 - Fy_C \qquad \textit{Eq. 6.5}$$

$$\Sigma F_x: Fx_C = Fx_A \qquad \textit{Eq. 6.6}$$

Substituting *Eq. 6.5* into *Eq. 6.4*

$$Fy_C = -13{,}500 - 0.95Fx_A \qquad \textit{Eq. 6.7}$$

Substituting *Eq. 6.7* into *Eq. 6.3*

$$\underline{Fx_A = 0\ N \therefore Fy_C = -13.5\ kN \ \therefore \ Fx_C = 0\ N \ \therefore Fy_A = -13.5\ kN}$$

Considering *BCD*

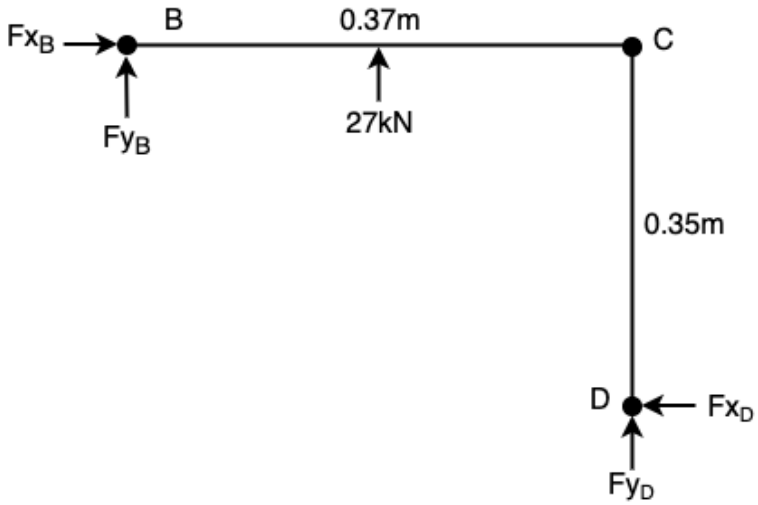

Figure 6.12: The free body diagram BCD.

By symmetry:

$$\underline{Fx_D = 0\ N\ \therefore Fy_D = -13.5\ kN\ \ \therefore\ Fx_B = \ 0\ N\ \ \therefore Fy_B = \ -13.5\ kN}$$

By being able to better understand the forces acting on the frame, it was possible to choose the material. In total three materials were considered: mild steel, carbon fibre, and aluminium. Ultimately, the chosen material was mild steel due to the fact that it comprised of adequate strength, was readily available and could be sourced relatively cheap.

It was also established, that the frame would comprise of two main elements:

1. Solid square sections;
2. Hollow square sections.

The solid square sections were utilised to take the majority of the bellow's impact and to be able to withstand this force, these sections were chosen to have a cross section of 40 x 40 mm. Four of these would be utilised, forming a band inside the frame, as highlighted in Figure 6.13.

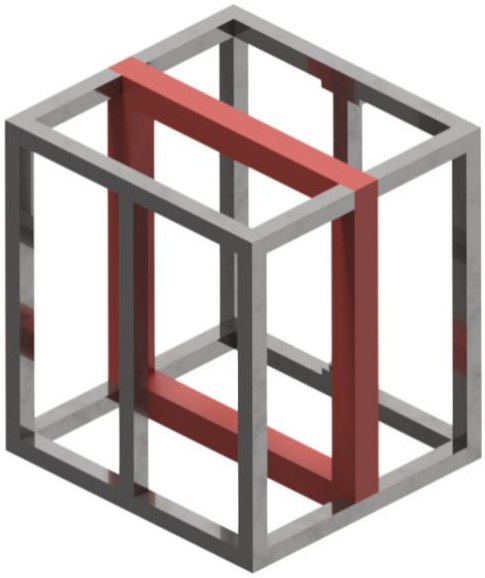

Figure 6.13: The frame structure with the highlighted solid square sections.

The remaining frame members were constructed using 25 x 25 mm hollow sections, with a wall thickness of 2 mm, making it possible to enclose the bellow. The reason for this selection was that these members are not subjected to as much force. By making use of these hollow sections, it did not only help in keeping the frame compact, but also decreased the overall weight of the frame by around 8 kg. It is also worth mentioning that one of the vertical hollow members was removable so as to make it possible to re-install or remove the bellow from the frame, as shown in Figure 6.14.

Figure 6.14: The finalised frame structure.

Ultimately, the overall dimensions of the set-up were 420 by 390 by 430 mm, adequately allowing for any inflation from the bellow, whilst also keeping in mind the imposed space restrictions. It is also good to note that in order to join the members together, welding was chosen as the solution. This is due to the fact that the weld penetrates through the metal hence offering additional structural rigidity. Furthermore this solution makes it possible to connect the members without drilling any holes, keeping the overall structural strength and integrity of the members intact.

Weld Sizing

Once the model was fully designed, the next step was to choose the weld size for the fillet welds to join each member. To do so, an FEA was performed using Autodesk Inventor. Through this analysis it could again be confirmed that the set-up was capable of withstanding the imposed forces, obtaining a safety factor of 1.6, which is adequate for the intended application since it is suggested that a safety factor of 1.5 or above should be used for structural frames [118].

The first step was to pinpoint the area which encounters the most stress whilst under loading. From the analysis performed, this was the area highlighted in Figure 6.15.

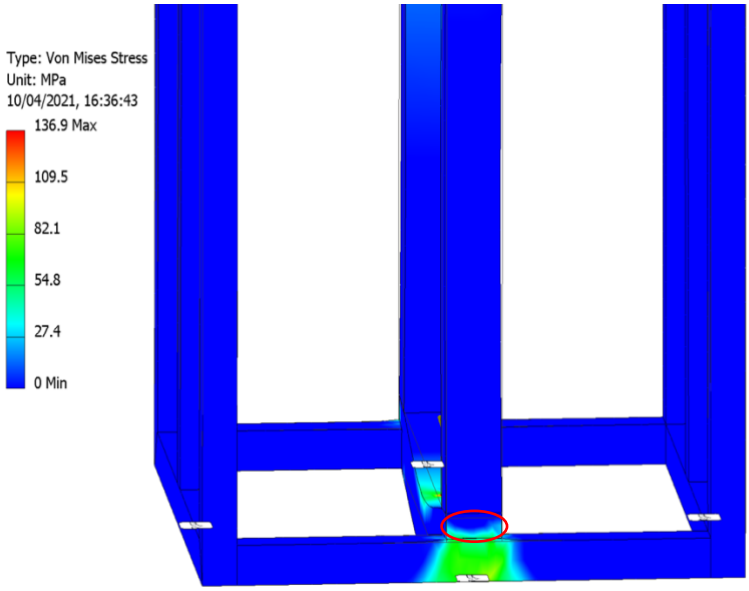

Figure 6.15: The highlighted area which encounters most stress during

By using the obtained results, the average stress experienced in this area was 43.5 MPa. This value was then converted into the force by using Equation 6.8.

$$\sigma = \frac{F}{A} \qquad \textit{Eq. 6.8}$$

Where σ = Stress experienced (Pa), F = Force experienced (N) and A = Cross-sectional area of effected member.

$$F = 43.5 \times 10^6 \times (0.04 \times 0.015)$$

$$\underline{F = 26.1\ kN}$$

By obtaining the force acting on these members and comprehending how these forces are distributed, as shown in Figure 6.16, the weld could be sized using Equation 6.9. Furthermore, Figure 6.17 illustrates the cross-sectional area of a fillet weld, which also helped in performing this calculation. It is also good to point out that the weld material

used was mild steel 6013, since it possesses adequate strength for this application, whilst being relatively inexpensive to purchase.

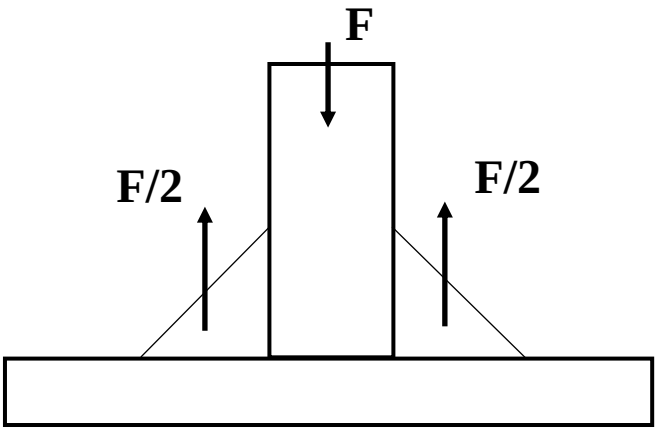

Figure 6.16: The forces acting on the fillet welds.

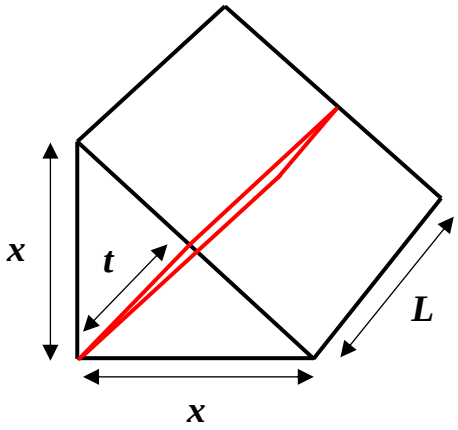

Figure 6.17: The dimension of one of the fillet welds together with cross-sectional area experiencing the force.

$$F = \frac{\sigma}{n} \times A \qquad \textit{Eq. 6.9}$$

Where: F = Force experienced (N), σ = Allowable weld stress (MPa), n = Design safety factor and A = Weld cross-sectional area that the force goes through (mm^2).

$$F = \frac{\sigma}{n} \times t \times L$$

Where: t = Weld throat (mm) and L = Length of weld (mm).

$$F = \frac{\sigma}{n} \times \sin(45) \times L \times x$$

Where: x = Size of weld (mm).

$$\frac{26.1 \times 10^3}{2} = \frac{410}{3} \times 0.707 \times 25 \times x$$

$$x = 5.40\ mm$$

$$\underline{\therefore x = 6\ mm}$$

Once the frame was fully designed, it was also important to ensure that it would adequately fit inside BPTB. In order to do so, the frame was rendered and mocked up inside the test-bed, as seen in Figure 6.18. Furthermore, Appendix 1 also includes a drawing of this frame.

Figure 6.18: The render of the finalised BPTB.

6.3.2 Implementation of the Set-up

By being able to finalise the design of the frame whilst also adding any additional elements required to make the set-up adequate for the study, the next step was to implement the set-up. In order to do so, both physical and digital implementations were required and in this section, detail will be given about both these elements.

6.3.2.1 Physical Implementation

The first step towards implementing the set-up was to complete the physical implementation of the system. As explained earlier in the study, the set-up made use of the CATB and the BPTB, with the former being mainly responsible for housing all the pneumatic end effectors relating to a typical BPS, whilst the latter contained the majority of the data monitoring equipment. During this stage, all the required

fabrication was completed and all the off-the shelf equipment was correctly installed and wired. Figure 6.19 shows the completed system which was located at the Industrial Automation Lab situated in the Faculty of Engineering at the University of Malta.

Figure 6.19: The finalised set-up comprising of the CATB (left) and the BPTB (right).

6.3.2.2 Digital Implementation

Following the completion of the set-up's physical implementation, the next step was to create a program capable of depicting the bus stop scenario, whilst also recording the required parameters during the simulations. In order to do so, Omron's Sysmac Studio was utilised to be able to adequately implement the system's digital elements.

Control Simulation Program

In order to depict the bus stop scenario using the BPTB, a program in the form of a ladder diagram, had to be created to instruct all the pneumatic equipment on when to actuate. Throughout this subsection, the main rungs of the program will be explained in detail. In Table 6-9 one can find the main variables used throughout the program.

Table 6-9: The main variables used throughout the program.

Variable Name	Representing function
B4	Solenoid valve responsible to inflate the bellow
B1	Solenoid valve responsible to deflate the bellow
R1R	Reed switch responsible to indicate the retraction of Cylinder *1*
R2R	Reed switch responsible to indicate the retraction of Cylinder *2*
R1E	Reed switch responsible to indicate the extension of Cylinder *1*
R2E	Reed switch responsible to indicate the extension of Cylinder *2*
C1E	Solenoid responsible to extend Cylinder *1*
C2E	Solenoid responsible to extend Cylinder *2*
C3E	Solenoid responsible to extend Cylinder *3*
C1R	Solenoid responsible to retract Cylinder *1*
C2R	Solenoid responsible to retract Cylinder *2*
C3R	Solenoid responsible to retract Cylinder *3*

The program commenced by pre-charging the bellow with CA whereby, solenoid valve *B4* was set (i.e. opened). This simulated the component to operate at ride height and rungs 0 to 3, shown in Figure 6.20, were dedicated to perform this function. It could be noted that in rung 1, a function block was created to limit the pressure inside the mentioned constituent, with the pressure being set at 4.5 bar. This was translated to a digital value of 13,499, so as to be understood by the PLC. Once the pressure was built up, the output fill was switched on in order to re-set (i.e. close) *B4*. Afterwards, in rung 3, a five second delay timer was also added so as to distinguish between the pre-charge phase and the start of the actual simulations.

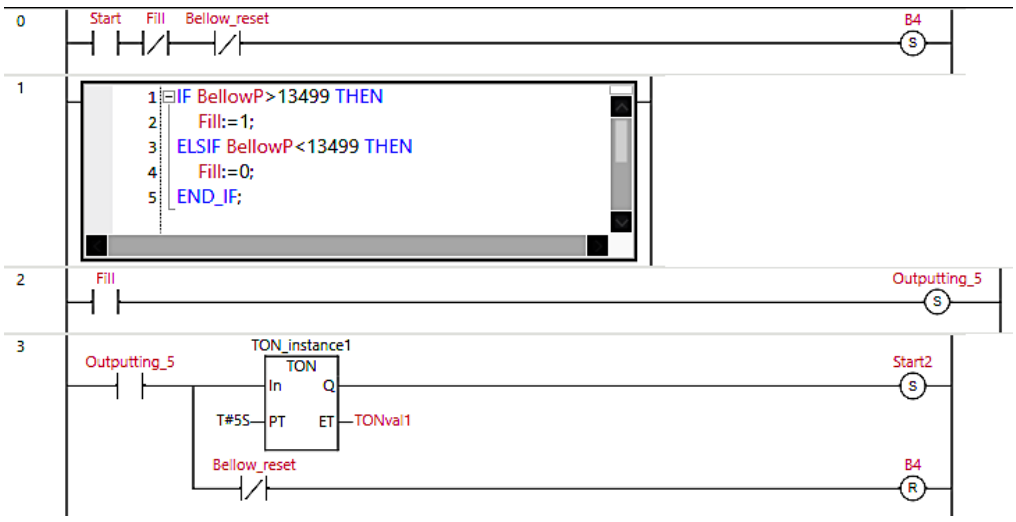

Figure 6.20: Rungs 0 to 3 for the control program.

In rung 4, the bus stop simulation commenced and the output *trans1* was switched on, resulting in both cylinders extending, by setting the solenoids *C1E* and *C2E*, and the bellow to deflate, by setting valve *B1*, simultaneously. This however, could only commence if both reed switches, *R1R* and *R2R* in rung 6, were on. Once both cylinders were fully extended, which was indicated when reed switches *R1E* and *R2E* were on, both cylinders stopped extending by resetting solenoids *C1E* and *C2E*. Additionally, the bellow stopped deflating when it reached a pressure of 2 bar, by de-energising *B1*, which was dictated by another function block. Figure 6.21 provides a snippet of rungs 4 till 6.

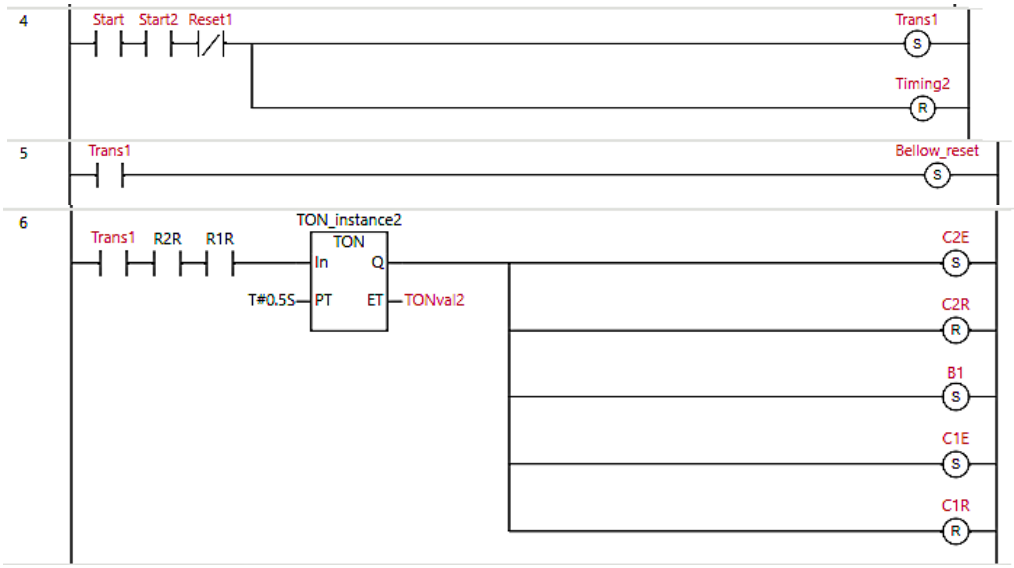

Figure 6.21: Rungs 4 to 6 for the control program.

Once the cylinders were opened and the bellow was deflated, an arbitrary timer of 5 seconds was added, which depicted the scenario of the passengers boarding or leaving the vehicle. Subsequently, when the time elapsed, both cylinders were retracted by switching on solenoids *C1R* and *C2R*, whilst simultaneously inflating the bellow, by switching on *B4*.

Finally, once the bus stop scenario was completed, which was instructed when both cylinders were retracted and the bellow stopped inflating, *Timing 2* was set, which also activated a 5 second timer, used to simulate when the bus was driving to its next stop. This variable also incremented the counter found in rung 19 and instructed the program to loop back to rung 1, in order to re-start the bus stop scenario. This looping was stopped when the pre-set counter value was elapsed, which was 31 bus stops, in order to include 10 runs per repeat, together with the extra pressurised run discussed in *Section 6.1.1.5*. Both rungs 19 and 20 can be seen in Figure 6.22. It is worth mentioning

that throughout the program, various short timers, such as the one in rung 6, were required so as to allow the PLC to switch on the required outputs.

Figure 6.22: Rungs 19 and 20 for the control program.

Additional Simulation Programs

The discussed program was for the control test, where both the double acting cylinders and the bellow were actuated simultaneously. However, in the case where these were actuated *separate*ly, minute program modifications were required. Such changes can be seen in Figure 6.23 where in rungs 13 and 14, both cylinders were instructed to retract and once this action was completed, outputs *R1R* and *R2R* were switched on, signalling the bellow to inflate via *B4*.

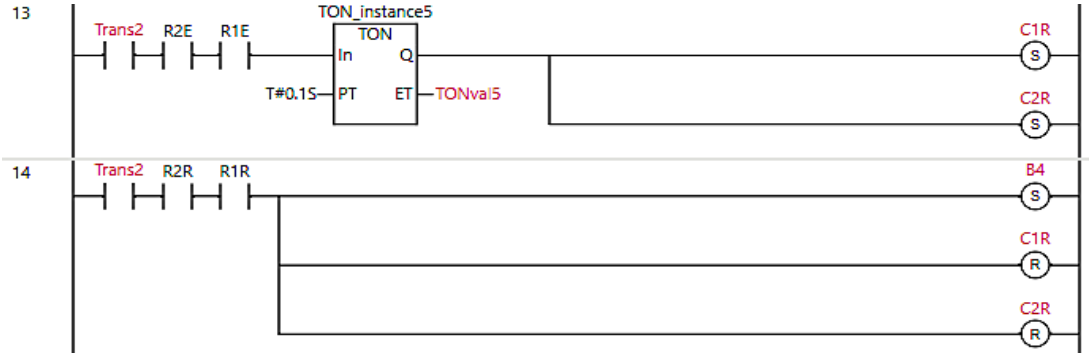

Figure 6.23: The changes required to make the actuators operate separately.

In the case where the faulty cylinder was utilised for the experiments, Cylinder *2* was replaced by Cylinder *3*. As a result, the program remained identical with the exception of changing the parameters associated with Cylinder *2* with those of Cylinder *3*. An instance of this can be seen in Figure 6.24, where the reed switch *R2E* was switched with *R3E* and *C2E* was swapped with *C3E*. Furthermore, in the simulations where the bellow ride height pressure was set to 3.5 bar, the program was left the same with the exception of adjusting the pressure values in function blocks accordingly.

Figure 6.24: The changes required to actuate Cylinder 3.

Data logging

Apart from developing the program tasked with actuating all the end effectors, care had to be taken to devise a system capable of recording all the required parameters during the simulations via the PLC. This was made possible using the Data Trace function provided by Sysmac Studio. During the experiments, two different types of data were logged: digital signals and analogue signals. The digital signals mainly involved the continuous switching of signals, such as the solenoid valves for the cylinders which were dictated by the signals of the reed switches. On the other hand, the analogue signals involved the data logging of the air flow sensor and the pressure transducers.

In order to record the data, the PLC had to be instructed on when it should log the required data and for this reason, the sampling interval was set to 40 milliseconds (ms). Other interval times were also considered however, it was determined that if the intervals were longer, the collected data would not have sufficient resolution, whilst if shortened, the amount of data collected would be too large to adequately analyse the data even though, a better resolution would be attained.

6.4 Conclusion

Throughout this chapter, the experimental and equipment set-up required to perform the BPS simulations was presented. In order to complete the experimental stage, two main elements were involved: the experimental procedure and the set-up itself. The first aspect dealt with all the components encompassing the actual experiments, establishing the scenario to be depicted and the parameters to be altered and recorded. On the other hand, the second aspect focused on the set-up used to perform the simulations. This entailed focusing on both the physical and cyber elements required to adequately perform the simulations. By doing so, the set-up paved the way to perform all the required simulations which would make it possible to answer research questions two and three.

Chapter 7-Results and Analysis

Following the completion of the set-up as presented in Chapter 6, the next step was to perform the devised bus stop simulations. This chapter delves into adequate detail regarding the analysis of the obtained results, using the chosen measured factors for the control scenario as a benchmark throughout all of the performed experiments. This would therefore make it possible to examine in detail the behaviour of such a pneumatic system. Additionally, the obtained data will also be compared with the data compiled in Chapter 5, in order to determine how a typical BPS performs as compared to the one constructed, whilst also investigating real life sustainable and financial repercussions, in order to fully answer research questions two and three.

7.1 Control Scenario

As discussed in Chapter 6, the first test to be performed was the control test, replicating a typical bus stop scenario. In order to depict such a situation, the input factors were set to those highlighted in Table 6-4, where no faults were introduced, the actuations were done *simultaneously* and the bellow pressure was set to 4.5 bar. As highlighted by M.Trompet [86], the importance of a benchmark test is to serve as a guide on how a system should perform. Thus, this data also served as a benchmark throughout the whole chapter, highlighting the operation of a typical fault-free bus stop scenario.

7.1.1 Control Experimental Data Plots

In order to better comprehend the behaviour of a fault free BPS, the data obtained from the whole duration of repeat one, for the control test, was scrutinised in detail.

The first step towards acknowledging the system's behaviour was to analyse the air flow and pressure readings. Figure 7.1 shows the plotted data for these readings.

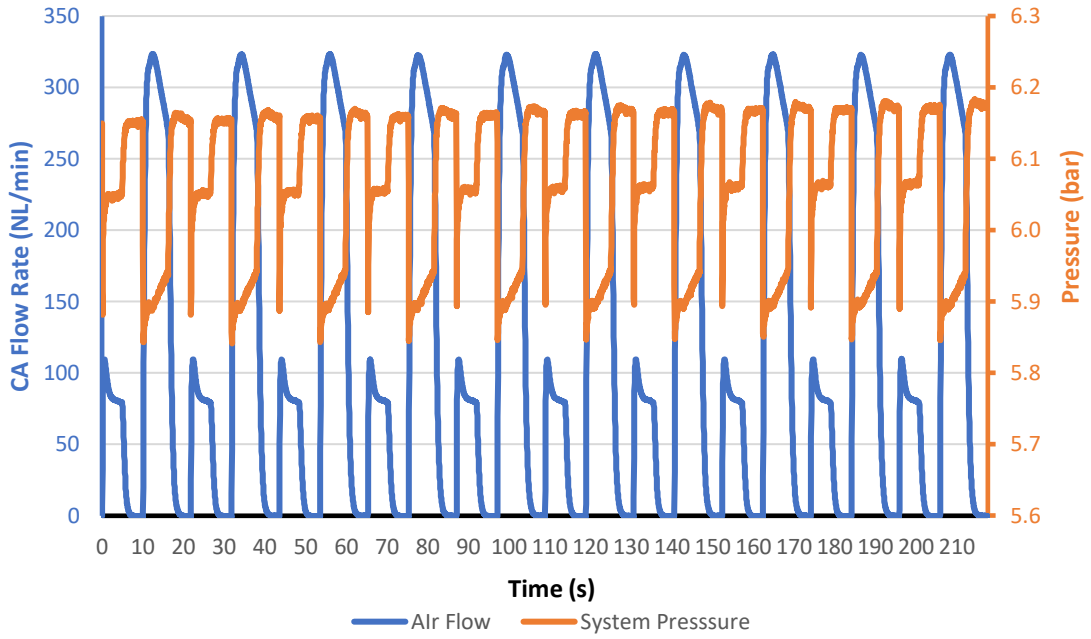

Figure 7.1: Flow and pressure data for the first repeat during the control test.

From the graph, it could be noted that although fluctuations were present for both of the recorded parameters, these were repeatable throughout the duration of the experiment, with the air flow readings ranging from 0 to 320 NL/min and the pressure readings ranging from 5.8 to 6.2 bar. During the simulations, the double acting actuators and the suspension bellow were actuated and as a result, CA was consumed in order to perform the actuations. Consequently, this resulted in a surge of CA flow, which also coincided with instantaneous drops in system pressure. This is due to Bernoulli's Principle, which states that the total system pressure is made up of two components, as shown in Equation 7.1.

$$P_{Total} = P_{Static} + P_{Dynamic} \qquad Eq.\ 7.1$$

To better understand this principle, one has to first comprehend what both types of pressures represent. Static pressure is defined as the force that a fluid (i.e. CA) exerts upon a particular surface while at rest, whilst the dynamic pressure is defined as the force that a fluid exerts whilst it is in motion [119]. During the experiment, transducer *P2*, which as shown in the schematic in Figure 6.5, was situated downstream of the conditioning equipment, measured the static system pressure since it was placed at right angles to the CA stream. By using Equation 7.1, the fluctuations in both the flow and pressure could still be explained due to the fact that during the actuations, CA flowed through the entire system, meaning that the dynamic pressure increased at this instance. Consequently, since the total pressure at the point of *P2* remains constant,

the static pressure drops to compensate for this increase, which was in fact reflected by the drop in the system pressure. It is good to note that Bernoulli's principle was used indicatively (to explain the measured increase/decrease in static pressure). It is also good to note that the unregulated pressure was kept higher than required system pressure throughout all the experiments. As a result, it could be concluded that all system pressure changes occurring during the simulations were a result of the performed actuations.

7.1.2 Detailed Account of Actuations

Once the overall system behaviour was understood, it was deemed appropriate to examine in detail the actuations taking place during the simulation. Due to the fact that the chosen data resolution was set at 40 ms, a substantial amount of data was collected throughout the entire experiment. Consequently, it was determined that for the purpose of this particular analysis, the first stop would be surveyed. By using Table 7-1, which summarises all the actuations of the simulation and the data plot in Figure 7.2, a detailed analyses could be performed. It is good to note that the outputs in the table were explained in detail in Table 6-9, where E denotes extension and R denotes retraction.

Table 7-1: Summary of the actuations performed during the simulation.

Labelled Zone	Performed Actuations	Outputs Set
A	• Cylinders *1* & *2* were fully extended from fully retracted state. • Bellow kneeled from ride height setting.	• C1E & C2E • B1
B	• Five seconds timed delay.	N/a
C	• Cylinders *1* & *2* were fully retracted from fully extended state. • Bellow inflated to ride height setting from kneeling setting.	• C1R & C2R • B4
D	• Five seconds timed delay.	N/a

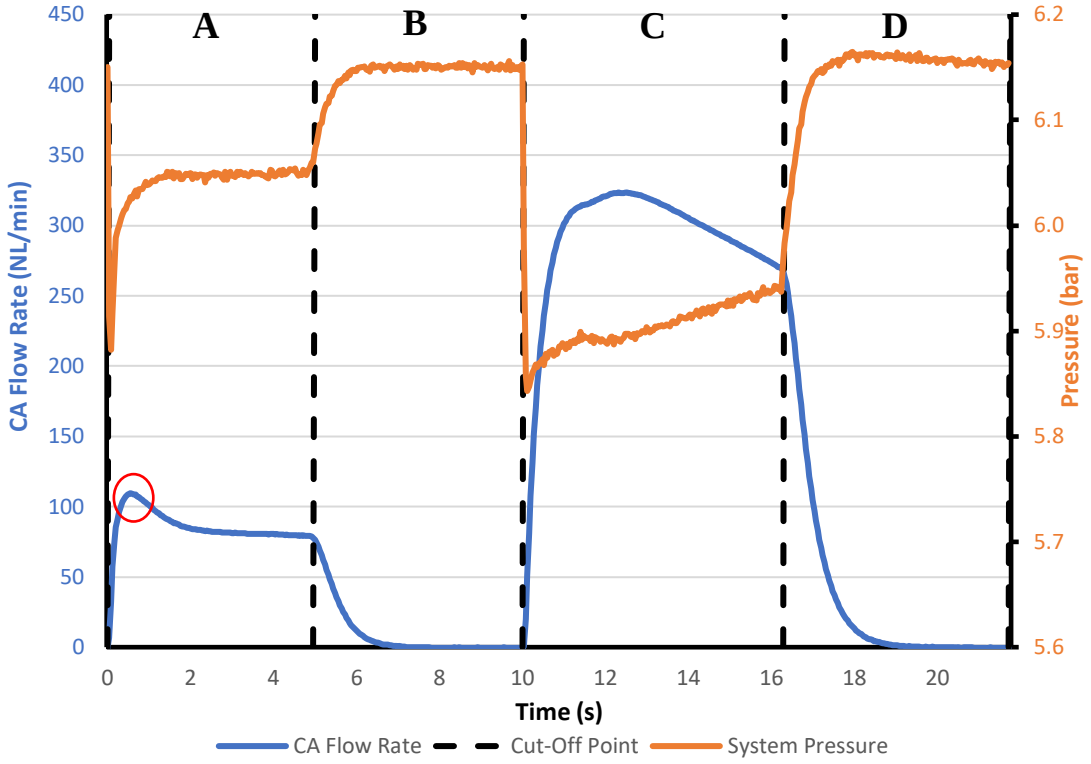

Figure 7.2: The data for the flow rate and pressure readings for the first repeat.

With regards to the actuations, each stop made both cylinders fully extend and the suspension bellow to deflate to 2 bar simultaneously, and the cylinder actuators to fully retract and the bellow to inflate to 4.5 bar. All the valve switching required to perform the actions highlighted in Table 8-1, were possible by using the reed switches to operate the cylinders using valves *C1* and *C2*, and pressure transducer *P3*, to monitor the pressure inside the bellow, thereby instructing the operation of valves *B1* and *B2*. Figure 7.3 and Figure 7.4 show the outputs for the valves which were required to actuate Cylinder *1* and the bellow, respectively. Although all of the actuations corresponded with the ones in the table, it was observed that the time to fully extend and retract the cylinders was not the same, regardless of the fact that both sets of flow restrictors were virtually set the same. This could be attributed to the design of the set-up's pneumatic system, in which both the doors and the bellow were supplied via the same set of tanks. As a result, whilst all of the actuators were actuated (i.e. Zone C in Figure 7.3 and Figure 7.4), the supply of CA had to be split between all three constituents, in contrast to Zone A, where only the cylinders were actuated. As a result, the time to close the doors was 25.6 per cent more than to open them. In theory, it was difficult to set both sets of flow restrictors identical, due to the element of human error involved. That said, this error would not have contributed to such a significant increase in the actuation time.

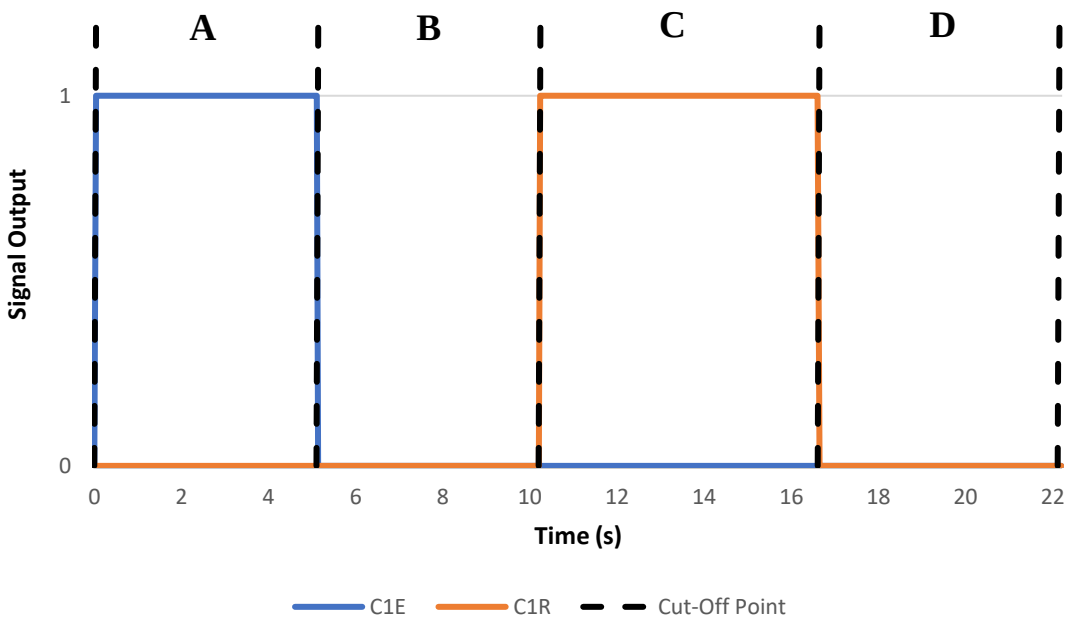

Figure 7.3: The valve signal outputs required to actuate Cylinder 1.

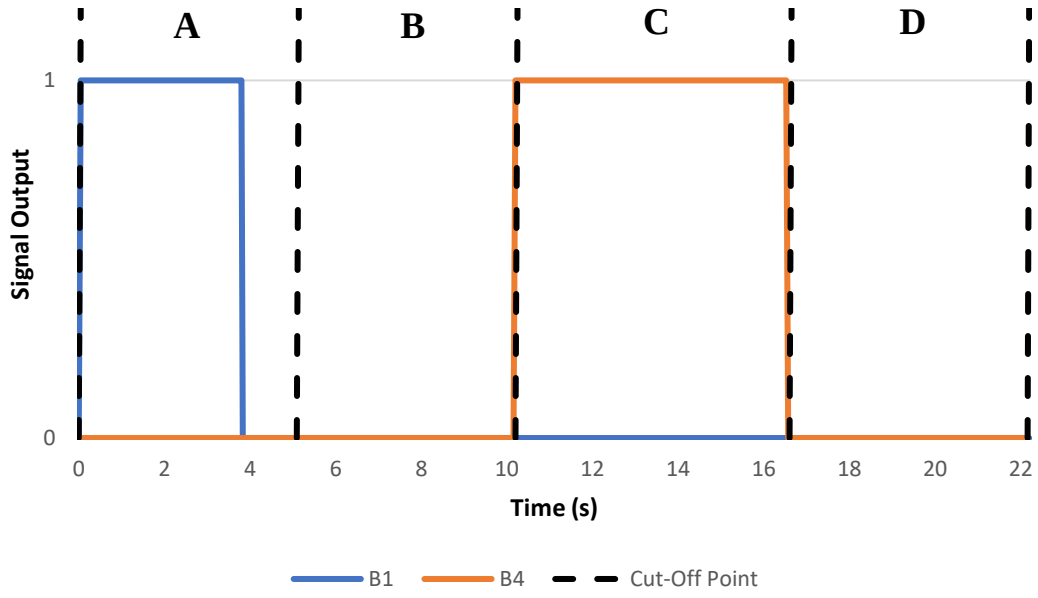

Figure 7.4: The valve signal outputs required to actuate the bellow.

Examining the actuations occurring in Zones A and C, it could be observed that in Zone C, significantly more CA was consumed, with the peak CA flow being 66 per cent more than the former. The reason for this is that in this zone, both the double acting actuators and the bellow consumed CA whilst in Zone A, only the cylinders consumed CA. This is because during kneeling CA was exhausted, hence not contributing to any consumption. It is worth mentioning however, that the bellow kneeling could also be considered as a source of leak which would therefore further

contribute to pressure loss due to the exhausting of CA. Nevertheless, it was apparent that none of the mentioned losses were recorded, both by sensors *F500* and *P2*. This was a result of the one-way pressure regulator installed upstream of the bellow, which isolated this part of the system from the rest, thereby not allowing the CA to flow back through.

In analysing the CA flow throughout the whole scenario, it could be noted that during the beginning of Zone A, a spike was present, which is highlighted in red, and levelled out throughout the rest of the actuation. The main reason for this could be attributed to the fact that once the valve was opened, a sudden surge of CA was required to initially move the piston rods for each double acting actuator. Additionally, this small surge could not be seen in Zone C, since the flow required to inflate the bellow was greater than the flow during this surge. For both Zones A and C, it could also be noted that although all the respective solenoid valves were reset and no actuations were taking place, CA was still being consumed for around two seconds. This is because although no actuations were performed, momentarily, CA was still being compressed, mainly in the cylinders' chambers.

By investigating all the previously mentioned zones in terms of system pressure, it could be noted that the obtained readings corresponded and followed the CA flow values. Analysing Zone A, it was noticed that whilst the flow of CA initially surged during the extension of the cylinders, the pressure dipped. This is because the valves had to exhaust air from the cylinders' retraction chamber in order to make it possible for the cylinders to extend, resulting in the pressure drop. Following this drop, the pressure inside the chamber was built up, increasing the value of the system pressure which levelled off to around 6.05 bar. This could again be attributed to the Bernoulli's Principle since the amount of CA required to fill the constituent was decreasing, which in turn decreased the dynamic pressure, hence increasing the static pressure. Moving on to Zone C, a significant pressure drop could be noticed whilst a surge in CA flow was present. In this instance however, pressure was not immediately built back to 6.05 bar due to the fact that the bellow was also being inflated, which required a considerable amount of CA. It is also worth mentioning that in theory, at the beginning of Zones A and C, the system pressure should have been recorded at 0 bar. This is because whilst the double acting cylinders were initially extended or retracted, valves *C1* and *C2*, initially exhausted CA from the opposing cylinder's chamber, making it

possible for the piston to move. Two reasons could be attributed as to why this behaviour was not recorded. Firstly, the data logging resolution was set at 40 ms which was too long to capture this rapid change, and secondly, the pressure transducer was placed further upstream in the set-up's distribution line, rather near the solenoid valves, which meant that the rest of the system's piping served as a temporary source of CA storage.

For the purpose of understanding every element of this set-up, the pressure readings for the bellow during this repeat were also plotted against the CA flow rate, as shown in Figure 7.5.

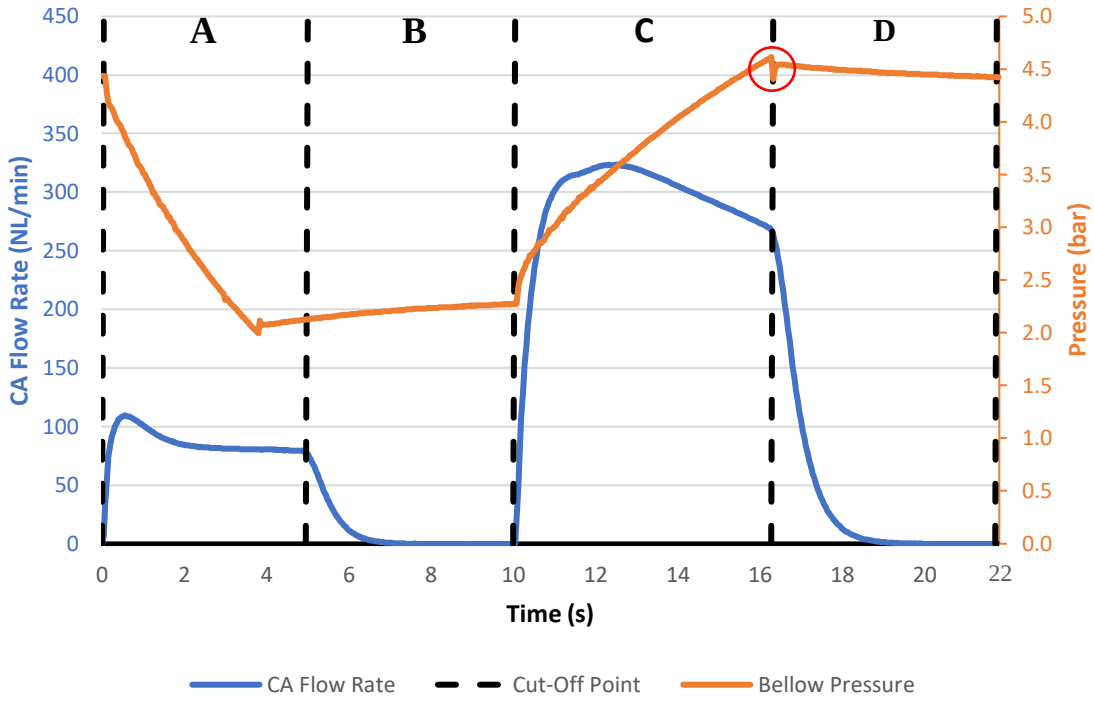

Figure 7.5: The bellow pressure during repeat 1.

From the figure, it could be noticed that all of the actions performed by the bellow corresponded with the summarised ones in Table 7-1, where at Zone A, the bellow was deflated and at Zone C, the bellow was inflated. Additionally, the minimum and maximum bellow pressures were recorded to be 2 and 4.6 bar, which represented the kneeling and ride height settings, respectively. That said, it is evident that although valves *B1* and *B2* operated correctly and actuated according to the pre-set cut-off pressures, the pressure inside the bellow fluctuated once the supply of CA was halted. This could be seen in Zones B and D in the figure, where the five second time delay was programmed. Observing the area in the proximity of the 2 bar cut-off point, the pressure kept on increasing throughout this zone, whilst the pressure near the 4.6 bar

cut-off point kept decreasing. This could be attributed to the behaviour of the rubber material which made up the bellow, where CA forced it to expand or retract, accordingly. Consequently, this meant that the bellow could not be considered to have a constant volume due to the hysteresis properties of the material [38]. As a result, whilst the CA flow was stopped abruptly, once the desired pre-set pressure was reached, when the vessel was being inflated, the rubber material kept on expanding, and if it was being deflated, the material kept on retracting. This meant that near the 2 bar cut-off point the rubber kept on retracting hence increasing in the pressure inside it, whilst near 4.6 bar cut-off point, the bellow kept on expanding, resulting in a decrease in pressure. It could also be recalled that, the ride height pressure was set to 4.5 bar however, as highlighted in the graph, the pressure was cut off at 4.6 bar. The reason for this was that during the short time delay of 0.5 s, which was introduced for PLC switching, CA kept being supplied, hence increasing the pressure by 0.1 bar.

7.1.3 Uncertainty Analysis

By being able to better comprehended the actuations taking place during the control experiment, the next step was to analyse the behaviour of the set-up whilst varying the chosen input parameters. For this reason, in order to accurately analyse the data, an uncertainty analysis had to be performed on all the recorded parameters. The reason for doing so is that each reading had an element of variation caused by unavoidable errors associated with the equipment and sensors utilised. That said, in this section, this process was conveyed solely for the control data set, together with all of their repeats found in Table 7-2, which served as a guide for all the tests.

Table 7-2: The collected data for the control test (experiment 1).

Measurement	Repeat 1	Repeat 2	Repeat 3	Average	Standard Deviation
Air Flow Meter					
Average System Flow Rate – *F500* (NL/min)	113.00	112.75	112.56	112.77	0.22
Volume per Stop (NL)	41.03	40.96	40.94	40.98	0.05
Pressure Transducer					
Unregulated Pressure – *P1* (bar)	7.09	6.76	6.50	6.78	0.29
Average System Pressure – *P2* (bar)	6.06	6.06	6.03	6.05	0.02
Pressure Standard Deviation Within Each Cycle (bar)	0.11	0.12	0.13	0.12	0.01
Solid State Switches & Digital Timing					
Test Time per Stop (s)	21.76	21.78	21.81	21.78	0.22
Door Average Actuation Time (s)	5.63	5.64	5.64	5.64	0.01
Bellow Average Fill Time (s)	6.21	6.22	6.34	6.26	0.07

Air Flow Meter

In order to determine the CA flow through the system, flow meter *F500*, highlighted in Figure 6.5, was utilised. This sensor offered the possibility to record flow readings in the range of 5-500 NL/min and this data was conveyed digitally to the PLC via 4-20 mA output signals.

According to the specification provided by the manufacturer, the factors affecting the accuracy (Δ_{Acc}) of the sensor's reading were the following: analogue output accuracy, i.e. ±3% Full Scale (F.S.), repeatability, i.e. ±1% F.S. and temperature characteristics, i.e. ±5% F.S. [120]. As a result, it could be determined that the total Δ_{Acc} associated for this sensor accounted to ±29.28 NL/min.

With regards to the uncertainty attributed to the resolution (Δ_{Res}), this was not determined by the sensor itself, but rather by the expansion module (NX-AD4208 [121]) utilised to interface with the sensor. According to the manufacturer, this module had a resolution of $\frac{1}{30000}$, equating to 1.66×10^{-3} NL/min. As a result, it could be concluded that Δ_{Res} for this component was $\pm 8.25 \times 10^{-3}$ NL/min.

The final factor affecting the uncertainty of the reading was accredited to the standard deviation between the readings (Δ_{Std}) in Table 7-2. In order to calculate this factor, the standard deviation between the readings had to be worked out and this resulted to 0.22 NL/min. Utilising this data, Δ_{Std} could be equated to: $\pm \frac{Standard\ deviation}{\sqrt{nr.\ of\ repeats}} = \pm\frac{0.22}{\sqrt{3}} =$ ±0.13 NL/min.

By obtaining values for Δ_{Acc}, Δ_{Res} and Δ_{Std}, the total reading uncertainty could be propagated by using Equation 7.2.

$$Propagated\ uncertainty = \pm\sqrt{{\Delta_{Acc}}^2 + {\Delta_{Res}}^2 + {\Delta_{Std}}^2} \qquad Eq.\ 7.2$$

$$Propagated\ uncertainty = \pm\sqrt{(29.28)^2 + (8.25 \times 10^{-3})^{\,2} + (0.13)^2}$$

$$Propagated\ uncertainty = \pm\mathbf{29.28\ NL/min} = \pm\mathbf{25.96\ per\ cent}\ \text{of the flow rate}$$

It could be noted that the percentage uncertainty value was quite high since the overall flow rate readings during this test were quite low, as compared to the maximum flow rate value of the sensor. This meant that as the overall flow rate increases during the tests, the uncertainty for this reading would also improve. Additionally, it could also be noted that both the uncertainties associated with the resolution and standard deviation were negligible.

Pressure Transducers *P1* & *P3*

In order to monitor the unregulated supply pressure, transducer *P1* was used, whilst to monitor the pressure inside the bellow, transducer *P3* was utilised. The WIKA A-10 [122] transducer, was chosen for both transducers, and this model had a pressure range from 0-10 bar and also worked by using the 4-20 mA current output principal. With regards to Δ_{Acc}, the manufacturer provided a test certificate which highlighted all the factors which attributed to this uncertainty. To comprehend what these factors consist

of, Table 7-3 provides this data for *P3*. By obtaining the current output uncertainty for each relevant property, it could be deduced that Δ_{Acc} for *P1* was ±0.17 mA, equating to ±0.11 bar and for *P3* was ±0.23 mA which equates to ±0.14 bar.

Table 7-3: Factors attributing to the uncertainty of P3.

Property	F.S. Analogue Output Uncertainty (%)
Non-Linearity	±0.18%
Analogue Output Accuracy	±1%
Temperature	±1%
Noise	±0.2%
Non-Repeatability	±0.1%
Long Term Drift	±0.1%

With regards to Δ_{Res}, the expansion module NX-AD4208 [121] was again used for *P1*, whilst for *P3* the expansion module NX-AD2208 was used. It could be said however, that both readings, Δ_{Res} could be considered negligible. Finally, the uncertainty attributed to the repeated readings was found to be 0.29 bar and 1.4×10^{-3} bar for *P1* and *P3*, respectively, which contributed to a Δ_{Std} of ±0.17 bar and $\pm0.81\times10^{-3}$ bar, where the latter could also be considered negligible. Using Equation 7.2, the propagated uncertainty for the unregulated pressure reading equated to **±0.20 bar**, which was equivalent to ±**2.95 per cent** of the full reading, whilst the total uncertainty for the bellow pressure amounted to **±0.14 bar**, corresponding to **±4.2 per cent** of the full reading.

Pressure Transducer *P2*

As seen in Figure 6.5, the transducer located downstream to the regulators and filters was tasked with monitoring the system pressure throughout the whole experiment. For this measurement, the WIKA S-10 [123] transducer was utilised. The behaviour of this sensor was similar to the WIKA A-10, where it recorded pressure from 0-10 bar and made use of the 4-20 mA current output principal. By using the test certificate supplied by the manufacturer, Δ_{Acc} could be calculated and equated to ±0.0357 bar. Since the expansion module NX-AD4208 [121] was again utilised, Δ_{Res} could be considered negligible. With regards to Δ_{Std}, the repeated readings found in Table 7-2, were used to calculate this value which amounted to ±0.01 bar. Finally, by using Equation 7.2, the uncertainty associated with this value could be deduced to be **±0.037 bar**, resulting

in a percentage uncertainty of **±0.6 per cent**. Due to the higher accuracy attributed to this sensor, as compared to the WIKA A-10 counterpart, it could be noted that the percentage uncertainty associated with this reading was less than those for transducers *P1* and *P3*. Thus, that is the reason why this transducer was used to measure the system pressure.

Uncertainty Survey Analysis

Through the uncertainty analysis performed for the sensory equipment, it was possible to complete the uncertainties for all their respective confounding parameters listed in Table 7-4, mainly the Volume per Stop. This was made possible by taking each parameter as a function of time. With regards to the uncertainty associated with time, this was considered negligible. It could also be concluded that the values associated with the air flow sensor had the highest amount of uncertainty. This offered one constraint during the experiments, mainly that although certain changes in the volume readings were repeatable, they could not be definitely concluded since they were within the range of the uncertainty of the sensor utilised.

Table 7-4: The uncertainty values for the recorded parameters for the control test.

Measurement	Average Reading	Standard Deviation	Reading Uncertainty
Air Flow Meter			
Average System Flow Rate – *F500* (NL/min)	112.77	0.22	±29.28 (26%)
Volume per Stop (NL)	40.98	0.05	±10.62 (26%)
Pressure Transducer			
Unregulated Pressure – *P1* (bar)	6.78	0.29	±0.20 (3.0%)
Average System Pressure – *P2* (bar)	6.05	0.02	±0.037 (0.6%)
Pressure Standard Deviation Within Each Cycle (bar)	0.12	/	/
Solid State Switches & Digital Timing			
Test Time per Stop (s)	21.78	0.22	/
Door Average Actuation Time (s)	5.64	0.01	/
Average Bellow Fill Time (s)	6.26	0.07	/

7.1.4 Control Test Observations

In order to comprehend the system's behaviour, the control experiment was scrutinised in detail throughout the previous sections. In *Section 7.1.1* the first repeat for the control test was briefly analysed to determine the overall system behaviour, whilst in *Section 7.1.2*, a single stop was examined in further detail. Finally, in *Section 7.1.3*, the uncertainty analysis was performed in order to determine the accuracy of the recorded data. This knowledge paved way to be able to interpret the results for the rest of the simulations.

7.2 Single Factorial Experiments

As discussed in *Section 6.1.1.4*, two sets of input parameters were altered, two operational (i.e. the bellow pressure and the actuation sequence) and two fault oriented (i.e. the 0.82 mm system leak and the faulty cylinder). This was done to understand how these alter the behaviour of the system. In order to quantify their effects, single factorial experiments were first performed and as indicated by J.Anthony [103]. Such experiments entail altering one factor per test. In Table 7-5, one can find the recorded data for all four experiments and in Table 7-6, one can find the percentage change for different parameters for each experiment, as compared to the control.

Table 7-5: The data obtained for the single factorial experiments.

Experiment Information	**Experiment**	**Actuation Sequence**	**Fault Type**	**Bellow Pressure**
	1 (Control)	*Simultaneous*	None	4.5
	2	*Simultaneous*	None	3.5
	3	*Separate*	None	4.5
	4	*Simultaneous*	System Leak	4.5
	5	*Simultaneous*	Faulty Cylinder	4.5

Parameter Analysed	**Experiment 1**	**Experiment 2**	**Experiment 3**	**Experiment 4**	**Experiment 5**
Air Flow Sensor					
Average System CA Flow Rate – *F500* (NL/min)	112.77	83.08	93.67	150.49	114.45
Standard Deviation of Repeats (NL/min)	0.22	0.23	0.06	0.46	0.35
Reading Uncertainty (NL/min)	±29.28	±29.28	±29.28	±29.28	±29.28
Percentage Uncertainty	25.96%	35.24%	31.26%	19.46%	25.58%
CA Volume per Stop (NL)	40.98	29.44	40.84	54.67	41.83
Standard Deviation of Repeats (NL)	0.050	0.025	0.021	0.055	0.049
Reading Uncertainty (NL)	±10.62	±10.37	±12.76	±10.64	±10.70
Percentage Uncertainty	25.92%	35.22%	31.24%	19.46%	25.58%
Pressure Transducers					
Average System Pressure – *P2* (bar)	6.05	6.05	6.07	6.00	6.02
Standard Deviation of Repeats (bar)	0.020	0.015	0.015	0.0017	0.026
Reading Uncertainty (bar)	±0.037	±0.037	±0.037	±0.037	±0.039
Percentage Uncertainty	0.61%	0.61%	0.61%	0.62%	0.65%
Pressure Standard Deviation Within Each Cycle (bar)	0.120	0.099	0.100	0.100	0.110
Solid State Switches & Digital Timing					
Test Time per Stop (s)	21.78	21.25	26.15	21.80	21.92
Standard Deviation of Repeats (s)	0.22	0.45	0.17	0.46	0.46
Door Average Actuation Time (s)	5.64	5.38	5.13	5.61	5.64
Standard Deviation of Repeats (s)	0.010	0.010	0.0058	0.00	0.0058
Bellow Average Actuation Time (s)	6.26	2.96	5.42	6.32	6.47
Standard Deviation of Repeats (s)	0.070	0.021	0.044	0.035	0.070

Table 7-6: The percentage difference for each parameter as compared to the control.

	Percentage Change of Experiments Compared to Control			
Parameter to be Compared	$\frac{Exp\ 2}{Exp\ 1}$	$\frac{Exp\ 3}{Exp1}$	$\frac{Exp\ 4}{Exp\ 1}$	$\frac{Exp\ 5}{Exp\ 1}$
Average System CA Flow Rate – *F500* (NL/min)	-26%	-17%	+33%	+2%
CA Volume per Stop (NL)	**-28%**	0%	**+33%**	**+2%**
Average System Pressure – *P2* (bar)	0%	0%	-1%	0%
Pressure Standard Deviation Within Each Cycle (bar)	-17%	-16%	**-16%**	**-6%**
Test Time per Stop (s)	**-2%**	**+20%**	**0%**	**+1%**
Door Average Actuation Time (s)	-5%	-9%	0%	0%
Bellow Average Actuation Time (s)	-53%	-13%	+1%	+3%

Where Exp = Experiment

7.2.1 Bellow Pressure at 3.5 bar (Experiment 2)

The first operational factor altered was the bellow pressure during the ride height setting, where it was set at 3.5 bar instead of 4.5 bar. This was done in order to depict a scenario where the bus was less loaded than the control. As one might predict, the 1 bar reduction would result in less CA being consumed and less time to inflate the bellow, as shown in Figure 7.6. This was confirmed by the obtained results in Table 7-6, where that the volume consumption was reduced by **28 per cent** and the time to inflate the bellow was decreased by 53 per cent. The reduction in inflation time also contributed to a reduction in the cylinders' actuation time by around 5 per cent due the bellow being inflated quicker. This is because of the CA being supplied to only the double acting actuators, once the bellow was inflated. Consequently, the overall time per stop also decreased by **2 per cent**, since the overall actuations were completed before.

An observation that could be noted was that although in Zone C, the bellow cut-off pressure was set at 3.5 bar, the actual cut-off point was around 3.66 bar. This was the same observation made in *Section 7.1.2*, which was attributed to the time delay required for the switching of valve *B4*. During this test, the bellow kneeling in Zone A, also finished considerably earlier than the cylinder actuations, due to the fact that less air had to be exhausted in the other test. With regards to the average system pressure, it was noted that the recorded value was virtually identical to the benchmark test. This is due to the fact that there were no elements attributing to pressure losses, such as system leaks or faulty components.

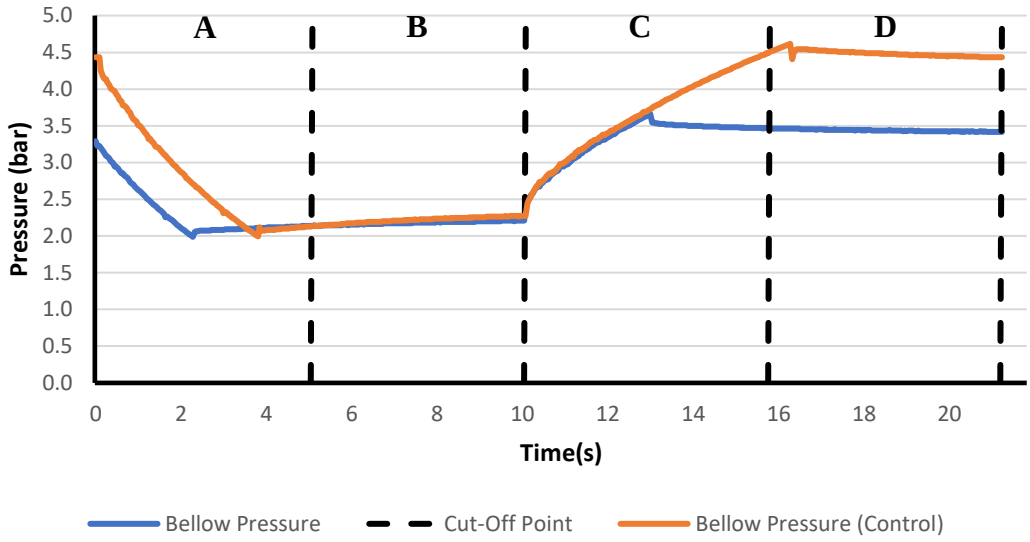

Figure 7.6: The bellow pressure readings for Experiment 2 for one of the runs.

7.2.2 Separate Actuations (Experiment 3)

As the title entails, this scenario revolved around the double acting cylinders and the bellow being *separately* actuated in Zone C, which meant that during these experiments, no changes were made to the system's hardware, as compared to the control test. Consequently, this was also confirmed by the values obtained for the volume per stop, which were identical to those of Experiment 1, since the volume required to actuate the constituents remained the same.

The main difference whilst comparing both sets of data was that as tabulated in Table 7-6, the time per bus stop was significantly more **(by 20 per cent)** due to the fact that the doors and the bellow were operated one after the other. This would therefore, also have an effect on the real life performance since this increases the waiting time per stop, directly contributing to an increase in the overall fuel consumed.

To better comprehend this scenario, Figure 7.7 provides a data plot for the CA flow rate for one of the randomly chosen repeats, with point X highlighting when the cylinders had been fully retracted and the bellow started to inflate to its original ride height.

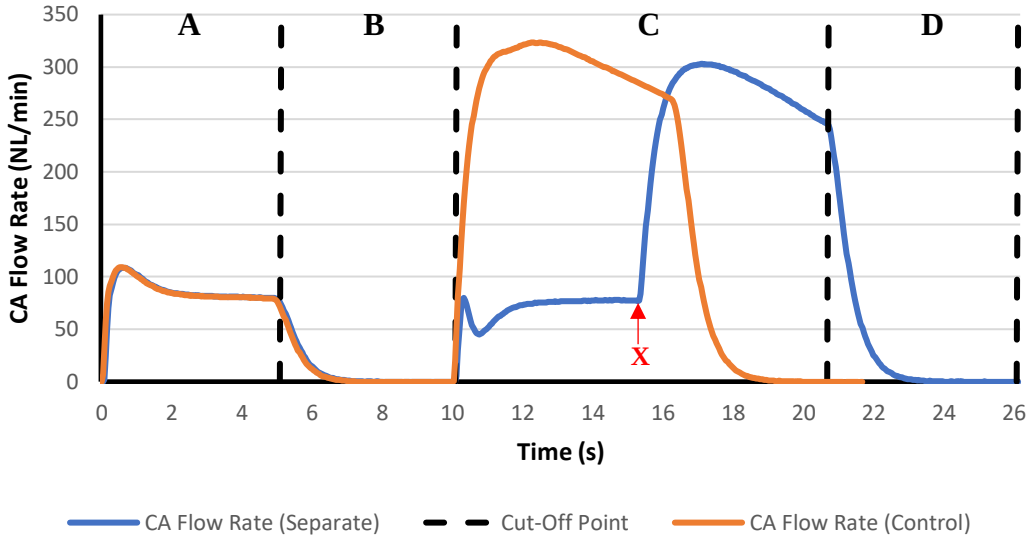

Figure 7.7: The CA flow data for Experiment 3 as compared to control.

Another observation which related to the timing of the components was that the time to individually actuate the cylinders and inflate the bellow was less than the control. Furthermore, the time taken to fully extend and retract the double acting actuators was virtually the same, keeping in mind the human error associated with the flow restrictor adjustments. This was illustrated by the plotted data in Figure 7.8, which shows the activity for the outputs responsible to extend and retract Cylinder *1* (i.e. *C1E* and *C1R*) for the previously mentioned repeat. From this data, it could be deduced that it took Cylinder *1*, 5 s to fully extend and 5.16 s to fully retract, whilst for the control test, the same cylinder took 5 s and 6.28 s to extend and retract, respectively. Therefore, the cylinder actuation time was reduced by 9 per cent and the bellow inflation time was reduced by 13 per cent. All of the highlighted time differences could again be attributed to the overall set-up of the BPS, where both of the mentioned sub-systems were supplied by the same reservoir tanks via the same distribution circuit. This meant that the supply of CA had to be divided between the two during the control test, which also explained why the average flow rate for the control test was on average 19.1 NL/min higher.

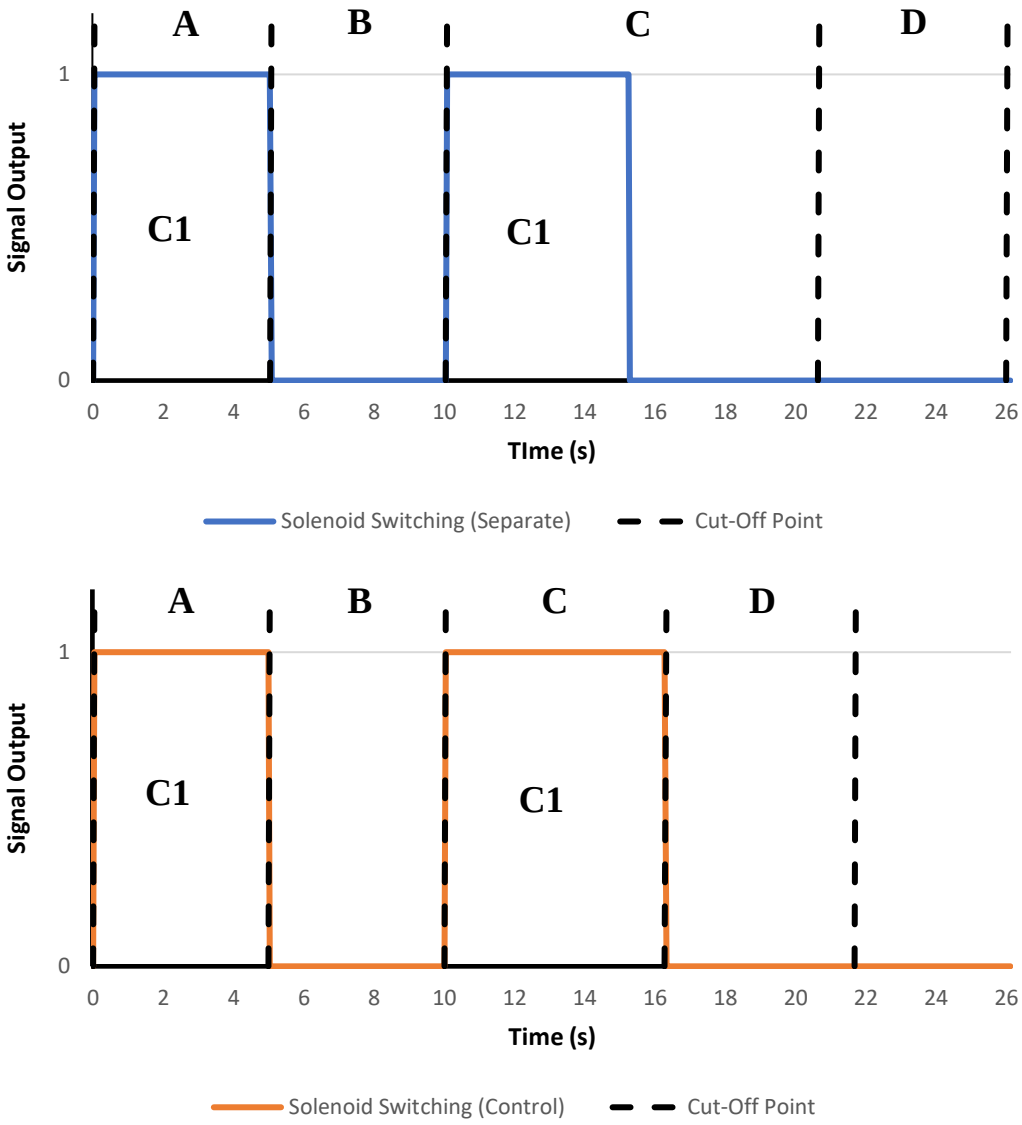

Figure 7.8: The valve signal outputs to actuate Cylinder 1 for Experiment 3 (Top) and the control signal outputs for the same cylinder (bottom).

From the recorded flow data points, the CA volume required to actuate the constituents could be calculated using the area under the graph. To determine the volume required to actuate the cylinders, the area under Zone A was calculated since only the double acting actuators were consuming CA at that instance. Consequently, in order to calculate the volume required to inflate the bellow from the kneeling setting to the ride height setting, the area under Zone C was computed. It could be concluded that in order to actuate the cylinders (i.e. extend or retract), **3.75 NL** of CA were required whilst to inflate the bellow from the kneeling setting to the ride height setting, **25.8 NL** of CA were required.

7.2.3 Introduction of System Leakage (Experiment 4)

By altering both operational parameters, the next step was to start exploring the effects imposed by the fault oriented parameters. Therefore, for this experiment, the system leak was induced. Upon inspection, the most obvious difference, when comparing this experiment to the control test, was the **33 per cent** increase in CA volume per stop, as highlighted in Table 7-6, which could be attributed to the 0.82 mm leak. Although this reading had a considerable amount of uncertainty, due to the sensor utilised, the recorded percentage increase was significant enough so as to not be attributed to this factor. It is good to note that as recalled in *Section 6.1.1.3*, a 5 s arbitrary timer was programmed for Zones B and D. Although this timer had no effect on the volume consumption for the previous experiments, this effected the volume when a fault was induced, since the longer the experiment, the more CA was lost through the leak and vice versa. Therefore, the obtained value is not finite and varies according to the time of the experiment.

Moving on to the average system pressure, theoretically according to the Bernoulli's Principle, the additional flowrates resulting from the leak, increased the dynamic pressure which directly contributed to a reduction in the system pressure (i.e. P_{static}). This could be confirmed by the reduction in the overall average system pressure, where the value decreased by 0.05 bar, translating to a one per cent reduction. At first glance, one may think that this did not have any significant effects on the performance of the system. However, in an effort to try and determine additional factors which may make it possible to identify the presence of faults, the standard deviation within each stop was also investigated. Indeed, the introduction of the fault led to the pressure standard deviation to be **16 per cent** less than the control. This meant that the leak helped in keeping the overall pressure more stable throughout the simulation, which was mostly evident in Zones A and B. In order to better comprehend this phenomenon, Figure 7.9 and Figure 7.10, show the pressure and CA flow data plots, respectively, while these two zones for two randomly chosen stops, one for the control experiment and one for the leakage experiment.

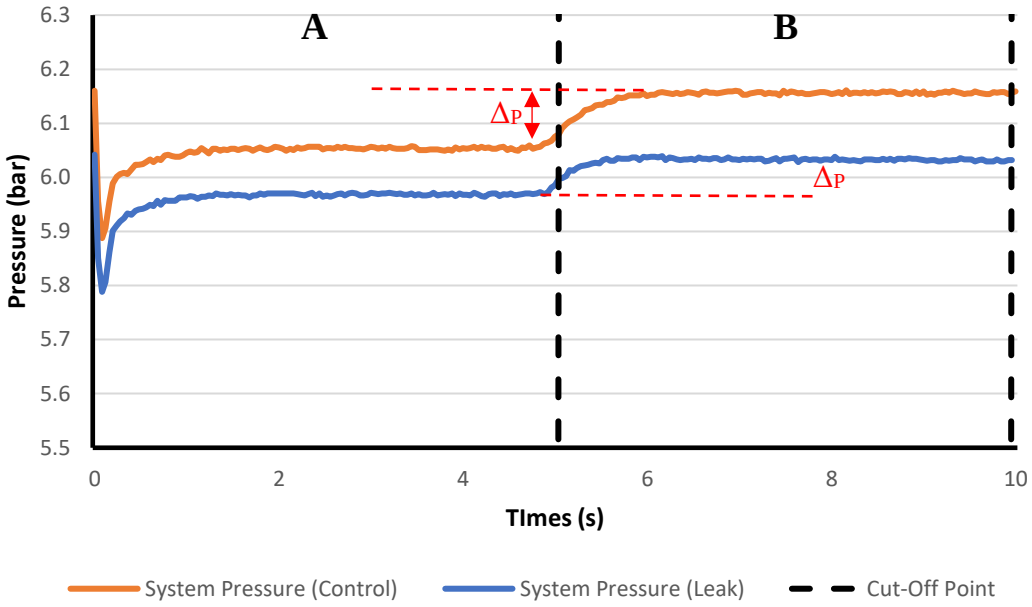

Figure 7.9: System pressure for Zones A and B for Experiment 4 and the control.

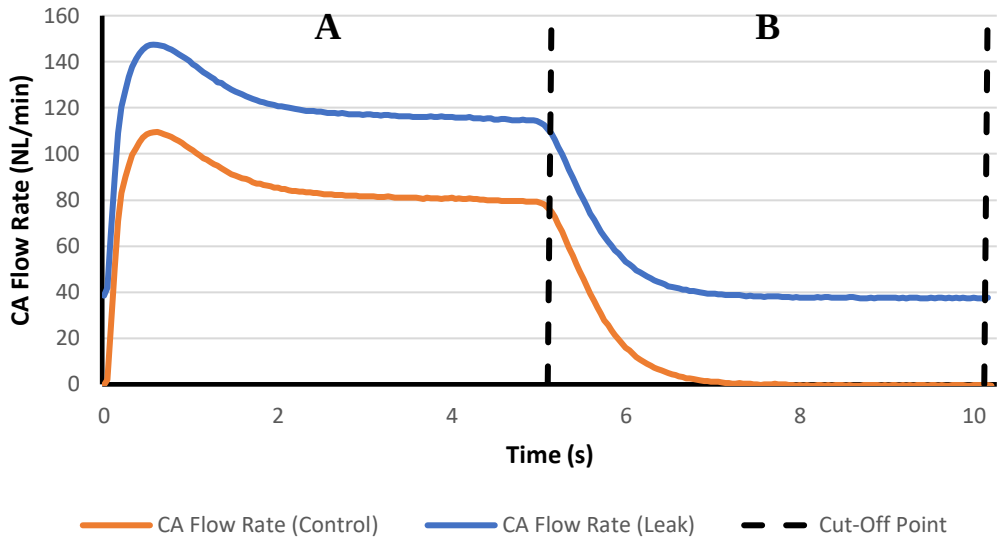

Figure 7.10: CA flow rate for Zones A and B for Experiment 4 and the control.

Analysing both graphs, it is evident that after the pneumatic cylinders were fully extended, i.e. transitioning from Zone A to Zone B, and the static system pressure was again built up, the change in pressure (Δ_P) between the zones for the leakage experiment was less than that of the control scenario. This is because the leak hindered the pressure build up. Again, this could also be attributed to Bernoulli's Principle since as stated previously, since the leak resulted in additional CA flow, the dynamic pressure increased, directly contributing to the reduction in the measured static pressure. If this parameter were to be monitored in actual buses, it would not require

any additional hardware since as underscored in *Section 3.5.3.2*, modern buses, such as those by Volvo [98], are equipped with various pressure transducers.

Conversely, the data showed that the leak had little to no effect on the time required to actuate the cylinder and inflate the bellow. This could be attributed to the fact that the system pressure did not decrease significantly, as highlighted earlier.

7.2.4 Faulty Double Acting Actuator (Experiment 5)

The final experiment to be performed was the bus stop scenario with the inclusion of the faulty cylinder, meaning that the pneumatic system comprised of a fault-free and faulty cylinder, together with a suspension bellow.

As stated in *Section 6.1.1.4*, the induced fault for the double acting actuator was a leak in the piston gasket, depicting typical seal wear. From the obtained results, it could be noted that as compared to the benchmark test, the volume per bus stop increased by 0.85 NL (**i.e. 2 per cent**), which equated to an average system flow rate increase of around **2 NL/min**. Again, it is good to note that the volume consumption of this fault is dependent on the duration of the experiment and therefore, it is not finite. Though the reported flow increase was repeatable, the uncertainty associated with flow sensor *F500* was well within the noted change. Therefore, it could not be definitely concluded that this increase was a result of this fault.

At first glance, one might think that the effects imposed by the fault were similar to the ones discussed for the system leak in the previous section, but on a smaller scale. However, by analysing Figure 7.11 and Figure 7.12, which include the data plots for both the CA flow and system pressure readings during Zones C and D, showed that the system's behaviour was quite different.

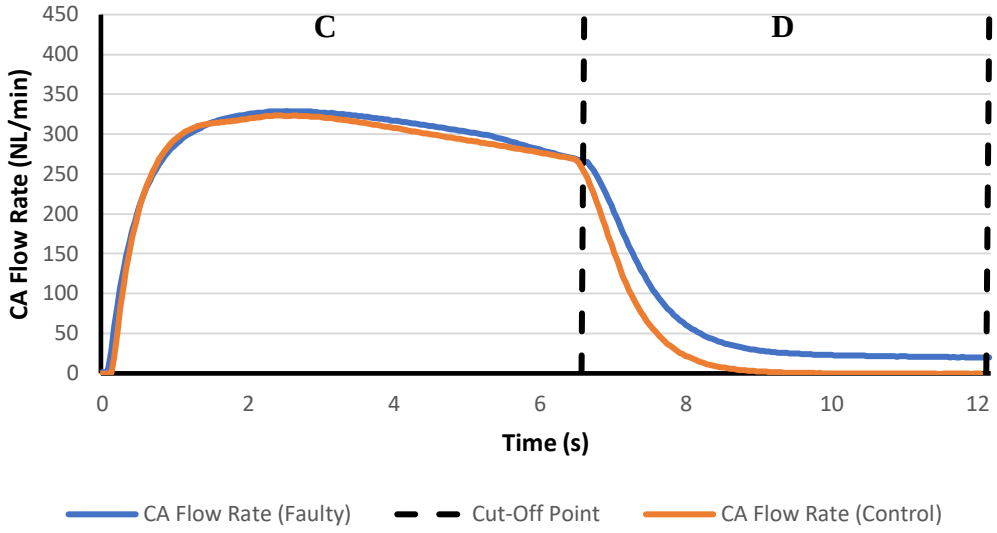

Figure 7.11: The flow readings for Zones C and D for Experiment 5 and the control.

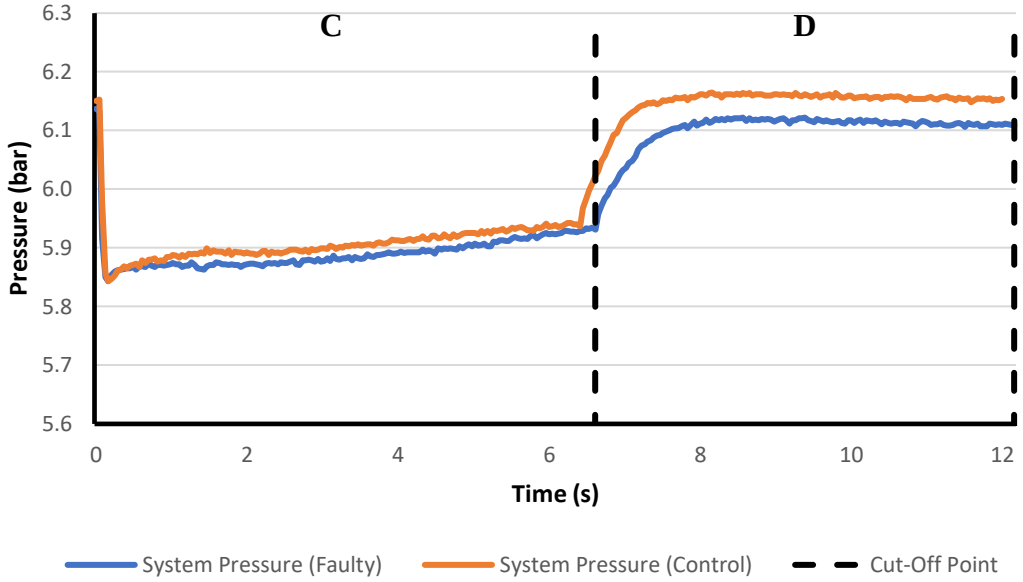

Figure 7.12: The pressure readings for Zones C and D for Experiment 5 and the control.

Firstly, it could be noted that the faulty seal did not impose a leak throughout the whole test but only whilst the double acting actuator was during its retraction stage. This is clearly shown in Figure 7.11 in the area highlighted in red, which was when the cylinder was fully retracted and all solenoids were re-set. This is different from the effects noticed whilst inducing the 0.82 mm system leak since the latter's effects were seen throughout the whole duration of the simulation, which was confirmed by the air flow readings being all transposed by around 40 NL/min, as compared to the control. This behaviour was attributed to the construction of the actuator itself and the

developed leak since whilst it was fully extended, the leak was sealed, imposing no other adverse effects.

With regards to actuation timings, the time to actuate the cylinders was virtually identical to those of the benchmark test. This was expected since the faulty cylinder was adjusted to actuate at the same rate as Cylinder *1*, by adjusting the flow restrictors accordingly. Nevertheless, the time to inflate the bellow was on average increased by 0.21s, which equated to around 3 per cent of the total inflation time. This was caused by the sudden leak prevailing during the faulty door's retraction phase, which had to be directly countered in order to inflate the bellow. Additionally, it could also be said that another reason for this time increase could be due to the fault being located further downstream in the circuit, i.e. closer to the bellow as compared to the system leak. Although in essence, this element did not hamper the CA flow inside the bellow, it hindered the build-up of pressure in the vicinity of the component, hence causing the increase in the time. Ultimately, the overall time per stop was increased by around **1 per cent**, which in the real world would also increase the additional fuel consumed due to the waiting time.

In order to confirm if the pressure standard deviation within each stop was able to reliably detect the presence of faults, this parameter was again scrutinised. It is evident that as shown in Table 7-6, the obtained value for this experiment was less than the benchmark by **6 per cent**. This could again be attributed to the Δ_P discussed in the previous section, where in Figure 7.12, the pressure was not able to build up as that of the control. It was observed however, that in this instance, the standard deviation value in Table 7-5, was more than the one reported for the system leak. This is the reason why the percentage value obtained was less than that of the leak. Indeed, during Zone C, when the faulty door was at retraction stage, the leak suddenly prevailed, which did not only increase the CA flow but also contributed to more fluctuations in the system pressure, resulting in an increase in the standard deviation value. Therefore, what could be noticed was that this parameter not only makes it possible to identify the presence of a fault, but it would also make it possible to identify the severity/type of fault. With regards to the overall system pressure, the simulations performed with the faulty actuator recorded virtually the same system pressure values as the control, with the minute difference experienced could be attributed to the uncertainty of sensor *P2*.

7.2.5 Synopsis of Single Factorial Experiments

By performing the single factorial experiments, one could better comprehend the system's behaviour as a consequence of the chosen input parameters. Firstly, a system leak of diameter 0.82 mm resulted in an increase in the CA volume consumption by 33 per cent and a faulty cylinder resulted in a volume increase of 2 per cent, confirming that this parameter would make it possible to identify faults. What was also noted was that although the increase noted for the faulty actuator was repeatable, it could not be definitely concluded that it was a result of the fault due to the uncertainty of the sensor utilised. With regards to time, it was determined that the sequence of actuation had the most effect on this factor, with the *separate* actuations resulting in an increase of 20 per cent in the stop time. The actuation sequence however, did not have any effect on the volume consumption since the same amount of CA was required to perform the actuations. The faulty double acting actuator also resulted in an increase in the total time per stop, due to the increase in the bellow inflation time however, the effects were not as significant as the previous parameter since only an increase of 1 per cent in the stop time was recorded.

Furthermore, both of the previously mentioned input factors would contribute to an increase in the total fuel consumed by the vehicle due to the additional waiting time per stop. It was also determined that the pressure standard deviation within each stop could also be used as a parameter which may help in reliably identifying the presence of faults whilst also being able to classify the severity/type of fault. This is because when both the system leak and the faulty cylinder were introduced, the value was less than that of the control, with the standard deviation reducing by 16 and 6 per cent, respectively. In the case of altering the bellow pressure, the results obtained were as expected, with the reduction in pressure attributing to a reduction in both the CA volume and overall bus stop time. Additionally, the volume of each constituent was also calculated where it was determined that 3.75 NL of CA were required to actuate the cylinders and 25.8 NL of CA were required to inflate the bellow from the kneeling setting to the ride height setting.

7.3 Full Factorial Experiments

After performing the single factorial experiments, a two-levelled full factorial experiment was also completed using the principles discussed in *Section 3.6*. Since a

total of 16 experiments were performed, a significant amount of data was collected. For this reason, this section will discuss four of these experiments, since they highlighted aspects which helped in further understanding the system, whilst also further helping to identify the presence of faults. These results are shown in Table 7-7. Consequently, to make the analysis process more straight forward, Table 7-8 also provides percentage comparisons for the chosen full factorial experiments. It is good to note that the remaining experimental results are outlined in Appendix 2 but will not be discussed in further detail in this section since these were all performed whilst the bellow cut off pressure was set at 3.5 bar. The reason why they were not reviewed was that this factor was introduced to better understand the behaviour of the bellow, which was sufficiently understood and discussed during the single factorial experiment in *Section 7.2.4.*

Table 7-7: The data obtained for four of the full factorial experiments.

Experiment Information	**Experiment**	**Actuation Sequence**	**Fault Type**	**Bellow Pressure**
	6	*Separate*	System Leak	4.5
	7	*Separate*	Faulty Cylinder	4.5
	8	*Simultaneous*	System Leak & Faulty Cylinder	4.5
	9	*Separate*	System Leak & Faulty Cylinder	4.5

Parameter Analysed	**Experiment 1**	**Experiment 6**	**Experiment 7**	**Experiment 8**	**Experiment 9**
Air Flow Sensor					
Average System CA Flow Rate – *F500* (NL/min)	112.77	131.10	98.86	152.45	136.99
Standard Deviation of Repeats (NL/min)	0.22	0.38	0.23	0.71	0.53
Reading Uncertainty (NL/min)	±29.28	±29.28	±29.28	±29.28	±29.28
Percentage Uncertainty	25.96%	22.33%	29.62%	19.21%	21.37%
CA Volume per Stop (NL)	40.98	57.19	43.44	55.91	60.29
Standard Deviation of Repeats (NL)	0.05	0.090	0.047	0.038	0.029
Reading Uncertainty (NL)	±10.62	±12.74	±12.88	±10.74	±12.88
Percentage Uncertainty	25.92%	22.28%	29.65%	19.21%	21.36%
Pressure Transducers					
Average System Pressure – *P2* (bar)	6.05	6.01	6.04	5.98	5.99
Standard Deviation of Repeats (bar)	0.02	0.021	0.025	0.021	0.029
Reading Uncertainty (bar)	±0.037	±0.038	±0.038	±0.039	±0.039
Percentage Uncertainty	0.61%	0.63%	0.63%	0.65%	0.65%
Pressure Standard Deviation Within Each Cycle (bar)	0.12	0.084	0.094	0.11	0.084
Solid State Switches & Digital Timing					
Test Time per Stop (s)	21.78	26.17	26.36	22.00	26.40
Standard Deviation of Repeats (s)	0.22	0.35	0.49	0.95	0.99
Door Average Actuation Time (s)	5.64	5.10	5.13	5.63	5.13
Standard Deviation of Repeats (s)	0.010	0.0058	0.0058	0.0058	0.0058
Bellow Average Actuation Time (s)	6.26	5.48	5.56	6.55	5.66
Standard Deviation of Repeats (s)	0.070	0.034	0.12	0.064	0.078

Table 7-8: The percentage difference for each parameter for selected experiments.

	Experiment	**Actuation Sequence**	**Fault Type**	**Bellow Pressure**
Reference Experiments	3	*Separate*	None	4.5
	4	*Simultaneous*	System Leak	4.5
Experimental Comparisons				
	***Simultaneous* Comparisons**		***Separate* Comparisons**	
Parameter to be Compared	$\frac{Exp\ 8}{Exp\ 1}$	$\frac{Exp\ 8}{Exp\ 4}$	$\frac{Exp\ 6}{Exp\ 3}$	$\frac{Exp\ 7}{Exp\ 3}$	$\frac{Exp\ 9}{Exp\ 3}$
Average System CA Flow Rate – *F500* (NL/min)	+35%	+1%	+40%	+6%	+48%
CA Volume per Stop (NL)	**+36%**	**+2%**	**+40%**	**+6%**	**+46%**
Average System Pressure – *P2* (bar)	-1%%	0%	-1%	0%	-1%
Pressure Standard Deviation Within Each Cycle (bar)	**-9%**	+9%	**-17%**	**-7%**	**-17%**
Test Time per Stop (s)	**+1%**	+1%	**0%**	**+1%**	**+1%**
Door Average Actuation Time (s)	0%	0%	0%	0%	0%
Bellow Average Actuation Time (s)	+5%	+4%	+1%	+3%	+4%

7.3.1 CA Consumption Trends

By being able to alter more than a single parameter per experiment, it was possible to determine the effects, if any, that the actuation sequence had on the system's behaviour, whilst introducing the system leak. As discussed in *Section 7.2.2* (i.e. Experiment 3), during the *separate* actuation test, the total actuation time during Zone C was longer, since the cylinders had to be closed in order to inflate the bellow. As a result, whilst comparing Experiments 3 and 6, with the latter being when the actuations where set to *separate* and a system leak was induced, it was observed that the additional time made it possible for the leak to pose a greater effect on the CA consumption, as compared to the same experiments performed with the actuation sequence set to *simultaneous*, i.e. Experiments 1 and 4. By analysing Table 7-8, it could be noted that the leak in the *separate* sequence caused an additional volume increase of **40 per cent**, as compared to its leak free counterpart. This meant that whilst comparing Experiments 4 and 6 to their fault free equivalent, i.e. Experiments 1 and 3, the leak in the *separate* actuation resulted in an additional 7 per cent of CA consumption, keeping in mind the arbitrary timers set. Therefore, it is evident that in any scenario, it would be better to actuate the constituents *simultaneously* since it not only reduces the downtime during the stop but also reduces the effect posed by the fault since the latter has less time to pose its effects.

During the single factorial Experiment 5, the effects of the faulty cylinder were also investigated, where it was determined that when the sequence of actuations was set to *simultaneous*, the faulty component caused an additional 2 per cent CA increase per stop as compared to the benchmark test. As also noted in *Section 7.2.4*, although this change was repeatable, it could not be definitely concluded that it was a result of the fault, due to the uncertainty of the sensor utilised. From the additional experiments performed, the repercussions of the faulty double acting actuator could also be assessed for the *separate* actuation setting. Using the obtained data from Experiment 7, where the actuations were performed *separately* whilst making use of the faulty cylinder, it could be deduced that this component increased the CA consumption by **6 per cent,** as compared to Experiment 3. Therefore, it was again established that the faulty door induced a greater effect when the actuation setting was set to *separate* due to the additional test time, as compared to the *simultaneous* actuation setting. This again suggested to avoid actuating the constituents *separately*.

In the instance that the BPS contains both a system leak and a faulty cylinder, the results showed that during the *simultaneous* actuation sequence, i.e. Experiment 8, an additional **2 per cent** of CA was consumed, as compared when the system solely contained a system leakage during Experiment 4. This meant that whilst the two faults were compounded together, in terms of air consumption, the faulty cylinder posed virtually the same effects as experienced during Experiment 5. Similarly, during Experiment 9, which contained both types of faults and the actuators actuating *separate*ly, the consumption of CA increased by around **6 per cent**, as compared to Experiment 6. This again meant that the effects of the faulty door remained the same as those reported in Experiment 7 whilst also confirming that when both faults are induced, their effect on the CA volume is compounded.

With regards to comparing the mentioned experiments with the control test, all experiments that included any fault type in junction with the *separate* actuation setting, resulted in a higher CA consumption, as compared to their *simultaneous* setting counterpart. This again was attributed to the longer test time in Zone C. In order to better comprehend each mentioned experiment in comparison with the control, Table 7-9 provides CA consumption data against the benchmark. Consequently, Figure 7.13 illustrates the CA consumption per experiment in a bar chart. It is worth mentioning that as discussed in previous sections, the values obtained for the flow rate values, which also determined the amount of CA consumption per stop, had a high element of uncertainty due to the sensor utilised. Having said this, the mentioned changes were quite substantial and repeatable, meaning that the highlighted changes could be attributed to the sequence of actuations.

Table 7-9: The CA consumption data for the chosen experiments, as compared to control.

Experiment	Depicted Scenario	Additional Volume Consumed/NL	Percentage Surge as Compared to the Control Test
4	*Simultaneous* (Leak)	13.69	+33%
5	*Simultaneous* (Faulty)	0.85	+2%
8	*Simultaneous* (Leak & Faulty)	14.93	+36%
3	*Separate*	0	0%
6	*Separate* (Leak)	16.21	+40%
7	*Separate* (Faulty)	2.46	+6%
9	*Separate* (Leak & Faulty)	19.31	+46%

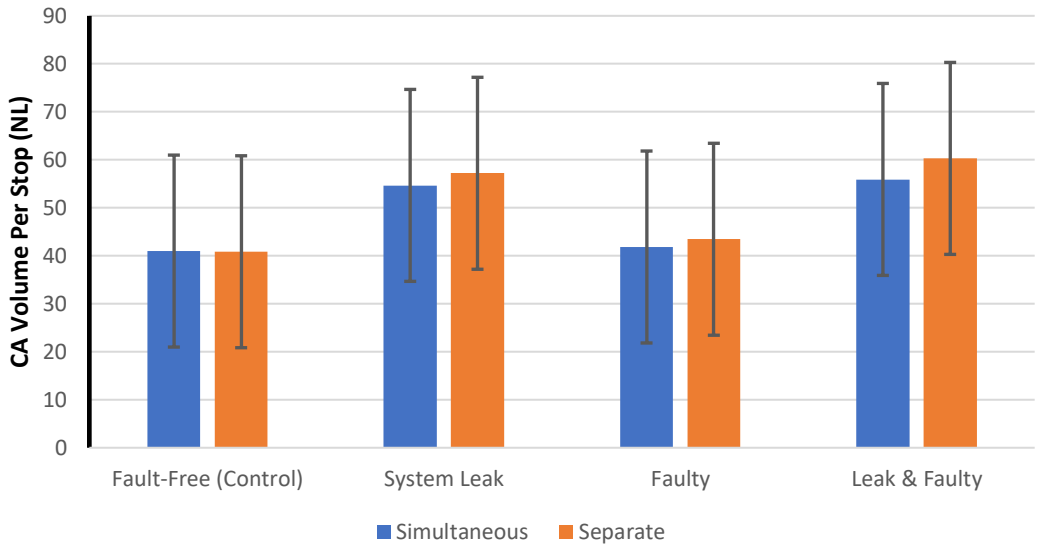

Figure 7.13: The CA consumption data for the chosen experiments.

7.3.2 System Pressure Trends

As reported in *Section 7.2.5*, leaks and faults both had an effect on the system's pressure behaviour, primarily on the standard deviation within each stop. By performing the additional experiments, it could be determined how the selected experiments behaved with regards to system pressure. This was done in order to confirm or deny if the pressure, mainly the standard deviation, can be used in order to reliably detect the presence of faults.

Firstly, it could be noted that whilst performing Experiment 6, which entailed inducing a system leak whilst the actuation sequence was set to *separate*, the average system pressure was reduced by 1 per cent, as compared to its leak free counterpart (i.e. Experiment 3). This behaviour was identical to the behaviour experienced in *Section 7.2.3*, which compared the same simulations but with the actuations occurring *simultaneously*. Subsequently, when analysing the pressure standard deviation within stops for the *separate* scenario, it could be deduced that the obtained value was **17 per cent** lower as compared to the same scenario without the leak, due the reduction in Δ_P caused as a consequence of Bernoulli's Principle. This behaviour virtually replicated what was reported in the previously mentioned section showing that the system behaved in the same manner. Therefore, it continued to show that monitoring this parameter also enabled the detection of leaks even when the sequence of actuations was altered.

The next step was to analyse the effect that the faulty cylinder had on the system's pressure behaviour. With regards to the *simultaneous* scenario, it was noted that during Experiment 5, the inclusion of the fault did not result in a leak which was significant enough to affect the system pressure. This was again observed for Experiment 7, which repeated the same experiment but for the *separate* scenario. During Experiment 5, it was also noted that the fault drastically reduced the pressure standard deviation, as compared to the control. Similar findings were made for Experiment 7, which showed that during this experiment, a **7 per cent** reduction was recorded for the pressure standard deviation. This was again virtually the same as the percentage obtained during the previously mentioned experiment, confirming that this parameter was capable of detecting the fault, irrespective of the actuation sequence.

The final set of experiments analysed the effects when the pneumatic system encountered both a system leak and a faulty double acting actuator, simultaneously, during the simulations. Consequently, it was deemed appropriate to investigate how these two parameters would together affect the system's pressure behaviour. From Table 7-8 it could be determined that whilst comparing Experiments 8 and 9, which induced both the leak and fault for both actuation sequences, the average pressure for the two sets of experiments was reduced by 1 per cent, as compared to their respective fault free counter parts. This reduction could again be attributed to the system leakage since as aforementioned previously, the faulty pneumatic cylinder did not affect the

system pressure. Additionally, when comparing the same experiments, a significant reduction in the pressure standard deviation was again noted. However, during Experiment 8, where the actuations were performed *simultaneously*, the reduction was recorded at **9 per cent** whilst during the *separate* actuation setting, i.e. Experiment 9, the reduction was computed at **17 per cent**. This difference in percentage was attributable to the effect that the actuation sequence plays during Zone C. The reason being that the during the *simultaneous* actuations, the faulty cylinder was actuated with the bellow, hence affecting the pressure whilst both were being actuated. On the other hand, during the *separate* actuations, the faulty double acting actuator only affected the system's pressure whilst it was being actuated, thereby reducing the fluctuations in the system pressure. In order to better comprehend the effects on the pressure standard deviation at each bus stop, Figure 7.14 contains a bar chart with all of mentioned the values.

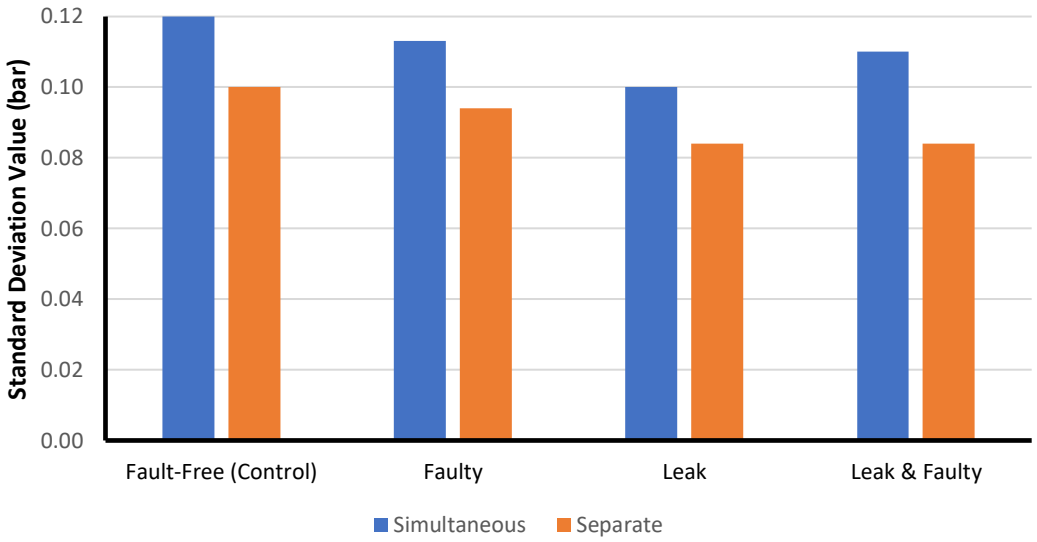

Figure 7.14: The obtained values for the pressure standard deviation within stops for the chosen experiments.

7.3.3 Bus Stop Timing Trends

The final aspect to be analysed for the chosen full factorial experiments was the bus stop timing. Firstly, in order to better comprehend the affect that the system leak posed with regards to the timing, Experiment 6 was performed, where the system leak was induced whilst the actuations were performed *separately*. Whilst comparing the results with its leak free counterpart, i.e. Experiment 3, it could be noted that that the leak had virtually no real effect on time, as confirmed in Table 7-8. This seconded the observations discussed in *Section 7.2.3*, where similar experiments were compared whilst undergoing the actuations *simultaneously*, i.e. Experiments 4 and 1.

While analysing Experiments 7 and 3, which compared the simulation for the faulty cylinder and *separate* actuations to its fault free counterpart, it was observed that this faulty component caused the time per bus stop to minutely increase by **1 per cent** and this was caused by the 3 per cent time increase to inflate the bellow, as explained in *Section 7.2.4*. These results showed that with regards to time, the faulty component posed the same effect as when comparing the *simultaneous* experiments, during Experiment 5. Consequently, it could be noted that with regards to real world repercussions, this type of fault would increase the downtime per stop.

Finally, in analysing the results obtained when the system leak was introduced in junction with the faulty cylinder for both actuation sequence settings, it was noted that for both Experiments 8 and 9, which was when both faults sources were induced whilst the actuation setting was set to *simultaneous* and *separate*, respectively, the overall time was virtually the same as when each respective system solely contained the faulty cylinder (i.e. **1 per cent** increase as compared to their faultless counterparts). This again confirmed that the system leak had no significant effects with regards to timing. Consequently, it could be deduced that for both sets of experiments, the time to inflate the bellow took 3 per cent more to inflate than the control experiment, with this being attributed to the effects posed by the faulty cylinder.

Furthermore, the duration to complete the simulations for the *separate* experiments was always longer than their *simultaneous* counterparts due to the additional time required to complete Zone C. This meant that when compared to the benchmark test, the percentage difference for the *separate* experiments were always around **20 per cent** greater, than those for the *simultaneous* experiments. This can be clearly highlighted in the bar chart shown Figure 7.15, where the time per stop was plotted. This therefore, confirms that the use of the *separate* setting should be avoided due to the additional down time.

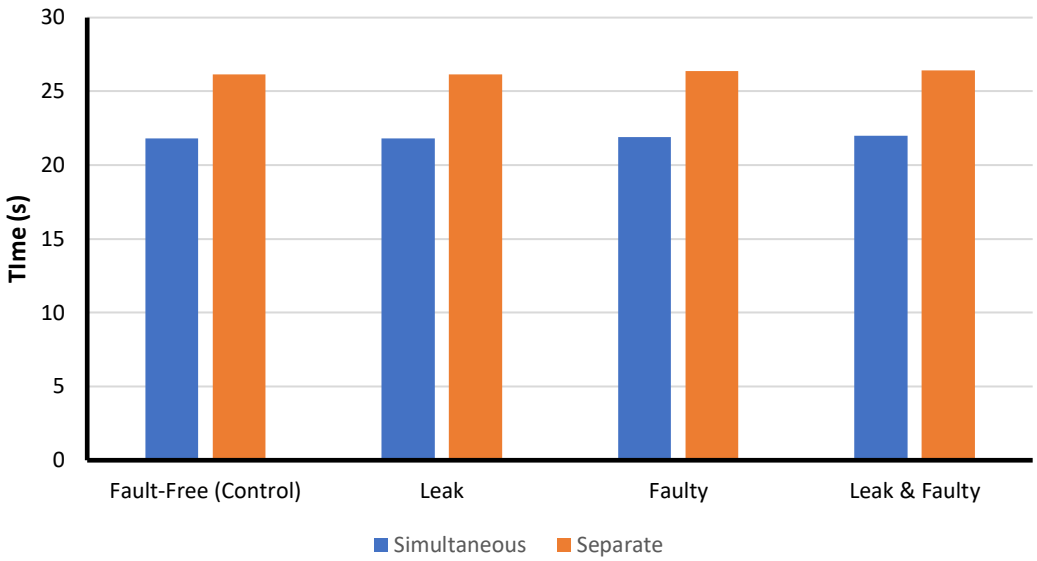

Figure 7.15: The obtained values for the time per stop for the chosen experiments.

7.3.4 Synopsis of Full Factorial Experiments

Through the additional experiments performed, more insight about the system's behaviour was gained, whilst also confirming the hypothesis established during the single factorial experiments. Furthermore, these tests helped in being able to answer research question two and three, whereby the effects imposed by different parameters on the system were analysed, together with assessing factors which make it possible to identify and quantify fault sources.

As expected, it was established that the CA flow rate would be able to identify and quantify the presence of faults since both when the system was induced with the system leak and the faulty pneumatic cylinder, additional CA was consumed during the simulations, with the former having a greater impact. Furthermore, it was evident that when the actuation setting was set to *separate*, the effects of both types of faults were amplified, due to the additional time required to complete the bus stop.

Moving on to the pressure characteristics, the obtained results showed that the system leak affected the system pressure by decreasing it by 1 per cent for all actuation settings whilst the faulty cylinder had no effect on this parameter. However, both faults resulted in the pressure standard deviation during stops to be significantly less as compared to a faultless system, irrespective of the actuation setting. Therefore, this parameter would make it possible to identify leaks using the pressure transducer infrastructure already present in buses. This would allow for the development of monitoring systems

which do not require additional flow rate sensors, such as the system proposed by M.Borg [17], or the need of conversion algorithms, designed by A.Erikson [99].

Finally, it was affirmed that for both actuation sequences, the system leak had virtually no effect with regards to the cycle time, whilst the faulty cylinder resulted in an additional 1 per cent on the overall time. Therefore, the time parameter can be used to identify faulty components. Furthermore, it was concluded that the major contributing factor which affected timing was the *separate* sequence setting. This was due to the additional time required to complete the actuations in Zone C, as compared to the *simultaneous* counterparts.

7.4 Real Life Data Analysis

Up to this point, one was able to better understand the behaviour of BPSs both by using the real life data compiled in Chapter 5 and by utilising the collected data of the BPTB. In order to further enhance the knowledge regarding this sector, whilst also exploring real life effects compounding the system, both sets of data were used conjointly.

Firstly, it was deemed appropriate to compare the values for both data sets in order to determine how the experimental data for the control test faired with that of Chapter 5, with the results tabulated in Table 7-10. It is worth mentioning that the same air flow sensor was used to measure both sets of data, meaning that the same element of uncertainty was present. Furthermore, the computed volume for each component was the average of three repeated readings.

Table 7-10: The CA consumption data for the real bus and BPTB.

	CA Volume Consumed per Actuation (NL)	
Component Measured	**Real Bus**	**BPTB**
Bellow	38.52	25.80
Pneumatic Cylinder	3.66	3.75

Comparing the performance of the cylinders, it was noted that the values obtained were very similar, with the difference most likely being attributed to the uncertainty associated with the air flow sensor. In contrast, the obtained volume values for the bellow were not as close with two main reasons being attributed to this. Firstly, as

stated in *Section 6.1.1.3*, the height to which the bellow is inflated varies from vehicle to vehicle, with the ride height setting for the actual bus being set to around 380 mm, whilst the setting for the test bed was set at 350 mm. Secondly, the loads being experienced by the vehicle were different from those imposed in the BPTB. All things considered, it could be said that the data recorded with the test bed was comparable to that in a real vehicle, showing that the set-up was capable of adequately portraying the performance of a typical BPS. Therefore, it could also be concluded that the experimental results were still valid since the data obtained using the test bed were relative hence not being effected by the mentioned discrepancies. Furthermore, the collected information made it possible to further investigate the real life performance of such a system.

7.4.1 Real Life Fault Repercussions

As underscored in both the studies by K.Abela [64] and L.Caurana *et al.* [80], it is essential for a pneumatic study to comprehend the real life effects regarding the financial and sustainable implications associated with faults. By being able to better comprehend the performance of BPSs, it was possible to determine the real life implications posed by faults on the system. To do so, the data compiled from the experiments was extrapolated and used with Equations 5.1 to 5.3. Therefore, for all scenarios, the number of bus stops was left the same as in *Section 5.4*. (i.e. 49 stops per hour). The obtained data was tabulated in Table 7-11. For this calculation, the flow rate value for the system leak was assumed to have a base line value of 40 NL/min, as established in *Section 7.2.3*. On the other hand, for the faulty cylinder, the baseline value had to be calculated since its effects only prevailed whilst the cylinder was retracted. According to research, the average time for a bus stop, whereby the cylinder is extended, is 30 s [124]. Therefore, since 49 stops occur each hour, the baseline value for the faulty cylinder could be calculated to 1.2 NL/min.

Table 7-11: The real life pneumatic data whilst induced with faults.

Parameter	Control	System Leak	Faulty Cylinder
Fuel Consumed By Pneumatic System (L/h)	0.305	0.395	0.308
Pneumatic Fuel Cost (€/h)	0.369	0.477	0.372
Pneumatic CO_2 Emissions (kg/h)	0.799	1.034	0.806

By initially looking at the obtained results, one might think that the overall impact imposed by the system leak on the pneumatic system is not significant. This could be attributed to the fact that whilst initially analysing certain parameters, such as the CO_2 emissions, a relatively minor increase of 0.235 kg per hour was recorded. Nevertheless, considering that a single bus is in operation daily for 16 hours [115], this increase becomes quite substantial, resulting in 1.37 tonnes of annual CO_2 emissions. To give context, if the solar panel set-up being proposed by the Malta Public transport [53] (discussed in *Section 3.2*) were to be implemented, it means that the fault would contribute to approximately a 50 per cent reduction in the quoted emission savings per vehicle. Additionally, considering how Malta is striving to decrease its carbon footprint through the push towards solar panel use for households, this would also hinder the overall progress. The reason being that since in Malta, 378 g of CO_2 per kWh [9] are emitted to produce electricity, if the additional CO_2 emissions were converted to electrical energy, this would equate to 3624 kWh. Therefore, since locally the power rating for solar systems is 1,600 kWh per kWp [9] and assuming that each panel has an output of 0.3 kW [125], than it means that in order to offset the additional emissions, 7 panels would be required. As pointed out in *Section 3.3.2*, maintenance is commonly overlooked since the down time associated with it accounts to 21 per cent [6] of the operational costs. Therefore, in terms of financial repercussions, if the operator chooses not to repair the system leak, the additional €0.11 per hour associated with the additional fuel costs required to operate the pneumatic system, translate to €640 in annual costs per vehicle. If it were assumed that each bus making up Malta's bus fleet (i.e. 430 buses [53]) would contain this leak, the costs associated with this fault would amount to a total of €280,000. It can also be concluded that with the introduction of the leak the pneumatic fuel percentage increases to 5.6 per cent, as compared to 4.4 per cent for a fault-free system. Furthermore, this leak would also contribute to an increase of 30 per cent in the pneumatic fuel consumption.

Whilst analysing the results for the faulty door, it could be noted that as expected, it also had financial and environmental repercussions but with a lesser effect than the system leak. By extrapolating the data, this fault would contribute to an additional €17.52 in annual fuel costs whilst increasing the annual CO_2 emissions by 40.9 kg.

As established, the *separate* actuation setting contributes to an additional 20 per cent in the total stop time, resulting in a longer period of waiting time. Since it was

previously stated that on average, a bus stop takes 30 s [124] to complete, it could be estimated that the percentage increase would result in an additional 6 s per stop, where for this scenario, 49 stops occur each hour. Therefore, since at idle, a diesel engine consumes 0.3 L per hour of engine displacement [126] and that a typical Maltese bus has an engine displacement of 8.9 L [34], the time increase would account to an additional 1,273 L of diesel per vehicle annually, equating to €1,540 in fuel costs and an increase in 3 per cent in the total fuel cost. Furthermore, an additional 3.3 tonnes of CO_2 emissions would also be emitted. Since in *Section 5.3.1*, it was estimated that the system fill-up takes 219 s to complete, this additional downtime could instead be used to perform 7,840 system fill-ups, again confirming that this setting should be avoided.

7.5 Conclusion

Throughout this chapter, the experiments performed helped to comprehend the behaviour of BPSs, by making use of the output parameters established in Chapter 6, i.e. CA flow, pressure and test timing. It was determined that the system leak and the faulty cylinder both had a significant impact on the CA flow, where both resulted in a significant increase in this parameter, therefore confirming that it could be used to identify fault sources. Additionally, in an effort to identify more parameters which could be used to identify faults, the pressure standard deviation within stops was also assessed and it was determined that for both types of fault, a sizable reduction in this value was recorded, when compared to their fault free counterparts. This was a result of the reduction in Δ_P, which made the system pressure more stable. Therefore, this parameter would allow for the finding of faults in BPSs, without the need of any additional equipment since buses are equipped with multiple pressure transducers. With regards to timing, the faults did not have a significant impact on this factor, with only the faulty cylinder recording any factual variations. On the other hand, the *separate* actuation setting posed the greatest effect with regards to the test time, since it increased it by 20 per cent, as compared to the *simultaneous* actuation setting. Furthermore, it was deduced that whilst actuating the end effectors *separately*, the losses associated with the faults were amplified, mainly the CA volume consumption, due to the longer actuation times during Zone C. However, the values obtained were not definite, due to the arbitrary times set during the simulations. During the tests, the performance of the bellow was also better understood and as expected, when the pre-

set ride height pressure was reduced, the volume required to fill the consistent reduced which reduced the time to fill the constituent.

The real life performance of BPSs was also examined, quantifying the effects imposed by different parameters, where it was determined that both types of faults resulted in the increase of fuel costs and emissions emitted. It was also established that the pneumatic fuel consumption increased by 30 per cent when the system was induced with the leak. The effects of the *separate* actuations were also underscored, as it was determined that it affected the performance of the system due to the increase in the waiting time. This resulted in an increase in the fuel costs and emissions emitted. By completing this chapter, it could also be concluded that research questions two and three were also fulfilled, as different parameters were analysed in relation to the performance of BPSs, followed by an analysis of the factors which make it possible to identify and quantify fault sources.

Chapter 8-Conclusion

This chapter presents the conclusions of this research study by discussing the results presented in Chapter 7, in view of the shortcomings identified in the state of the art and literature review. A discussion is also presented on how the research questions were tackled in this study.

The established research questions were the following:

1. How much fuel/energy do elements in a typical BPS consume during operation (e.g. the bellows, doors and brakes)?
2. What are the effects that different parameters have on the performance of the BPS?
3. Which parameters can be used to identify and quantify fault sources in BPSs?

Although this study gave a better insight on how BPSs behave and which factors affect it the most, there are still areas where future work or further advancements would be beneficial towards better comprehending and developing these set-ups. This chapter also discusses these improvements and work opportunities.

8.1 Principal Research Outcomes

In a typical bus, the pneumatic auxiliaries are frequently used throughout the time of the operation of the vehicle, with the main ones being the air suspension, double acting actuators and the air brakes. These consume a considerable amount of energy, with the study by D.Tretsiak *et al.* [5], claiming that for a hybrid bus, the electric compressor consumes 24 per cent of the total electrical energy. It is also known that all CAS are inefficient, with research claiming that industrial set-ups are only capable of converting 5 to 30 per cent of their input energy into useable output [47, 48]. Additionally, all pneumatic systems are inevitably exposed to faults, with one of the most prevalent ones being leaks. In buses, these faults not only result in additional fuel consumption and emissions but may also lead to safety hazards. This was underscored by S.Ramarathnam *et al.* [67], who concluded that a leak led to the braking distance to increase by 2.7 m. In the public transport sector, these type of faults are not frequently attended to due to the fact that maintenance causes a considerable amount

of downtime, which accounts to 21 per cent [6] of the overall operational costs. It is also known that repairs have a high potential in improving the sustainability performance of a system where in industrial systems, demand side improvements account for up to 70 per cent [54] of the total CA improvement potential.

Whilst reviewing literature, in Chapter 3, it became evident that information in terms of both the behaviour and performance of these systems is lacking. This observation was also highlighted by M.Trompet [86], since during a benchmarking process performed in collaboration with several companies, focus was given towards the financial side of the operation, therefore totally neglecting the BPS. Other bus related audits were also found, such as the ones by A.Thiruvengadam *et al*. [78] and Volvo [79], which focused on the sustainability of the vehicle. However, these concentrated on improving the drivetrain of their bus fleet, rather than improving the BPS.

Although knowledge regarding this sector is lacking, developments have been made towards improving BPSs. One of the main areas of these advancements was the development of monitoring systems, with the aim of reducing the downtime associated with the repairs. One such example was the set-up by A.Eriksson [99], where by using the built-in pressure sensor infrastructure already present in these vehicles, a monitoring system was designed to detect fault sources. However, such system was not reliable due to the frequent false alarms, whilst also not being able to successfully identify the fault location. Another monitoring set-up for buses was also designed by M.Borg [17], which made use of additional air flow sensors to monitor the set-up. However, the performance of this system could not be assessed since it was not fully implemented. By gaining insight on the current lack of information regarding this sector, together with the potential that monitoring systems have in making the overall repair process easier, the need to develop the three research questions was ensued.

To answer research question one, real life data from an actual bus was collected in Chapter 5, to better comprehend the performance of a typical BPS. During the monitoring session, the actuations taking place throughout a bus stop scenario were chosen to be observed. The reason being that this scenario is performed regularly and entails the actuations of the three most frequently used pneumatic end effectors, i.e. the pneumatic cylinders, the air suspension and the air brakes. By monitoring the CA flow rate of all constituents, it was concluded that each stop required 168 NL of CA

which translates to 4.96 L of diesel daily. In addition, it was also established that the pneumatic system consumes 4.4 per cent of the vehicle's total fuel.

The second and third research questions of this research study sought to identify the effects that different parameters, both operational and fault oriented, have on the performance of BPSs, whilst also finding parameters which determine and quantify fault sources in such systems. These questions were answered through the performance of further simulations which depicted the bus stop scenario, where the first step was to perform a DOE. To perform the tests, a set-up comprising of both the BPTB and the CATB was used since it was capable of depicting and monitoring a typical BPS. During the simulations, three output factors were monitored: CA flow which derived the volume consumption, system pressure which derived the pressure standard deviation within each stop and cycle time. From the obtained data, it could be confirmed that the losses were well monitored using:

- A pressure transducer monitoring the system pressure;
- An air flow sensor monitoring the system CA flow rate;
- Reed switches monitoring the actuations of the doors;
- A pressure transducer monitoring the bellow pressure.

By performing the simulations and using the variations from the three output parameters measured, whilst inducing each fault, it was possible to determine the effects that faults have on the set-up and any factors which help in identifying them. In analysing the data whilst the system was induced with the system leak, the obtained results when comparing Experiment 1 (i.e. control) to 4 in Table 7-5 were:

- A 33 per cent increase in the CA volume;
- A 16 per cent decrease in the pressure standard deviation between stops;
- No change in the time per stop.

With regards to the faulty cylinder, comparing Experiments 1 and 5 in Table 7-5, the system reacted as follows:

- A 2 per cent per cent increase in CA volume;
- A 6 per cent decrease in the pressure standard deviation between stops;
- A 1 per cent increase in the time per stop.

The results showed how the system reacted whilst exposed to the faults and also indicated that all three factors could be used to identify and quantify faults in BPSs. However, in analysing each parameter, it was determined that the pressure standard deviation within each stop would be most adequate for use in these vehicles. The reason being that apart from the obtained values being quite significant, making it more easy to differentiate between the type of fault, multiple pressure transducers are pre-installed in buses, as indicated by Volvo [98]. Consequently, this makes it possible to monitor the set-up without the need of additional equipment allowing for the overall process to be simpler than other proposed set-ups, such as the one by A.Eriksson [99], which made use of complex algorithms to obtain volume readings, or the set-up by M.Borg [17], which made use of additional flow meters. Additionally, the time parameter can also be used conjointly with the pressure standard deviation to ensure further reliability during the fault finding process. This parameter can also be monitored in buses without the need of additional equipment since the vehicle's ECU, also monitors the actuation timing of the equipment. The system's behaviour whilst induced with each fault is summarised in Table 8-1.

Table 8-1: A summary of the system's behaviour for each type of fault

Fault Induced	System Pressure	Pressure Standard Deviation	CA Volume	Time per Stop
System Leak	-	--	++	/
Faulty Cylinder	/	-	+	-
System Leak & Faulty Cylinder	-	--	++	-

Where + is increase and – is decrease

In analysing the operational factors, it was established that the *separate* actuation sequence resulted in a considerable increase in the time per stop due to the actuations in Zone C being performed in succession. In addition, due to the longer time, the effects posed by both faults, most notably the CA volume consumption, were amplified. Therefore, it could be suggested that this setting should always be avoided during typical bus use. Furthermore, whilst analysing the effects of the reduction of the bellow pressure during the ride height setting, the results obtained were as expected, since the volume required to fill the constituent decreased, reducing the time to inflate it. Ultimately, it could be established that both research questions two and

three were fulfilled since the performance of the system was examined in relation to different parameters, whilst parameters which help in finding and quantifying fault sources were also assessed.

Moving onto the real life data obtained whilst performing the tests on an actual bus, it could be recalled that a fault free pneumatic system consumes 4.4 per cent of the total fuel. This however, increased to around 5.6 per cent whilst being induced with the system leak, contributing to an increase of 30 per cent in the pneumatic fuel consumption. This shows that the effects are quite considerable. In addition, although maintenance is often overlooked due to downtime associated with it, by seeing the financial and environmental repercussions highlighted in *Section 7.4.1*, it should give further incentive to properly maintain these systems, whilst also highlighting the importance that monitoring systems can have in these set-ups.

Therefore, by being able to investigate the behaviour that both operational and fault oriented factors pose on the BPS, both through the experiments and through real life repercussions, whilst also identifying parameters which make it possible to identify and quantify fault sources, research question two and three were also answered. This consequently led to fulfilling the overarching aim of the study, whereby using the knowledge gathered from all three research questions, it would help towards the development of better monitoring systems catered for BPSs.

8.2 Future Work

By completing the study and thereby fulfilling all three research questions, one was able to comprehend the performance of a typical BPS, whilst identifying the factors which highlight the presence of faults. Although this provides crucial data towards this particular sector, it still paves way to future work.

Seeing the potential that the study has with regards to improving BPSs it would be beneficial for the obtained knowledge to be used to further evolve cyber-physical monitoring systems, such as the one designed by M.Borg [17]. Additionally, by implementing such a set-up, it would also make it possible to gather further holistic pneumatic data contributing to further knowledge towards this area, whilst also helping to develop audits in this sector. This information will become more valuable

as time goes by since as highlighted throughout Chapter 3, emphasis in recent years has been made towards improving the drivetrain of these vehicles. Thus, there will come a point where further drastic improvements in this area would not be possible, thereby shifting improvement efforts towards other areas, such as pneumatic systems, in order to improve the vehicle's sustainability performance.

Another possible opportunity towards the further development of the monitoring system is to be able to develop an intelligent BPS, in the sense that it would be able to interpret the data on its own. This could be achieved by further evolving the concept of IoV, such as the supply oriented ones by J.Laurikko [102] and D.Tretsiak *et al.* [5], whilst also incorporating the concept of Artificial Intelligence (AI), where the system is able to continuously study and learn the behaviour of the set-up using adequate models. This would also allow for the system to be dynamic thereby, automatically performing demand oriented reactive actions. By applying such a concept, the overall fault-finding process is more stream lined and user friendly, giving incentive for companies to implement such set-ups into their bus fleet.

One of the problems encountered by current monitoring systems, including the one by A.Eriksson [99], which was not tackled in this study, is the identification of the fault location. This therefore, presents the final future work opportunity whereby the monitoring system would be further developed and improved in order to locate the area where the fault/s reside.

8.3 Concluding Reflections

The output efficiency of all pneumatic systems is regarded to be considerably low and riddled with losses. The BPS is no exception, with the difference being that current knowledge regarding such set-ups is still quite scarce. With the completion of this study, where the significance that the pneumatic system plays towards the sustainable performance of the vehicle was underscored, an incentive to further investigate these systems was provided. Additionally, the gathered quantitative and qualitative data, which helped to further enhance the knowledge of these systems, encourages further development towards state-of-the art monitoring systems catered for these vehicles. This would make the overall leak repair process more user friendly, hence drastically reducing the down time associated with repairs, giving incentive for companies to

adopt such set-ups. Ultimately, such improvements will contribute towards the reduction of emissions and fuel costs, making the transportation sector overall cleaner.

Appendices

Appendix 1

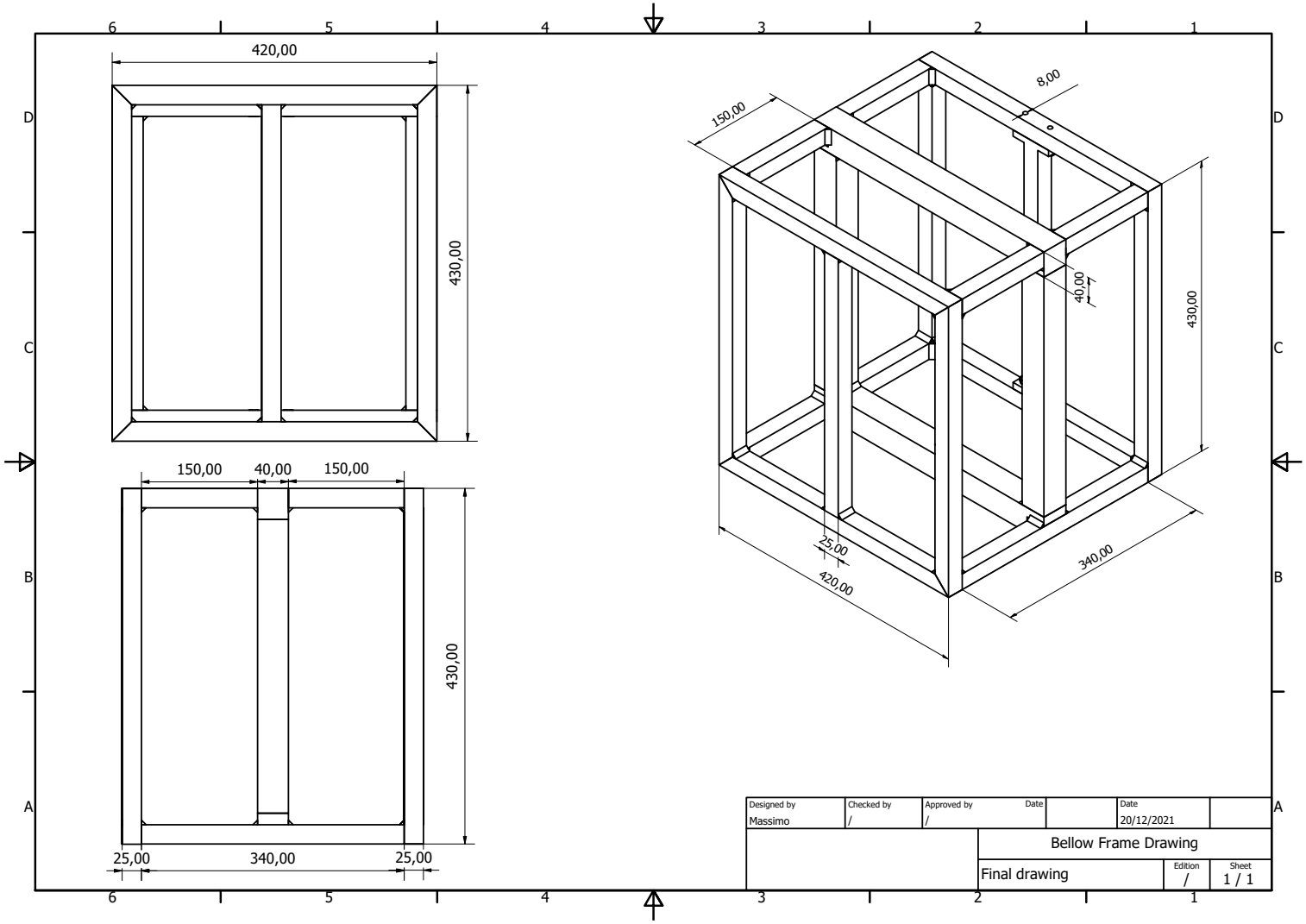

Figure 9.1: The CAD drawing for the bellow's frame.

Appendix 2

Table 9-1: The data obtained for the remaining eight experiments.

Experiment Information	**Experiment**	**Actuation Sequence**	**Fault Type**	**Bellow Pressure**
	10	Together	System Leak	3.5
	11	Separate	None	3.5
	12	Separate	System Leak	3.5
	13	Together	Faulty Door	3.5
Parameter Analysed	**Experiment 10**	**Experiment 11**	**Experiment 12**	**Experiment 13**
Air Flow Sensor				
Average System CA Flow Rate – *F500* (NL/min)	120.83	75.09	112.64	84.91
Standard Deviation of Repeats (NL/min)	0.22	0.29	0.22	0.23
Reading Uncertainty (NL/min)	±29.28	±29.28	±29.28	±29.28
Percentage Uncertainty	24.23%	38.99%	25.99%	34.48%
CA Volume per Stop (NL)	42.74	29.27	43.88	30.04
Standard Deviation of Repeats (NL)	0.11	0.046	0.05	0.038
Reading Uncertainty (NL)	±10.35	±11.40	±11.41	±10.36
Percentage Uncertainty	24.22%	38.94%	26%	34.48%
Pressure Transducers				
Average System Pressure – *P2* (bar)	6.01	6.06	6.01	6.05
Standard Deviation of Repeats (bar)	0.031	0.025	0.02	0.021
Reading Uncertainty (bar)	±0.04	±0.039	±0.038	±0.038
Percentage Uncertainty	0.67%	0.64%	0.63%	0.63%
Pressure Standard Deviation Within Each Cycle (bar)	0.09	0.09	0.08	0.10
Solid State Switches & Digital Timing				
Test Time per Stop (s)	21.22	23.37	23.38	21.23
Standard Deviation of Repeats (s)	0.18	0.5	0.53	0.5
Door Average Actuation Time (s)	5.36	5.14	5.1	5.37
Standard Deviation of Repeats (s)	0.003	0	0.0058	0.036
Bellow Average Actuation Time (s)	2.99	2.64	2.67	2.99
Standard Deviation of Repeats (s)	0.035	0.02	0.03	0.021

Experiment Information	Experiment	Actuation Sequence	Fault Type	Bellow Pressure
	14	Together	System Leak & Faulty Door	3.5
	15	Separate	Faulty Door	3.5
	16	Separate	System Leak & Faulty Door	3.5
Parameter Analysed	**Experiment 14**	**Experiment 15**	**Experiment 16**	
Air Flow Sensor				
Average System CA Flow Rate – *F500* (NL/min)	123.45	79.21	117.90	
Standard Deviation of Repeats (NL/min)	0.33	0.24	0.33	
Reading Uncertainty (NL/min)	±29.28	±29.28	±29.28	
Percentage Uncertainty	23.72%	36.97%	24.83%	
CA Volume per Stop (NL)	43.69	30.95	46.10	
Standard Deviation of Repeats (NL)	0.04	0.061	0.085	
Reading Uncertainty (NL)	±10.36	±11.44	±11.44	
Percentage Uncertainty	23.71%	36.97%	24.82%	
Pressure Transducers				
Average System Pressure – *P2* (bar)	6.00	6.04	6.01	
Standard Deviation of Repeats (bar)	0.023	0.01	0.031	
Reading Uncertainty (bar)	±0.038	±0.036	±0.04	
Percentage Uncertainty	0.63%	0.6%	0.67%	
Pressure Standard Deviation Within Each Cycle (bar)	0.089	0.08	0.08	
Solid State Switches & Digital Timing				
Test Time per Stop (s)	21.23	23.44	23.45	
Standard Deviation of Repeats (s)	0.39	0.53	0.23	
Door Average Actuation Time (s)	5.36	5.14	5.14	
Standard Deviation of Repeats (s)	0.0058	0.0058	0.01	
Bellow Average Actuation Time (s)	3.03	2.66	2.69	
Standard Deviation of Repeats (s)	0.032	0.02	0.029	

References

[1] "MAN Lion's City." MAN, München, 2015.

[2] "Why does public transport uses compressed air to open doors instead of electromotors?," *Engineering Beta*, 2015. [Online]. Available: https://engineering.stackexchange.com/questions/2917/why-does-public-transport-uses-compressed-air-to-open-doors-instead-of-electromo. [Accessed: 05-Jan-2021].

[3] "8 Advantages of Pneumatic Systems," *SMC*, 2019. [Online]. Available: https://www.smcpneumatics.com/8-Advantages-of-Pneumatic-Systems_b_31.html. [Accessed: 07-Jan-2021].

[4] "How to Decide Between Pneumatic and Electric Actuators," *Automation World*, 2012. [Online]. Available: https://www.automationworld.com/products/motion/article/13307480/how-to-decide-between-pneumatic-and-electric-actuators. [Accessed: 07-Jan-2021].

[5] D. Tretsiak, T. Häberlein, and B. Bäker, "Energy Efficient Control of the Air Compressor in a Serial Hybrid Bus based on Smart Data," *IFAC-PapersOnLine*, vol. 49, no. 11, pp. 385–392, 2016.

[6] A. Haghani and Y. Shafahi, "Bus maintenance systems and maintenance scheduling: Model formulations and solutions," *Transp. Res. Part A Policy Pract.*, vol. 36, no. 5, pp. 453–482, 2002.

[7] "Climate Change Consequences," *European Commision*, 2021. [Online]. Available: https://ec.europa.eu/clima/climate-change/climate-change-consequences_en. [Accessed: 01-Dec-2021].

[8] IPCC, "IPCC report Global warming of 1.5°C," 2018.

[9] Ministry for Energy and Water Management, "Malta's 2030 National Energy and Climate Plan," 2019.

[10] United Nations, "The 17 Goals," 2021. [Online]. Available: https://sdgs.un.org/goals. [Accessed: 01-Dec-2021].

[11] "Decarbonisation," *Euroean Commision-Mobility and Transport*, 2020. .

[12] O. Kostoska and L. Kocarev, "A novel ICT framework for sustainable development goals," *Sustain.*, vol. 11, no. 7, pp. 1–31, 2019.

[13] Bosch, "Bosch and Weichai Power increase efficiency of Weichai truck diesel engines to 50 percen," 2021. [Online]. Available: https://www.bosch-presse.de/pressportal/de/en/bosch-and-weichai-power-increase-efficiency-of-

weichai-truck-diesel-engines-to-50-percent-218880.html. [Accessed: 01-Dec-2021].

[14] Volvo, “Volvo 7900 Electric,” 2021. [Online]. Available: https://www.volvobuses.com/en/city-and-intercity/buses/volvo-7900-electric.html. [Accessed: 01-Dec-2021].

[15] N. Nakajima, “Green advertising and green public relations as integration propaganda,” *Bull. Sci. Technol. Soc.*, vol. 21, no. 5, pp. 334–348, 2001.

[16] FIA, UN Environment, UNECE, ICAO, and IMO, “Accelerating SDG 7 Achievement Policy Brief 16 - Interlinkage between Energy and Transport,” 2018.

[17] M. Borg, P. Refalo, and E. Fracalanza, “Development of a Vehicle Cyber Physical System for Sustainability Analysis,” Univeristy of Malta, 2020.

[18] K. Abela, P. Refalo, and E. Fracalanza, “Real Time Monitoring for the Efficient Use of Industrial Pneumatic Applications,” University of Malta, 2020.

[19] C. R. Kothari, *Research Methodology Methods and Techniques*. New Delhi: New Age International Publishers, 2004.

[20] A. Papson, F. Creutzig, and L. Schipper, “Compressed air vehicles: Drive-cycle analysis of vehicle performance, environmental impacts, and economic costs,” *Transp. Res. Rec.*, no. 2191, pp. 67–74, 2010.

[21] T. Verge, “The Tata AirPod: India’s tiny air-powered prototype car,” 2012. .

[22] F. Creutzig, A. Papson, L. Schipper, and D. M. Kammen, “Economic and environmental evaluation of compressed-air cars,” *Environ. Res. Lett.*, vol. 4, no. 4, 2009.

[23] S. S. Verma, “Latest Developments of a Compressed Air Vehicle: A Status Report Latest Developments of a Compressed Air Vehicle A Status Report Latest Developments of a Compressed Air Vehicle: A Status Report,” *Glob. J. Res. Eng. Automot. Eng.*, vol. 13, no. 1, 2013.

[24] T. Nehler, “Linking energy efficiency measures in industrial compressed air systems with non-energy benefits – A review,” *Renew. Sustain. Energy Rev.*, vol. 89, no. November 2016, pp. 72–87, 2018.

[25] E. M. Talbott, *Compressed Air Systems A Guidebook on Energy and Cost Savings*, Second. Lilburn: The Fairmont Press, Inc., 1993.

[26] Circle, “Electric outswing bus door system,” 2022. .

[27] “Electric sliding door system,” *Access Ability*. [Online]. Available:

https://www.access-ability.eu/en/products-for-people-with-disabilities-or-reduced-mobility/electric-sliding-door/. [Accessed: 07-Jan-2021].

[28] H. Heisler, *Advanced Vehicle Technology*. Oxford: BUTTERWORTH HEINEMANN, 2002.

[29] "Air Brake Parts," *Bus Parts*. [Online]. Available: http://www.busparts.com/assets/pdf-files/brakes-pdf/brakes-air-pdf/brakes-air-page-1-pdf.pdf. [Accessed: 05-Jan-2021].

[30] "Daily inspection test," *Ministry of Transportation*, 2017. [Online]. Available: http://www.mto.gov.on.ca/english/trucks/handbook/section6-1-4.shtml. [Accessed: 05-Jan-2021].

[31] "VOLVO B7R – Bellow Circuit and Suspension," *Volvo Service Manual*. [Online]. Available: https://svmchaser.wordpress.com/2014/11/18/volvo-b7r-bellow-circuit-and-air-suspension/. [Accessed: 05-Jan-2021].

[32] "VOLVO B7R – Brake Circuit," *Volvo Service Manual*. .

[33] *Understanding Trailer Air Suspensions*. Canton: Hendrickson, 2020.

[34] King Long, "Operation Manual King Long Buses." Xiamen, pp. 1–40, 2014.

[35] Firestone, "Engineering Manual & Design Guide." Indiana, p. 96, 2020.

[36] "What's the purpose of a kneeling bus?," *Right Driver*, 2019. [Online]. Available: https://mocktheorytest.com/highway-code-questions/bus/passengers/5-25-the-purpose-of-a-kneeling/. [Accessed: 24-Feb-2021].

[37] Laz, "LAZ A-183-CNG," 2012. .

[38] E. Klavebäck, "Improved Weight Estimation for Vehicles with Air Suspension Improved Weight Estimation for Vehicles with Air Suspension," Uppsala University, 2019.

[39] N. Einstein, "Safety Compromises, Part 5 - Failing to Kneel the Bus or Coach," 2018. .

[40] M. Grunwald and I. L. Barroso, "The Accesibility of Urban Transport to People with Reduced Mobility," Berlin, 2003.

[41] "Public Service Vehicles Accessibility Regulations 2000 - Guidance Table of contents," Lodnon, 2000.

[42] The American Public Transportation Association, "Recommended Practice for Transit Bus In-Service Brake System Performance Testing," Washington, 2005.

[43] *Air Brakes*. Glasgow: Ritchies Training Centre, 2016.

[44] SMC, “ISO Cylinder CP96 Series.” .

[45] Alibaba, “Pneumatic Outswing Door,” 2022. .

[46] “MAN - Pneumatic door motor for buses,” *MAN*, 2016. .

[47] R. Boehm and J. Franke, “Demand-Side-Management by flexible generation of compressed air,” *50th CIRP Conf. Manuf. Syst.*, vol. 63, pp. 195–200, 2017.

[48] S. Mousavi, S. Kara, and B. Kornfeld, “Energy efficiency of compressed air systems,” *Procedia CIRP*, vol. 15, pp. 313–318, 2014.

[49] “Cars, Trucks, Buses and Air Pollution,” *Union of Concerned Scientists*, 2018. [Online]. Available: https://www.ucsusa.org/resources/cars-trucks-buses-and-air-pollution. [Accessed: 21-Jan-2021].

[50] “Air Pollution costing the life of more than one person a day in Malta.,” *Malta Association of Public Health Medicine*, 2020. [Online]. Available: https://maphm.org/2020/05/16/air-pollution-costing-the-life-of-more-than-one-person-a-day-in-malta/. [Accessed: 19-Jan-2021].

[51] “Quarter of new public buses to be ‘clean’ in 2025,” *European Federation for Transport and Environment*, 2019. [Online]. Available: https://www.transportenvironment.org/news/quarter-new-public-buses-be-‘clean’-2025. [Accessed: 07-Jan-2021].

[52] “Emissions of most harmful air pollutants dropped in 2018, marking EU progress under UN Convention,” *European Enviroment Agency*, 2020. [Online]. Available: https://www.eea.europa.eu/highlights/emissions-of-most-harmful-air. [Accessed: 21-Jan-2021].

[53] Times of Malta, “Solar panels to be installed on top of route buses,” 2021. [Online]. Available: https://timesofmalta.com/articles/view/solar-panels-to-be-installed-on-top-of-route-buses.892429. [Accessed: 09-Aug-2021].

[54] M. Unger and P. Radgen, “Energy Efficiency in Compressed Air Systems – A review of energy efficiency potentials, technological development, energy policy actions and future importance,” in *Energy Efficiency in Motor Driven Systems (EEMODS) 2017*, 2018, no. November, pp. 207–233.

[55] E. A. Abdelaziz, R. Saidur, and S. Mekhilef, “A review on energy saving strategies in industrial sector,” *Renew. Sustain. Energy Rev.*, vol. 15, no. 1, pp. 150–168, 2011.

[56] CDC, “Too Loud! For Too Long!,” 2020. .

[57] “Reducing noise in the automotive industry,” Brussels, 2014.

[58] “Addendum 50: Regulation No. 51 Revision 2; Uniform provisions

concerning the approval of motor vehicles having at least four wheels with regard to their noise emissions," Geneva, 2011.

[59] ISC, "JORC Ultrasonic Air Leak Detector Kit," 2022. .

[60] H. Q. Shanghai and A. McKane, "Improving Energy Efficiency of Compressed Air System Based on System Audit," California, 2013.

[61] WABCO, "WABCO ULTRASONIC LEAKAGE DETECTOR," 2014.

[62] R. Dindorf, "Estimating potential energy savings in compressed air systems," *Procedia Eng.*, vol. 39, pp. 204–211, 2012.

[63] J. Billep and H. Fleischhacker, "Reduce energy costs in compressed air systems by up to 60%," 2013.

[64] K. Abela, P. Refalo, and E. Fracalanza, "Design, Construction and Testing of a Compressed Air Test Bed," University of Malta, 2019.

[65] V. K. Sharma and K. D. Prajapati, "Reduction of Friction in Pneumatic Actuator," *IOSR J. Mech. Civ. Eng. e-ISSN*, vol. 14, no. 4, pp. 1–07, 2017.

[66] "PHILADELPHIA: James Derbyshire Killed In Bus Accident After SEPTA Bus Crashed Through Pool And Into House By Frankford Avenue and Morrell Avenue In Torresdale," *Edgar Snynder & Associates*, 2018. [Online]. Available: https://www.edgarsnyder.com/breaking-news/2018-07/philadelphia-james-derbyshire-killed-in-bus-accident-after-septa-bus-crashed-through-pool-and-into-house-by-frankford-avenue-and-morrell-avenue-in-torresdale.html. [Accessed: 05-Jun-2021].

[67] S. Ramarathnam, S. Dhar, S. Darbha, and K. R. Rajagopal, "Development of a model for an air brake system with leaks and a scheme for the estimation of the steady-state pushrod stroke," *Veh. Syst. Dyn.*, vol. 49, no. 8, pp. 1267–1282, 2011.

[68] A. Azzi, A. Maoui, A. Fatu, S. Fily, and D. Souchet, "Experimental study of friction in pneumatic seals," *Tribol. Int.*, vol. 135, no. October 2018, pp. 432–443, 2019.

[69] "How to Avoid the Most Common Bus/Coach Kneeling Failures," *Compressed Air Best Practices*. .

[70] T. Ceh, "4 signs you've got a leak in your compressed air system," 2017. .

[71] "Get Rid of Stick-slip Trouble With These Tips," 2013. [Online]. Available: http://blog.parker.com/get-rid-of-stick-slip-trouble-with-these-tips. [Accessed: 22-Jan-2021].

[72] ISO, "ISO 3583:1984," 2020. [Online]. Available:

https://www.iso.org/standard/8991.html. [Accessed: 25-Mar-2021].

[73] "Poor maintenance of TNSTC buses, a cause for concern," *The Hindu*, 2018. [Online]. Available: https://www.thehindu.com/news/cities/Coimbatore/poor-maintenance-of-tnstc-buses-a-cause-for-concern/article24216275.ece. [Accessed: 22-Jan-2021].

[74] "Air suspension systems on vehicles, Health and Safety Executive - Safety alert," *Health and Safety Executive UK*, 2020. [Online]. Available: https://www.hse.gov.uk/safetybulletins/air-suspension-systems-on-vehicles.htm. [Accessed: 22-Jan-2021].

[75] Distrelec, "KEW6305 - Energy Analyzer," 2022. [Online]. Available: https://www.distrelec.de/en/energy-analyzer-channels-600-vac-70hz-kyoritsu-kew6305/p/11071750. [Accessed: 06-Jan-2022].

[76] R. Saidur, N. A. Rahim, and M. Hasanuzzaman, "A review on compressed-air energy use and energy savings," *Renew. Sustain. Energy Rev.*, vol. 14, no. 4, pp. 1135–1153, 2010.

[77] "ISO 50002:2014," 2014.

[78] A. Thiruvengadam, S. Pradhan, P. Thiruvengadam, M. Besch, and D. Carder, "Heavy-Duty Vehicle Diesel Engine Efficiency Evaluation and Energy Audit," West Virginia, 2018.

[79] E-hike, "Volvo/KPMG analysis finds cities could save millions with electric buses instead of diesel," 2015. .

[80] L. Caruana and P. Refalo, "Sustainability analysis of a compressed air system," *Eng. Sustain. Sustain. Energy 2018*, no. May, pp. 39–45, 2018.

[81] "Performance Audit: Assesing the Public Transport Contract and Transport Malta's Visibility on the Service," 2020.

[82] C. W. Marshall, "Public Transport Performance Model.," Parliament of Victoria, Victoria, 2012.

[83] "Bus Inspection & Maintenance," *JRS Innovation LLC*, 2019. [Online]. Available: https://businspectionmaintenance.com/index.html. [Accessed: 28-Dec-2020].

[84] T. P.Dinapoli, "Metropolitan Transportation Authority Selected Aspects of Bus Fleet Maintenance," New York, 2014.

[85] "Best Operational and Maintenance Practices for City Bus Fleets to Maximize Fuel Economy Helping Cities Meet Their Energy Challenges of the New Century," 2011.

[86] M. Trompet, B. J. Condry, and E. R. Randall, “International Bus System Benchmarking : Performance Measurement,” in *Transportation Research Board 86th Annual Meeting (2007)*, 2007, no. January 2007.

[87] M. Benedetti, F. Bonfa, I. Bertini, V. Introna, and S. Ubertini, “Explorative study on Compressed Air Systems’ energy efficiency in production and use: First steps towards the creation of a benchmarking system for large and energy-intensive industrial firms,” *Appl. Energy*, vol. 227, no. January 2017, pp. 436–448, 2018.

[88] “Air Compressor with Integrated Clutch,” *WABCO*, 2010. [Online]. Available: https://www.wabco-auto.com/WabcoWeb/media/Library/Assets/WABCO-pictures/Documents (PDF)/Brochures/c-comp_820_010_046_3.pdf?ext=.pdf. [Accessed: 16-Jan-2021].

[89] “Energy-efficient on all road types Air compressors,” *Voith*, 2019. [Online]. Available: https://d2euiryrvxi8z1.cloudfront.net/asset/445934742530/6a92e0a5c237bb6f1920bf5161b73b44. [Accessed: 16-Jan-2021].

[90] Steinert and Frank, “Challenges of Pure Electric Driving in the Field of Public Transport - Energy Efficiency as Necessity for Usability,” 2015, pp. 117–184.

[91] C. Andersson, “On auxiliary systems in commercial vehicles,” Lund University, 2004.

[92] M. Khodabakhshian, J. Wikander, and L. Feng, “Fuel efficiency improvement in HEVs using electromechanical brake system,” *IEEE Intell. Veh. Symp. Proc.*, no. Iv, pp. 322–327, 2013.

[93] R. Folkson, *Alternative Fuels and Advanced Vehicle Technologies for Improved Environmental Performance: Towards Zero Carbon Transportation*. Woodhead Publishing Limited., 2014.

[94] “OptiLevel™ - Electronically Controlled Air Suspension (ECAS),” *WABCO*, 2019. [Online]. Available: https://www.wabco-customercentre.com/catalog/en_GB/trailer/suspension-controls/optilevel---electronically-controlled-air-suspensionecas. [Accessed: 12-Jan-2021].

[95] “High Performance Electric Door Actuator for Transit Buses.” Vapor Bus International, Illinois, 2014.

[96] “Troubleshooting Transit Bus Air Systems,” Washington, 2020.

[97] P. Killeen, B. Ding, I. Kiringa, and T. Yeap, “IoT-based predictive maintenance for fleet management,” *Procedia Comput. Sci.*, vol. 151, no.

2018, pp. 607–613, 2019.

[98] "VOLVO Trucks Dashboard Warning Lights," *Dashboard lights*. [Online]. Available: https://www.dash-lights.com/volvo/trucks-dashboard-warning-lights/. [Accessed: 05-Jan-2021].

[99] A. Eriksson, "Detecting Leakages in the Pneumatic System of Heavy Vehicles Modelling Using Simulink," Upsala University, 2010.

[100] "Driver's Manual Volvo B10 M." Volvo.

[101] KAESER, "Sigma Air Utility: Air as a Service," 2022. .

[102] J. Laurikko, "Guideline for Including Energy Efficiency in Procurement Material Process," Brussels, 2018.

[103] J. Anthony, *Design of Experiments For Engineers and Scientists*. Elsevier, 2014.

[104] A. Kochsiek, "Pneumatic system for motor vehicles," 16175894.1, 2017.

[105] F. Rosero, N. Fonseca, and J. C. Lopez, "Real-world fuel efficiency and emissions from an urban diesel bus engine under transient operating conditions," *Appl. Energy*, vol. 261, 2020.

[106] "Know Which Gear is More Efficient?," *Max Power Gears*, 2017. .

[107] "Extreme 3 30LT. 12/24 Volt," *Nardi*, 2021. [Online]. Available: https://www.nardicompressori.com/prodotti/extreme-3-30lt-12-24-volt/. [Accessed: 08-Nov-2021].

[108] US Department of Energy, "Determining Electric Motor Load Ranges," 2014.

[109] "What is Energy and How Much do You Use?," *Sustainability Exchange*, 2021. [Online]. Available: https://www.sustainabilityexchange.ac.uk/files/cambridge_regional_college_sus_how_much_energy_do_you_use_pdf.pdf. [Accessed: 08-Dec-2021].

[110] H. Shauna L., W. Bo, Q. Yu, and S. Robert, "Evaluation of In-Use Fuel Economy for Hybrid and Regular Transit Buses," *J. Transp. Technol.*, vol. 03, no. 01, pp. 52–57, 2013.

[111] Z. Gao, T. J. LaClair, C. S. Daw, D. E. Smith, and O. Franzese, "Simulations of the Fuel Economy and Emissions of Hybrid Transit Buses over Planned Local Routes," *SAE Int. J. Commer. Veh.*, vol. 7, no. 1, pp. 216–237, 2014.

[112] "Malta Diesel prices, 13-Dec-2021," *Global Petrol Prices*, 2021. [Online]. Available: https://www.globalpetrolprices.com/Malta/diesel_prices/. [Accessed: 13-Dec-2021].

[113] R. Kawamoto *et al.*, "Estimation of CO2 Emissions of internal combustion

engine vehicle and battery electric vehicle using LCA," *Sustain.*, vol. 11, no. 9, 2019.

[114] "Route X1," *Malta Public Transport*, 2021. .

[115] "Route 49," *Malta Public Transport*, 2021. .

[116] J. Warczek, R. Burdzik, and G. Peruń, "The method for identification of damping coefficient of the trucks suspension," *Key Eng. Mater.*, vol. 588, no. January 2016, pp. 281–289, 2014.

[117] "Air Cylinder Selection Basics," *Misumi*, 2011. [Online]. Available: https://www.misumi-techcentral.com/tt/en/lca/2011/01/068-air-cylinder-selection-basics.html. [Accessed: 13-Nov-2021].

[118] Budynas-Nisbett, *Mechanical Engineering : Shigley's Mechanical Engineering Design 8th Edition*. McGraw−Hill, 2006.

[119] R. K. Mobley, *Plant Engineering Handbook*, 2nd ed. Tennessee: Butterworth-Heinemann, 2001.

[120] SMC, "Series PFMB, 2-Color Display Digital Flow Switch," 2013. [Online]. Available: https://www.smcpneumatics.com/pdfs/PFMB.pdf. [Accessed: 06-Nov-2021].

[121] Omron, "NX-series Analog I/O Unit," 2020. [Online]. Available: https://assets.omron.eu/downloads/datasheet/en/v8/nx-series_analog_i_o_unit_-_nx-ad_da_datasheet_en.pdf. [Accessed: 05-Nov-2021].

[122] WIKA, "Pressure transmitter For general industrial applications Model A-10." p. 2, 2021.

[123] WIKA, "High-quality pressure transmitter For general industrial applications Model S-10." p. 3, 2021.

[124] S. Arhin, E. Noel, M. F. Anderson, L. Williams, A. Ribisso, and R. Stinson, "Optimization of transit total bus stop time models," *J. Traffic Transp. Eng. (English Ed.*, vol. 3, no. 2, pp. 146–153, 2016.

[125] Hyundai, "Hyundai Solar Module." 2019.

[126] A. Buchroithner, "How many liter of petrol burn when car is in idle state while the engine is turning on?," 2017. .